INSTITUTE FOR AEROSPACE STUDIES

UNIVERSITY OF TORONTO

EXPERIMENTAL EVALUATION OF THE TENSOR POLYNOMIAL FAILURE CRITERION FOR THE DESIGN OF COMPOSITE STRUCTURES

by

R. C. Tennyson

A Progress Report Submitted to the

NATIONAL AERONAUTICS AND SPACE ADMINISTRATION
LANGLEY RESEARCH CENTER

Under Grant No. NGR 52-026-039

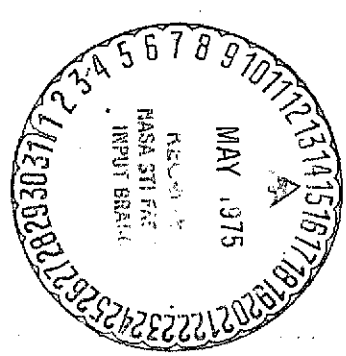

MARCH 1975

EXPERIMENTAL EVALUATION OF THE TENSOR POLYNOMIAL FAILURE CRITERION FOR THE DESIGN OF COMPOSITE STRUCTURES

by

R. C. Tennyson

A Progress Report Submitted to the

NATIONAL AERONAUTICS AND SPACE ADMINISTRATION
LANGLEY RESEARCH CENTER

Under Grant No. NGR 52-026-039

MARCH 1975

ACKNOWLEDGEMENT

The author would like to acknowledge the contributions made in this research programme by his Research Engineers; Mr. F. Mueller, Mr. P. Palmer and Mr. J. Young. In addition, the financial aid provided by the National Research Council of Canada (Grant No. A-2783) enabled us to purchase and modify a belt wrapper apparatus for manufacturing all composite tubes used in this investigation. We are also particularly appreciative to the National Aeronautics and Space Administration for their continued interest and financial support of this work (Grant No. NGR 52-026-039).

CONTENTS

NOTATION

A_{ij}	$\sum_{k=1}^{n} \bar{Q}_{ij}(t_k - t_{k-1})$
$\tilde{B}_{ij}$	$\frac{1}{2} \sum_{k=1}^{n} \bar{Q}_{ij}\, k\, (t_k^2 - t_{k-1}^2)$
B_{ij}	biaxial stress ratio σ_i/σ_j
E_{11}, E_{22}	orthotropic elastic moduli of the lamina measured in the fiber and transverse directions, respectively
F_i, F_{ij}, F_{ijk}	strength tensors
F_1, F_2, F_6	$\frac{1}{X} - \frac{1}{X'}$, $\frac{1}{Y} - \frac{1}{Y'}$, $\frac{1}{S} - \frac{1}{S'}$, respectively
F_{11}, F_{22}, F_{66}	$\frac{1}{XX'}$, $\frac{1}{YY'}$, $\frac{1}{SS'}$, respectively
F_{12}	quadratic interaction strength parameter
F_{112}, F_{122} F_{166}, F_{266}	cubic interaction strength parameters
G_{12}	orthotropic elastic shear modulus
ksi	1000 lbs/in^2
L	tube length
N_x, N_y	normal forces per unit length measured in the x and y directions, respectively
N_{xy}	in-plane shear force per unit length
p	internal pressure

Q_{11}, Q_{22}	$E_{11}/(1-\nu_{12}\nu_{21})$, $E_{22}/(1-\nu_{12}\nu_{21})$ respectively
$Q_{12} = Q_{21}$	$\nu_{21}E_{11}/(1-\nu_{12}\nu_{21})$
Q_{66}	G_{12}
$\overline{Q}_{ij}$	see Eq. (20)
R	tube radius measured to median surface
S,S'	positive and negative lamina shear failure stresses, respectively
t	lamina thickness
T	torque
X,X'	uniaxial lamina strength in fiber direction, tensile and compressive, respectively
Y,Y'	uniaxial lamina strength transverse to fibers, tensile and compressive, respectively
β	$(1-\nu_{12}\nu_{21})$
γ, ε	shear and normal strain, respectively
θ	fiber orientation relative to structural axis (see Fig. 3)
ν_{12}, ν_{21}	major and minor orthotropic Poisson ratios, respectively
σ	stress
τ	shear stress

SUBSCRIPTS

i, j, k	integers, 1, 2, 6
x,y	structural axes, axial and circumferential, respectively
1, 2	principal lamina axes corresponding to the fiber and transverse directions, respectively
6	in-plane shear

1. INTRODUCTION

One of the major difficulties associated with the design and use of composite materials for load-bearing structural applications is the current lack of a suitable failure criterion for both the individual laminae and the laminated structure as a whole. Although many lamina failure criteria have been proposed (see Refs. 1, 2 and 3, for example), insufficient experimental data particularly under combined states of stress have been accumulated to indicate which criterion is best able to predict the failure stresses. The difficulty is of course that each strength criterion has been developed empirically with certain interaction parameters being neglected and they are all phenomenological in nature. In other words, they can predict the occurrence of failure but they do not describe the physics or mode of failure.

It would appear that the most general failure criterion proposed up to the present is that given by Wu (Refs. 4, 5, 6) in the form of a tensor polynomial

$$f(\sigma_i) = F_i \sigma_i + F_{ij} \sigma_i \sigma_j + F_{ijk} \sigma_i \sigma_j \sigma_k + \ldots = 1 \qquad (1)$$

(where i, j, k = 1, 2, 3, ...6)

which can be shown to encompass all other failure criteria which are currently available. The simplest form of Eq. (1) which retains the interaction tensor strength components is (Refs. 7, 8)

$$F_i \sigma_i + F_{ij} \sigma_i \sigma_j = 1 \qquad (2)$$

This quadratic tensor polynomial defines a failure surface in stress space in terms of two strength tensors F_i and F_{ij} of the second and fourth ranks, respectively. Of particular interest in this formulation is the existence of the linear terms in σ_i which can account for the observed differences between positive and negative stress induced failures. However, in order to employ the stress tensor polynomial strength equation, one is faced with the difficulty of evaluating not only the standard principal strength parameters as defined by the (F_i, F_{ii}) relations, but also determining the interaction terms (F_{ij}, F_{ijk}, etc.) which are regarded as independent material properties. Since the failure surface may not be ellipsoidal in shape (i.e., the principal directions of strength may not always be orthogonal), it is necessary to include higher order terms in the tensor polynomial equation (such as the sixth-order failure tensor F_{ijk}). Thus the number of independent strength parameters that have to be determined experimentally can become inordinately large. It might be noted that a compromise "hybrid" method has been recently proposed (Ref. 6) in which fewer experimentally measured interaction parameters are required. One other formulation that has also been published recently (Ref. 9) is based on strain energy and matching the shape of the failure surface to experimental data. However, only the three principal strength parameters are utilized and no interaction terms are included.

Most of the experimental studies that have been undertaken with composite materials have employed flat plate specimens, particularly for evaluating the orthotropic stiffness and principal strength parameters. For example, two reports by Azzi and Tsae (Refs. 10, 11) have demonstrated remarkably well how the plane stress anisotropic Hill failure condition was able to predict the strength for transversely isotropic configurations, including unidirectional off-axis, cross and angle ($\pm\theta$) ply laminates. In this failure criterion, only the primary strength parameters were used, with no allowance for compression/tension differences. Since theory and experiment were in good agreement, one must conclude that for the specimens tested, the interaction terms must either have been reasonably well approximated or their influence on the strength prediction was of second order. However, in general this may not be the case for all materials and load configurations. In particular, for the flat off-axis test specimen, Pipes and Cole (Ref. 12) recently showed very well that the F_{12} term did not contribute significantly to the tensile strength prediction as a function of fiber orientation (θ). Moreover, it was proven that this specific test configuration was not sufficiently sensitive to accurately measure F_{12}. Other difficulties associated with flat plate specimens include:

- specimen geometry can affect the measured strength - thus it is necessary to use samples having very high (free length/width) ratios (Ref. 13);

- existence of free edges can lead to large interlaminar shear strains and premature cracking of matrix (Ref. 14);
- effect of end constraints and coupled deformations can lead to erroneous results;
- obtaining a homogeneous stress state requires a sufficiently wide specimen, but this makes it difficult to overcome the first problem.

Consequently, a great deal of theoretical and experimental work has been devoted to assessing the circular cylindrical tube as an optimum specimen configuration for both stiffness and strength characterization. However, considerable care must also be exercised in the proper design of the cylinder to ensure absence of edge constraint effects, failure in the test section and a uniform stress field. In general, to employ "thin wall" shell theory for calculating stress levels requires that the (diameter/thickness) ratio should be $\geq$ 20 (Refs. 15, 16) and the specimen length should equal twice the mean diameter plus the desired gauge length (Ref. 15). The limits on (diameter/thickness) however are dependent on the material system and ply orientations. It was shown, for example, that it was difficult to achieve a uniform stress distribution in a helical unidirectional wound tube and thus one should use $\pm \theta$ symmetric configurations for characterization tests. Perhaps the most difficult parameter to assess experimentally is the degree of end attachment needed to obtain a relatively uniform stress distribution

in the gauge section without failure occurring at the ends (Refs. 17, 18). For a good review of current static testing techniques, one can refer to Bert's paper (Ref. 19).

At this point, it is worthwhile reviewing the extent to which tubular specimens have been utilized to evaluate strength criteria. Aside from the preliminary burst pressure results published by Sandhu et al (Ref. 20), the first measurements of an interaction component (F_{12}) were made by Wu (Ref. 8). More details on the actual test programme can also be found in Ref. 21. Later, when Wu expanded his failure criterion to include higher order terms (F_{ijk}), he also reported additional data (Ref. 6) in the form of a failure surface for direct comparison with various failure theories. These results were also given in Ref. 5 in which it was shown that the tensor failure polynomial provided the best comparison. However, the scatter was substantial and the configurations tested were quite restrictive, i.e., specially orthotropic and symmetric. One noteworthy investigation involved the testing of $\pm\theta$ cylinders under axial tension, torsion and internal pressure (Ref. 22). The failure criterion adopted consisted of evaluating the in-plane stresses and determining when their fracture stress levels had been reached (based on four fracture stress parameters - tensile and compressive stresses for fibers, tensile stress normal to fibers and shear stress). An empirical expression was used to calculate

the ultimate shear stress as a function of orientation with respect to the fibers. Furthermore, it was assumed that the matrix failed first and the stresses could be re-calculated based on an assumed zero modulus for the matrix. With this approach, good agreement between experiment and predicted behaviour was achieved. Whether or not this method would yield similar results for other laminates is not known. Finally, one last report which was recently published (Ref. 23) contains experimental data on tubes subjected to uniaxial loading, internal pressure and torsion. Some comparisons with failure theories were presented but no attempt to evaluate the tensor strength polynomial terms or its strength predictions was made.

The following report describes the experimental measurements and techniques used to obtain the strength tensor components, including cubic terms. Based on a considerable number of biaxial pressure tests together with specimens subjected to a constant torque and internal pressure, a modified form of the plane stress tensor polynomial failure equation was obtained that was capable of predicting ultimate strength results reasonably well. Although only glass-epoxy tubular test configurations have been studied, it is felt that the failure criterion should apply equally well to other material laminates. In addition, preliminary data were obtained to determine the effect of varying post cure times and ambient temperature (- 80°F to 250°F) on the change in

two tensor strength terms, F_2 and F_{22}. Other laminate configurations presumably should yield corresponding variations for the remaining strength parameters.

2. FABRICATION OF SPECIMENS

2.1 Belt Wrapper

The belt wrapper, as shown in Figure 1, is an apparatus which applies constant pressure around approximately 340° of a mandrel through the use of a silicone coated fibreglass belt under tension. The mandrel is positioned on the loose silicone/fibreglass belt between two rollers. One of these rollers can be moved forward in a groove and tightened down so that there is a gap of about 1.5 inches between the two rollers (Figure 2). One of the lower rollers is mounted at both ends on air cylinders and these cylinders are connected through a pressure regulator to an air supply. When the air cylinders are pressurized, the lower roller is pushed forward so that tension is applied to the belt. This causes the mandrel to be pressed up against the two upper rollers and the belt applies pressure around the mandrel. There is a reversible, variable speed motor connected to one of the lower rollers. When the motor is engaged, the roller rotates causing the belt to move, which, in turn, causes the mandrel to rotate. In this way, the prepreg tape can be wrapped tightly onto the mandrel.

The mandrels can be made from either steel or aluminum tubing of the desired outside diameter. The tube must be cut to a length of 46 inches so that it will fit in this particular belt wrapping apparatus and then, its surface must be ground to ensure a uniform circular cross-section along

the entire length and be very smooth. The tube is then fitted with a vacuum connection at one end. Now, the finished mandrel is thoroughly cleaned to remove all traces of dirt and oil from its surface and an even continuous film of Frekote 33 Releasing Interface is sprayed on. This film is then baked on at 125°C for about 15 minutes to increase its durability as suggested by the manufacturer.

2.2 Geometry of Pre-Preg Sheets for Wrapping

In order to wrap a particular fibre angle on the mandrel and to avoid overlapping or gaps at the seams of the material, the pre-impregnated (pre-preg) tape must be cut very accurately to the desired width. The following procedure is used to determine the length and width of the tape required to fabricate a specimen having any fibre angle, θ.

Figure 3 shows the dimensions of the finished specimen and of the tape required to make that specimen. In this figure, D is the outside diameter of the mandrel, L is the required length of the test specimen, C is the outside circumference of the mandrel, W is the width of the pre-preg tape, l is the length of the pre-preg tape and θ is the fibre angle. The dimensions of the pre-preg tape are calculated using the following relations:

$$C = \pi D, \quad W = \pi D \sin \phi \ , \text{ and } l = L / \cos \theta$$

where $\phi = 90 - \theta$ degrees. When performing these calculations for additional laminae other than the first, the value of D must be increased by twice the thickness of the pre-preg

tape each time.

2.3 Wrapping Procedure

The material used to make all of the test specimens was "Scotchply" Reinforced Plastic Type 1002 fibreglass/epoxy preimpregnated tape.

The feed guides on the belt wrapper are adjusted to produce butt seams using a paper pattern of the desired orientation. The first ply of pre-preg is then placed on the working table of the belt wrapper with the paper backing against the belt. The circumferential edge of the tape is positioned against the feed guide and the material is slowly rolled onto the mandrel in such a way that the paper backing faces outwards. If the tape has been cut correctly and the guides adjusted carefully, there should be no overlaps or gaps in the tube, but rather a smoothly butted seam. The paper is then peeled away from this first ply by running the belt wrapper backwards and carefully lifting the paper from the tape. Additional laminae are wrapped in the same manner. With thick-walled structures, the air cylinder pressure should be reduced as successive layers are wrapped to avoid buckling the material.

Once all of the plies are wrapped onto the mandrel, a porous teflon coated fibreglass cloth is wrapped around the tube again using the belt wrapper to ensure a wrinkle-free application. The specimen is then removed from the belt-wrapper and bagged in Vac-Pak type E3760 film and sealed

with a vacuum bag sealant. Canvas strips are placed along the bag seam and around the ends of the mandrel, inside the vacuum bag, to allow a vacuum over the entire tube (Figure 4). Using a vacuum pump, a vacuum of 29 inches of Hg is established and maintained in the bag around the specimen for three hours while the tube is curing at 150°C. The bag and release cloth are removed from the tube after four hours and the specimen is postcured for seventeen hours at 150°C. The oven temperature is then raised to 200°C for forty-five minutes. After this, the tube is removed from the oven and slid off the mandrel.

The tubes are cut to the desired length by sliding them over a cutting mandrel mounted on a lathe (Figure 5). Using a slow lathe speed, the tube is turned and an air operated abrasive cutting disc, mounted in the tool post, is used to make a square cut. The tube ends are sanded smooth and thickness measurements are taken at eight positions equally spaced around the circumference at both ends and in the middle section in order to obtain an average tube wall thickness. The specimens are then readied for testing by reinforcing the ends with stepped down layers of cotton cloth, fine fibreglass cloth and epoxy and potting them in end plates, made of a suitable material, to a depth of one inch with a room temperature curing epoxy. Several specimens were strain gauged with 350 ohm, 0.5 inch foil gauges to provide stress-strain data up to failure.

2.4 Specimen Design

Thin-walled cylindrical test specimens offer definite advantages for experimentally characterizing the mechanical behaviour of fibre/matrix composite materials. All of the loadings required to fully characterize the composite system with respect to its mechanical properties can be applied to this type of specimen. However, particular care must be taken to ensure that reasonably uniform stresses across the wall thickness are obtained. As noted earlier, the stresses induced in an anisotropic tube which is subjected to combined axial load, torsion, and internal pressure are approximately uniform across the wall thickness provided that the ratio of wall thickness to radius is sufficiently small.

A major problem remains in the use of tubular test specimens which are usually rigidly clamped (i.e., potted) to end plates. This method of end attachment prohibits the transverse and radial displacements of the tubular specimen and this induces relatively large bending stresses in the region near the end plates. These bending stresses can lead to premature failure of the tube in the end regions.

If the magnitude of these bending stresses can be predicted before any testing is done, then sufficient reinforcement can be applied to the ends of the tube in order that they do not fail prematurely. Also, if the variations in the induced stresses along the length of the test specimen are known, then it can be designed more accurately so as to

ensure a uniform stress distribution in the test section.

In Appendix A, the governing equations for orthotropic symmetric laminates ($A_{16} = A_{26} = B_{ij} = 0$) under symmetric loading are derived using an extension of Flugge's shell theory (Ref. 24) provided by Cheng and Ho (Ref. 25). These equations were then solved to determine the proper dimensions of the tubular test specimens used for composite characterization.

3. EVALUATION OF STRENGTH TENSORS

The general form of the tensor polynomial strength equation proposed by Wu (Ref. 4) is

$$F_i \sigma_i + F_{ij} \sigma_i \sigma_j + F_{ijk} \sigma_i \sigma_j \sigma_k + \ldots = 1 \qquad (3)$$

where i, j, k = 1, 2, ... 6, and F_i, F_{ij}, F_{ijk} are tensors of the 2nd, 4th and 6th ranks, respectively. For a plane stress state, i, j, k = 1, 2, 6. The purpose of this section of the report is to provide a description of the experimental methods used to evaluate the principal strength components (F_1, F_2, F_6, F_{11}, F_{22}, F_{66}) and the quadratic interaction parameters (F_{12}, F_{16} and F_{26}), assuming the material system is symmetric (i.e., $F_{ij} = F_{ji}$ for $i \neq j$). In this formulation, each of the tensor strength terms (F_i, F_{ij}, F_{ijk}, etc.) is considered to be an independent material property. Although experimental results have only been obtained for the linear and quadratic terms, analysis in Section 6 was used to estimate the required cubic terms (F_{ijk}) necessary for the strength equation.

3.1 Principal Strength Tensor Components (F_i, F_{ii})

From the analysis by Wu (Ref. 8), it was shown that the principal strength tensor components (F_i and F_{ii}) can be readily calculated from the experimentally determined values of the uniaxial tensile and compressive failure stresses in the fiber direction (X and X'), perpendicular to the fibers (Y and Y') and from positive and negative pure shear failure

stresses (S and S', respectively). The appropriate relations are given by:

$$F_1 = \frac{1}{X} - \frac{1}{X'} \qquad F_2 = \frac{1}{Y} - \frac{1}{Y'}$$
$$F_6 = \frac{1}{S} - \frac{1}{S'} \qquad F_{11} = \frac{1}{XX'} \qquad (4)$$
$$F_{22} = \frac{1}{YY'} \qquad F_{66} = \frac{1}{SS'}$$

where the F_{iii} terms are not considered since they were shown in Ref. 6 to be redundant and not necessary for the strength criterion.

To determine the tensile strength in the fibre direction, four tubes were tested. These tubes all had an inside diameter of approximately 2 inches and were 8 inches long between end-plates. They were fabricated from two plies of material with the fibers aligned along the longitudinal axis of the tube, (i.e., $\Theta = 0$). Figures 6 to 8 show the test set-up used and a specimen before, during and after failure. The results are summarized in Table I. A typical stress-strain curve, obtained using a strain gauge oriented longitudinally at the midpoint of the specimen, is shown in Figure 9.

For the compressive strength in the fiber direction, seven tubes were tested. It was necessary to fabricate these tubes with a smaller inside diameter (approximately one inch) and a larger wall thickness in order to avoid buckling. They were made from eight plies of material and the fibers were

also aligned in the longitudinal direction. The test set-up and a failed specimen are pictured in Figures 10 and 11. Figure 9 also shows a stress-strain curve for one of the tubes.

Seven unidirectional, four ply, laminated tubes with $\theta = 90^{\circ}$ were tested in tension to determine the value of the ultimate transverse tensile strength. These tubes had an inside diameter of about 2 inches and were 5 inches long between end-plates. They were wrapped from a single piece of the pre-preg tape in order to provide continuous fibres in the circumferential direction. This resulted in two seams opposite each other on the inside and the outside walls of the tube. Although a slight discontinuity occurs at the seam, it does not affect the determination of the transverse strength at all. A tube is shown in the test set-up, after tensile failure, in Figure 12. The tensile strength results are contained in Table I and Figure 14 shows the stress-strain behaviour of one of the test specimens.

The compressive strength of the material transverse to the fiber direction, was determined by applying axial compression to failure on seven specimens, similar to those used in the transverse tension tests. Figure 13 shows a typical failure of one of the tubes. These results are also summarized in Table I and Figure 14 shows a stress-strain curve for this type of loading.

Seven tubes were tested to failure under pure torsional loading to obtain the ultimate shear strength of the material. As expected, the direction of the torque did not significantly change the failure stress. The tubes were four-ply laminates with $\theta = 90^{o}$, fabricated in the same way as those that were used in the tests for the transverse tensile and compressive strengths. Strain gauges were applied at $\theta = \pm 45^{o}$ to some of the tubes so that the stress-strain data to failure could be obtained. One of these curves is shown in Figure 15. The shear failure data are presented in Table I and Figures 16 and 17 show the test set-up and a failed tube, respectively.

Once the five basic failure strengths of the material are known, the simple strength tensors can be easily calculated using the relations given in Eq. (4). These values are listed in Table II. Using the stability condition (Ref. 7) $F_{ii} F_{jj} - F_{ij}^{2} \geq 0$, the bounds on the interaction strength tensors can also be calculated (Table II).

3.2 Quadratic Interaction Strength Tensor Components (F_{ij})

It was shown in the previous section that the determination of the F_i and F_{ii} (i = 1, 2, 6) strength tensors requires only simple uniaxial tension, compression and torsion tests. On the other hand , the interaction tensors F_{12}, F_{16} and F_{26} require biaxial stress experiments in which very strict control must be maintained over the biaxial stress ratio, $B = \sigma_i/\sigma_j$ in order to achieve sufficient test accuracy

to correctly measure the F_{ij} terms. In Ref. 8, Wu has shown that the best resolution of the interaction tensors is obtained by using an optimal value of the biaxial stress ratio together with the most suitable stress state since the resolution of the interaction tensor is dependent on both of these variables. However, the major difficulty that immediately arises is the fact that the full strength equation (1) must be employed, thus introducing cubic (and higher order) terms. As noted earlier, we shall restrict our attention only to a cubic formulation.

Consider, for example, the relative scatter (or resolution) of the interaction tensor component F_{12}. From Ref. (6) this is given by

$$\Delta F_{12} = \left.\frac{\partial F_{12}}{\partial \sigma_2}\right|_{\tilde{\sigma}_2} \Delta \tilde{\sigma}_2 \qquad (5)$$

where $\tilde{\sigma}_2$ is the failure stress of a biaxial test at a given stress ratio of $B_{12} = \sigma_1/\sigma_2$. $\tilde{\sigma}_2$ is obtained as a root of the failure equation (1) which can be re-written in the form (Ref. 6),

$$\left(3F_{112}B_{12}^2 + 3F_{122}B_{12}\right)\tilde{\sigma}_2^3 + \left(F_{12}B_{12}^2 + 2F_{12}B_{12} + F_{22}\right)\tilde{\sigma}_2^2 + \left(F_1 B_{12} + F_2\right)\tilde{\sigma}_2 = 1 \qquad (6)$$

where $\sigma_6 = 0$ by definition.

In order to alleviate the experimental requirements for determining F_{12}, as a first approximation we shall assume

that the cubic contribution to the strength (i.e., F_{122} and F_{112} terms) is negligible for the 0° and 90° configuration. Consequently, one can then estimate F_{12} and subsequently employ other complex load tests to assess the accuracy of its value. Based on these results, it is possible to estimate values for F_{122}, F_{112} and then reiterate to correct F_{12}. This procedure can be repeated to arrive at final values for F_{12}, F_{112} and F_{122}.

Hence, neglecting the cubic terms one obtains

$$\left.\frac{\partial F_{12}}{\partial \sigma_2}\right|_{\tilde{\sigma}_2} = -\left(F_{11} B_{12} + 2 F_{12} + \frac{F_{22}}{B_{12}} + \frac{F_1}{2\tilde{\sigma}_2} + \frac{F_2}{2B_{12}\tilde{\sigma}_2} \right) \tilde{\sigma}_2^{-1} \tag{7}$$

where

$$\tilde{\sigma}_2 = -(F_1 B_{12} + F_2) \pm \left[(F_1 B_{12} + F_2)^2 + 4 (F_{11} B_{12}^2 + 2 F_{12} B_{12} + F_{22}) \right]^{1/2} \Big/ 2 (F_{11} B_{12}^2 + 2 F_{12} B_{12} + F_{22}) \tag{8}$$

The optimum biaxial stress ratio B_{12} occurs when

$$\left.\frac{d \psi_{12}}{d B_{12}}\right|_{F_{12}} = \frac{\partial \psi_{12}}{\partial B_{12}} + \frac{\partial \psi_{12}}{\partial \tilde{\sigma}_2} \frac{d \tilde{\sigma}_2}{d B_{12}} = 0 \tag{9}$$

where $\psi_{12} = \left(\frac{\Delta F_{12}}{F_{12}} \right) \Big/ \left(\frac{\Delta \tilde{\sigma}_2}{\tilde{\sigma}_2} \right)$

$\equiv$ scatter magnification factor (Ref. 6).

Substituting into Eq. (9) yields

$$\frac{2\tilde{\sigma}_2 (F_{11} B_{12} + F_{12}) + F_1}{2\tilde{\sigma}_2 (F_{11} B_{12}^2 - F_{22}) - F_2} = \frac{-\left[2\tilde{\sigma}_2 (F_{11} B_{12}^2 + 2 F_{12} B_{12} + F_{22}) + F_1 B_{12} + F_2 \right]}{B_{12} (B_{12} F_1 + F_2)} \tag{10}$$

where $\tilde{\sigma}_2$ can be determined from Eq. (8). To obtain the best estimate for F_{12}, a set of experiments must be performed since the optimal value for B_{12} depends on F_{12}, assuming the other tensor strength components are known.

Before any strength tests could be carried out to determine the interaction tensor components, an analysis had to be done to determine the optimal biaxial stress ratios for each stress state. This was accomplished once the bounds on each of the interaction tensors were known (Table II).

Again, for example, consider the F_{12} interaction tensor. Once the constants F_1, F_2, F_{11}, F_{22} and the bounds on F_{12} are determined, it is a simple matter to substitute these into Eqs. (8) and (10) to estimate the optimal biaxial stress ratio for various values of F_{12} within the bounds of the stability condition. There are four roots of Eq. (8) for each value of F_{12}, one for each stress quadrant. Then, the resolution of F_{12} for the optimal ratios B_{12} must be plotted to determine in which stress quadrant the testing should be done. The resolution of F_{12} is given by the following relation;

$$\frac{\Delta \tilde{F}_{12}}{\Delta \sigma_2/\sigma_2} = -\left(F_{11} B_{12} + 2 F_{12} + \frac{F_{22}}{B_{12}} + \frac{F_1}{2\sigma_2} + \frac{F_2}{2 B_{12} \sigma_2}\right) \qquad (11)$$

When these two graphs have been obtained, it remains to decide on the method of application of the biaxial stress state and then to begin the iterative procedure to determine the value of F_{12}. This method is equally applicable to the determination of F_{16} and F_{26}.

F_{12} Interaction Tensor

Figures 18 and 19 are graphs of the optimal biaxial stress ratio to be used in the determination of F_{12} and the attainable resolution of F_{12} for a given optimal B_{12}. From these figures it is evident that for $F_{12} > 0$, a longitudinal tension-transverse compression ($\sigma_1 > 0, \sigma_2 < 0$) experiment with the ratio B_{12} in the range of - 14.4 to - 15.6 is optimal, and a longitudinal compression-transverse compression ($\sigma_1 < 0, \sigma_2 < 0$) experiment with the ratio B_{12} in the range 13.2 to 15.4 is optimal for $F_{12} < 0$. The tension-compression experiment was chosen because it was the most convenient test for a tubular specimen. A combination of internal pressure and axial compressive loading was used to provide the required biaxial stress state.

The specimens tested were unidirectional three ply laminates with $\theta = 90^{\circ}$. The tubes were continuously wrapped from a single piece of pre-preg tape and had a 1/4 inch overlap at the seam for load transfer. A 1/16 inch polyurethane liner was spuncast inside each specimen to prevent any damage that might be caused by the oil used in the internal pressure apparatus.

A schematic diagram and pictures of the actual test set-up are shown in Figures 20 and 21. An air-operated hydraulic oil pump was used to maintain the reservoir at a pressure of approximately 6,000 psi. The specimens were pressurzed from this reservoir by adjusting a flow valve

while monitoring the internal pressure by means of a pressure transducer downstream from the valve. The specimens were mounted in a Tinius Olsen 60,000 lb. Universal Testing Machine which provided the axial compressive load. This load was converted to a voltage by means of a potentiometer mounted in the testing machine. By knowing the pressure transducer's calibration in psi/volt and the testing machine's calibration in lb/volt, the required pressure versus axial compressive load curve can be plotted for a particular biaxial stress ratio B_{12}. This curve was recorded on an X - Y plotter having internal pressure and axial compressive load as inputs. The valve was opened just enough to allow a slow, steady increase in pressure in the tube, while the amount of axial load applied by the testing machine was controlled manually to ensure that the loading followed the pre-calculated load curve up to failure. In this way, a constant biaxial stress ratio was maintained throughout the test. Using the values of the internal pressure and compressive load at failure, the failure stresses σ_1 and σ_2 were calculated and a value for the F_{12} tensor was determined from the following equation:

$$F_{12} = \frac{1}{2\sigma_1\sigma_2}\left[1 - (F_{11}\sigma_1^2 + F_{22}\sigma_2^2 + F_1\sigma_1 + F_2\sigma_2)\right] \quad (12)$$

This method provided a controlled, constant ratio biaxial loading as is evident in Figure 22 which shows the actual loading curve in comparison to the calculated loading curve for a biaxial stress ratio of - 14.2. The results of the

iteration procedure to determine the value of F_{12} are listed in Table III. The average value of the F_{12} tensor for this material was determined to be - 6.387×10^{-4} $(K.S.I.)^{-2}$.

Even though the experimentally determined value of F_{12} lies in the range - 5.933×10^{-4} to - 6.690×10^{-4} $(K.S.I.)^{-2}$, tension-compression tests were used instead of compression-compression tests, as is indicated in Figure 19, to obtain the best resolution of the F_{12} tensor because the latter mode of testing was quite inconvenient to use with tubular specimens and this testing machine. Figures 23 and 24 show typical failure modes for the F_{12} test specimens. Other failure tests were conducted to verify this value of F_{12}. Details of these results and analysis of the cubic int eraction terms can be found in Section 6.

F_{16} and F_{26} Interaction Tensors

The tests to determine the values of F_{16} and F_{26} strength tensors have not yet been done. However, the optimal biaxial stress ratios for the four stress states and the attainable resolutions of the tensors have been calculated. These are plotted in Figures 25 to 28 and are summarized in Table III.

However, it should be noted that since $F_6 = 0$, this would indicate that the sign of the shear stress does not affect the failure stress. Consequently, to remove this shear stress "sign" effect from the failure equation, all odd-order

terms in σ_6 should be set to zero. Thus it is proposed to let $F_{16} = F_{26} = 0$ in our subsequent failure analyses. This will of course also apply to the cubic terms involving odd-order σ_6 components.

3.3 The Effect of Temperature on the Strength Tensor Components

A preliminary test programme was undertaken to evaluate the effects of varying ambient temperature from - 80°F to + 250°F on the orthotropic elastic constants and burst strength of 3-ply, 90° laminated tubes. Appendix B contains a detailed discussion of the test methods used together with the required analysis. A summary of the experimental results is contained in Table IV. It should be noted that two test conditions were investigated using internal pressure loading; (1) free axial expansion of ends, and (2) zero axial displacement due to imposed external constraints. The actual burst pressures recorded in Table IV are for case (1) loading.

In order to demonstrate how this test data can be used to estimate the variation in strength tensors with temperature, one must first consider the ability of the strength criterion to predict failure at room temperature where the strength components are already known. For a $\theta = 90°$, 3-ply laminated tube under internal pressure,

$$\begin{aligned} \sigma_1 &= \sigma_Y \cong pR/3t \\ \sigma_2 &= \sigma_X \cong pR/6t \\ \sigma_6 &= 0 \end{aligned} \tag{13}$$

Neglecting the cubic terms F_{122}, F_{112}, the strength equation can be written as,

$$4\sigma_2^2\left(F_{11}+\frac{F_{22}}{4}+F_{12}\right)+2\sigma_2\left(F_1+\frac{F_2}{2}\right)=1 \qquad (14)$$

Substituting for the strength components (see Tables II and III), the predicted failure stress is σ_2 = 3365 psi. This agrees quite well with the average measured value of 3442 psi (within 3%) shown in Table IV at T = 70°F. Thus, the assumption of F_{122} and F_{112} being of second order (for θ = 90°) appears valid. The interesting feature of Eq. (14) is that if one neglects the F_{11}, F_{12} and F_1 terms for the θ = 90° configuration tests, then the resulting approximation yields a failure stress (σ_2) of 3246 psi. This value lies within 4% of the predicted strength based on the inclusion of all terms. Consequently, one can now obtain an estimate of the temperature variation of the F_{22} and F_2 terms from the following strength equation;

$$\sigma_2^2 F_{22} + F_2 \sigma_2 = 1 \qquad (15)$$

where we shall define the reference temperature (RT) strength tensor components as

$$F_{2_{RT}} = \frac{1}{Y} - \frac{1}{Y'} = \frac{Y' - Y}{YY'} \qquad (16)$$

$$F22_{RT} = \frac{1}{YY'}$$

We shall further assume that at some arbitrary temperature (T), these strength components can be estimated by

$$F_2(T) = \frac{F_{2_{RT}}}{(1 \pm k)}$$

$$F_{22}(T) = \frac{F_{22_{RT}}}{(1 \pm k)^2} \qquad (17)$$

where $Y(T) = (1 \pm k)Y$

$Y'(T) = (1 \pm k)\ Y'$

k = a constant

Using the strength equation (15) to predict failure at some temperature T, one has

$$F_{22}(T)\,\sigma_2^2(T) + F_2(T)\,\sigma_2(T) = 1$$

or substituting for $F_{22}(T)$ and $F_2(T)$ from Eq. (17) gives,

$$\alpha^2 - \alpha F_{2_{RT}}\sigma_2(T) - F_{22_{RT}}\sigma_2^2(T) = 0 \qquad (18)$$

where $\alpha = (1 \pm k)$.

Consequently, knowing the $F_{2_{RT}}$ and $F_{22_{RT}}$ values as well as the failure stresses $\sigma_2(T)$ at various temperatures, one can solve for $\alpha(T)$. Thus one can construct plots of the variation in the strength tensor components $F_2(T)$ and $F_{22}(T)$ as a function of temperature.

Based on the data shown in Table IV for circular cylindrical tubes with a mean radius R = 1.015" and a ply thickness t = 0.010", the strength terms were then calculated for the various temperatures. These results are shown in Figure 29.

3.4 The Effect of Post Cure Time on the Strength Tensor Components

Similar to the temperature study, an investigation

was made on the effects of varying post cure times (0 to 24 hrs) on the measured orthotropic elastic constants and the burst pressure. A description of this work can be found in Appendix C, with a summary of the results listed in Table V. Since the test procedures and analysis are identical to the thermal study previously discussed, it is only necessary to consider the appropriate strength tensors F_2 and F_{22}.

Based on the 0_{HR} post cure data, an average failure stress of σ_2 = 3112 psi was obtained. This can be compared with the predicted (room temperature) value of 3365 psi for a 3 ply, $\theta = 90^{\circ}$ configuration which agrees within 8%. Again, using the same argument posed in Section 3.3, the variation in F_2 and F_{22} with post cure time was estimated and the results plotted in Fig. 30.

4. MATERIAL PROPERTY CHARACTERIZATION TESTS

Although this report is primarily concerned with the evaluation of a strength criterion for the design of composite structures, it is also necessary to include the determination of the lamina orthotropic stiffness parameters. This arises because in the analysis of laminated configurations consisting of many plies oriented at arbitrary angles θ relative to the structural axes, it is necessary to compute the individual ply stresses (σ_1, σ_2, σ_6 or σ_x, σ_y, τ_{xy}) and strains. This will be discussed later in Section 7. Suffice it to say at this point that the plane stress distrubution in some lamina of orientation θ (see Fig. 3) is related to the overall structural strain matrix in the following way;

$$\begin{bmatrix} \sigma_x \\ \sigma_y \\ \tau_{xy} \end{bmatrix}_\theta = \begin{bmatrix} \overline{Q}_{11} & \overline{Q}_{12} & \overline{Q}_{16} \\ \overline{Q}_{21} & \overline{Q}_{22} & \overline{Q}_{26} \\ \overline{Q}_{61} & \overline{Q}_{62} & \overline{Q}_{66} \end{bmatrix} \begin{bmatrix} \varepsilon_x \\ \varepsilon_y \\ \gamma_{xy} \end{bmatrix} \tag{19}$$

where

$$\begin{aligned} \overline{Q}_{11} &= U_1 + U_2 \cos 2\theta + U_3 \cos 4\theta \\ \overline{Q}_{22} &= U_1 - U_2 \cos 2\theta + U_3 \cos 4\theta \\ \overline{Q}_{12} &= \overline{Q}_{21} = U_4 - U_3 \cos 4\theta \\ \overline{Q}_{16} &= \overline{Q}_{61} = (U_2/2)\sin 2\theta + U_3 \sin 4\theta \\ \overline{Q}_{26} &= \overline{Q}_{62} = (U_2/2)\sin 2\theta - U_3 \sin 4\theta \\ \overline{Q}_{66} &= U_5 - U_3 \cos 4\theta \end{aligned} \tag{20}$$

and

$$U_1 = \frac{1}{8}(3\,Q_{11} + 3\,Q_{22} + 2\,Q_{12} + 4\,Q_{66})$$

$$U_2 = \frac{1}{2}(Q_{11} - Q_{22})$$
$$U_3 = \frac{1}{8}(Q_{11} + Q_{22} - 2\,Q_{12} - 4\,Q_{66}) \qquad (21)$$
$$U_4 = \frac{1}{8}(Q_{11} + Q_{22} + 6\,Q_{12} - 4\,Q_{66})$$
$$U_5 = \frac{1}{8}(Q_{11} + Q_{22} - 2\,Q_{12} + 4\,Q_{66})$$

and

$$Q_{11} = E_{11}/(1 - \nu_{12}\nu_{21})$$
$$Q_{22} = E_{22}/(1 - \nu_{12}\nu_{21}) \qquad (22)$$
$$Q_{12} = Q_{21} = \nu_{21}\,E_{11}/(1 - \nu_{12}\,\nu_{21})$$
$$Q_{16} = Q_{26} = 0 \text{ for an orthotropic lamina}$$
$$Q_{66} = G_{12}$$

Equations (19) to (22) are based on three major assumptions:

(a) linear response;

(b) the laminae exhibit identical structural strains under a given load system;

(c) the individual laminae can be regarded as homogeneous orthotropic materials.

Clearly the assumption of linear stress/strain behaviour requires experimental verification to define the limits for which this is true. Furthermore, one must also evaluate the actual orthotropic constants as defined by E_{11}, E_{22}, ν_{12} (or ν_{21}) and G_{12}.

The following sections describe the experimental methods used to determine the orthotropic constants and the results obtained.

4.1 EVALUATION OF ORTHOTROPIC ELASTIC CONSTANTS

The material properties E_{11}, E_{22}, and G_{12} were obtained from stress-strain data of tubes with $\theta = 0^{\circ}$ and 90° loaded in axial tension and tubes with $\theta = 90^{\circ}$ loaded in pure torsion respectively.

These material properties were calculated from basic relationships and are listed in Table VI.

Four other specimens were also characterized using the method outlined in Ref. 26. These specimens were all made up of four plies and had the following fibre orientations: 0°, 0°, 0°, 0°; -30°, 30°, 30°, -30°; -60°, 60°, 60°, -60°; 90°, 90°, 90°, 90°. Three 350 ohm, 0.5 inch strain gauges were bonded onto each tube, oriented in the axial, circumferential and -45° directions. All of the strain gauges were positioned at the midlength of the specimens. Each tube was then potted in aluminum endplates using a room temperature curing epoxy.

The characterization procedure consisted of applying separately to each tube pure axial compression, internal pressure and pure torsion. By monitoring the load transducers and strain gauges on an X-Y plotter, a plot of load versus strain was obtained during each of the loading cycles for each of the strain gauges. From these curves, the nine values of load/strain were calculated for each tube. These values along with the ply thickness and fibre orientation were the input data for the material properties characterization computer program listed in Ref. 26. This program calculated, among other things, the material properties E_{11}, E_{22}, G_{12}, ν_{21} and ν_{12} and these are also listed in Table VI along with the manufacturer's specifications.

It can readily be seen by comparing the unidirectional tube data with the calculated values for the $\pm\,\theta$ laminated tubes that for the E_{11}, E_{22} and G_{12} parameters, the results agree within 11%.

In the subsequent failure analyses, the unidirectional tube data will be used for these three orthotropic constants, while the major and minor Poisson ratio terms obtained from the $\pm\ \theta$ tests will be employed.

Of particular interest for stress calculations is the range of linear behaviour as shown in Figs. 9, 14 and 15. From this data, the following limits should be considered on the use of Eq. (19):

$$\begin{aligned} &-88\ \text{ksi} \leq \sigma_1 \leq 121\ \text{ksi} \\ &-6\ \text{ksi} \leq \sigma_2 \leq 3.3\ \text{ksi} \\ &|\sigma_6| \leq 3\ \text{ksi} \end{aligned} \tag{23}$$

where 1 and 2 denote the fiber and transverse directions, respectively.

4.2 THE EFFECT OF TEMPERATURE ON THE ORTHOTROPIC CONSTANTS

The effect of varying ambient temperature not only changes the strength parameters (as shown previously in Section 3.3) but also the orthotropic stiffness coefficients. Appendix B contains a complete description of the tests performed over a temperature range of $-80^{\circ}F$ to $+250^{\circ}F$. As far as the elastic constants are concerned, Figs. B.4 to B.10 illustrate the stress/strain curves obtained which are quite linear except near fracture in the high temperature range ($T \geq 200^{\circ}F$). The actual variations in the moduli E_{11} and E_{22} are shown in Figs. B.11 to B.14 and summarized in Table IV. The major thermal effect is found in E_{22} as expected since it reflects primarily the epoxy matrix response. Estimates of the temperature variation in the Poisson ratio terms were also made. Again, the

dominant change is in the ν_{21} parameter.

Knowing both the change in strength and orthotropic stiffness parameters with temperature permits the designer to calculate the failure loads of composite structures at various thermal conditions. Although all parameters have not yet been determined as a function of temperature, the methodology outlined in this report should provide the means for obtaining the necessary data.

4.3 THE EFFECT OF POST CURE TIME ON THE ORTHOTROPIC CONSTANTS

As in the thermal investigation, the effect of varying the post cure time was studied to assess the change in the orthotropic constants. This aspect of the programme is discussed in Appendix C, with a summary of the results contained in Table V. In general, it would appear that substantial variations in post cure time do not drastically alter either the stiffness or strength parameters. This is quite useful from a manufacturing viewpoint since over-curing of the material does not appear to be degrading. This of course would not hold true when one imposes too short a cure time. Other fabrication parameters such as cool-down rate should also be investigated to determine the tolerance limits in terms of their effect on mechanical properties.

5. STRENGTH TESTS ON LAMINATED TUBES

An extensive experimental investigation was undertaken to evaluate the strength of laminated 4 ply tubes having a symmetric

configuration $(-\theta, +\theta, +\theta, -\theta)$ with respect to the mid-plane. Two different load conditions were employed, internal pressure and combined loading of internal pressure plus torsion. The major purpose of both series of tests was to obtain failure data as a function of fibre orientation to compare with predicted values based on the tensor polynomial strength criterion which is discussed in Section 6.

5.1 BIAXIAL STRENGTH TESTS OF $\pm\theta$ LAMINATED TUBES

In the biaxial strength tests used to obtain the complex failure strengths, the tubes with the orientations listed below were loaded to failure by internal pressure. A total of fifteen four ply tubes were tested - three each of the following fibre orientations (see Table VII);

$0^\circ, 0^\circ, 0^\circ, 0^\circ$; $-30^\circ, 30^\circ, 30^\circ, -30^\circ$; $-45^\circ, 45^\circ, 45^\circ, -45^\circ$;
$-60^\circ, 60^\circ, 60^\circ, -60^\circ$; $90^\circ, 90^\circ, 90^\circ, 90^\circ$.

The same air operated hydraulic oil pump that was used in the F_{12} tests was also used in this set of tests (see Fig. 31). The tube's internal pressure was again monitored by a pressure transducer and its output was plotted on an X-Y recorder to obtain an accurate determination of the failure pressure.

Fracture was evident by a "weeping" through the walls of the tube in which small droplets of oil appeared on the surface of the tube indicating that the matrix had failed. In the three tubes other than the circumferential and longitudinal wraps, this "weeping" was not localized at all, but rather, it occurred at many places around the circumference of the tube at the same time. The

internal pressure started to drop and could not be maintained even with an increased flow rate when the "weeping" started. Fracture was more pronounced in the $\theta = 0^{o}$ and $\theta = 90^{o}$ tubes as actual splits appeared in the matrix parallel to the fibre direction. A summary of the experimental results is contained in Table VIII. Later, in Section 6, a comparison between the predicted values and this data will be made.

5.2 STRENGTH OF $\pm \theta$ LAMINATED TUBES SUBJECTED TO INTERNAL PRESSURE AND TORSION

Of the fifteen tubes manufactured for this investigation (see Table IX), twelve were tested to failure under combined torsion and internal pressure loading. Each tube was first subjected to a positive constant torque of 500 in.-lb. and then loaded to failure under internal pressure. The constant torque was applied using a Tinius Olsen universal testing machine modified for torsional loading. Internal pressure was generated using a specially designed hydraulic pump. In each case, the test specimen was completely filled with hydraulic fluid before being mounted into the testing machine, with care taken to bleed all trapped air from the hydraulic lines. Hydraulic pressures were recorded using a Kistler Model 607A quartz pressure transducer with the output plotted on an X-Y recorder.

The test specimens were in all cases judged to have failed when the first signs of hydraulic fluid could be seen on the outer surface of the tube. Accompanying these first signs of hydraulic fluid was an immediate drop in the recorded pressure.

Figure 32 shows a photograph of the test apparatus used to accomplish the required combined loading. A summary of the failure

pressures can be found in Table X. Again, as with the biaxial strength tests, a comparison with predicted values will be done in Section 6.

6. EVALUATION OF THE TENSOR POLYNOMIAL FAILURE CRITERION

The general form of the tensor polynomial failure criterion proposed by Wu is

$$F_i \sigma_i + F_{ij} \sigma_i \sigma_j + F_{ijk} \sigma_i \sigma_j \sigma_k + \cdots\cdots$$

$$= f(\sigma) \begin{cases} < 1 & \text{no failure} \\ = 1 & \text{failure} \\ > 1 & \text{exceeded failure} \end{cases} \tag{24}$$

for i, j, k, = 1, 2, 3, ... 6. F_i, F_{ij} and F_{ijk} are strength tensors of the 2nd, 4th and 6th rank, respectively. If one restricts the analysis to a plane stress state and considers only a cubic formulation as being a reasonable representation of the failure surface, then Eq. (24) reduces to

$$F_1\sigma_1 + F_2\sigma_2 + F_6\sigma_6 + F_{11}\sigma_1^2 + F_{22}\sigma_2^2 + F_{66}\sigma_6^2$$

$$+ 2F_{12}\sigma_1\sigma_2 + 2F_{16}\sigma_1\sigma_6 + 2F_{26}\sigma_2\sigma_6 + 3F_{116}\sigma_1^2\sigma_6$$

$$+ 3F_{126}\sigma_1\sigma_2\sigma_6 + 3F_{112}\sigma_1^2\sigma_2 + 3F_{221}\sigma_1\sigma_2^2 + 3F_{166}\sigma_1\sigma_6^2$$

$$+ 3F_{226}\sigma_2^2\sigma_6 + 3F_{266}\sigma_2\sigma_6^2 + F_{111}\sigma_1^3 + F_{222}\sigma_2^3 + F_{666}\sigma_6^3 = 1 \tag{25}$$

if it is further assumed that the material has some form of symmetry (Ref. 6) such that $F_{ij} = F_{ji}$ for $i \neq j$ and $F_{ijk} = F_{ikj} = F_{jik} = F_{jki} = F_{kij} = F_{kji}$. Since it has also been shown (Ref. 6) that inclusion of the cubic terms F_{iii} (for i = 1, 2 and 6) is redundant, therefore they can be omitted. One other important simplification of Eq. (25) can also result if it can be experimentally determined that a lamina exhibits identical strength for both positive and negative shear. If this condition is satisfied, then all odd-order terms in σ_6 can be set to zero to remove the shear stress "sign" dependence. Hence Eq. (25) reduces to

$$F_1\sigma_1 + F_2\sigma_2 + F_{11}\sigma_1^2 + F_{22}\sigma_2^2 + F_{66}\sigma_6^2$$

$$\pm 2F_{12}\sigma_1\sigma_2 + 3F_{112}\sigma_1^2\sigma_2 + 3F_{221}\sigma_2^2\sigma_1$$

$$+ 3F_{166}\sigma_1\sigma_6^2 + 3F_{266}\sigma_2\sigma_6^2 = 1 \qquad (26)$$

Based on the experimental results (refer to Table I) used to evaluate the strength tensor components (F_i and F_{ij}) described in Section 3, it was found (Fig. 15) that the sign of the shear stress did not significantly affect the failure stress. Thus Eq. (26) is proposed as a failure criterion for the glass-epoxy material being studied. As shown earlier, the following strength tensor components have been determined experimentally;

$$F_1 = -3.076 \times 10^{-3} \ (\text{ksi})^{-1}$$

$$F_2 = 2.344 \times 10^{-1} \ (\text{ksi})^{-1}$$

$$F_6 = 0$$

$$F_{11} = 9.398 \times 10^{-5} \ (\text{ksi})^{-2} \qquad (27)$$

$$F_{22} = 2.270 \times 10^{-2} \ (\text{ksi})^{-2}$$

$$F_{66} = 2.142 \times 10^{-2} \ (\text{ksi})^{-2}$$

$$F_{12} = -6.387 \times 10^{-4} \ (\text{ksi})^{-2}$$

ESTIMATE OF CUBIC INTERACTION TERMS (F_{ijk})

Since no direct experimental measurements were made with the intension of evaluating the cubic interaction terms, it is necessary at this stage to attempt to estimate their values based on the test data obtained.

It can be shown that as $\theta \to 60^{\circ}$, the shear stress term σ_6 becomes very small for internal pressure loading acting alone. However, since the failure pressure increases by over a factor of five compared to the 0° laminate (see Table VIII), then the interaction terms F_{122} and F_{112} must play a significant role for this 60° orientation. On the other hand, since the quadratic form of the failure criterion provides accurate estimates of the strength for

the 0° and 90° configurations, then the cubic terms must have a small influence in these fiber angle ranges. Similarly, one can argue that for the internal pressure + torque tests, the major contributions from the cubic terms should occur in the 40°-70° range. Consequently, to evaluate the four cubic terms F_{112}, F_{122}, F_{166}, F_{266}, it was assumed that the other tensor components were known (i.e., see Eq. (27)) and the cubic polynomial (Eq. 26) was fitted to the test data at 45° and 60° for both the pressure and pressure-torsion cases. This yielded the following values for the cubic terms;

$$F_{112} = 1.6671 \times 10^{-4} \ (\text{ksi})^{-3}$$

$$F_{122} = -1.0575 \times 10^{-3} \ (\text{ksi})^{-3} \qquad (28)$$

$$F_{166} = 3.9985 \times 10^{-4} \ (\text{ksi})^{-3}$$

$$F_{266} = -1.3726 \times 10^{-3} \ (\text{ksi})^{-3}$$

One of the difficulties associated with a cubic formulation is that of ensuring a real positive root corresponding to a failure pressure. This of course depends on the value of the discriminant of the coefficients. For example, consider a general cubic polynomial of the form

$$x^3 + bx^2 + cx + d = 0 \qquad (29)$$

Hence, the discriminant can be defined by

$$\Delta = 18\ bcd - 4\ b^3d + b^2c^2 - 4c^3 - 27\ d^2$$

< 0 one real root, two complex

$= 0$ all roots real, two are equal

> 0 three roots real and unequal

Since the strength coefficients vary from the mean values defined by Eqs. (27) and (28), it is quite possible for Δ to assume any of the three conditions stated above for a particular laminate configuration. This is readily apparent in Fig. 33 where the cubic failure polynomial has been plotted for the $\pm$ 45° laminae. In one case ($\theta = -45^\circ$), two distinct positive roots were obtained differing by a factor of two. Hence, from a physical viewpoint, the lowest value should be taken. On the other hand, for $\theta = +45^\circ$, the polynomial does not cross, but the "error" is very small. In other words, because of coefficient variations, one can consider the maximum as a "double root", thus yielding a failure load.

One other comparison that can be made is between the quadratic and cubic failure predictions. Figure 34 contains both polynomial solutions for the case of symmetric laminated tubes subjected to internal pressure. In this instance, failure of the $+\theta$ and $-\theta$ laminae is assumed to occur at the same load. It is quite evident that the cubic terms are most significant in the fiber angle range of 40° to 70°. Although the quadratic solution provides the best estimates of the failure pressures at 0° and 90°, there is some discrepancy in the cubic solution near 90°. One other feature worth noting is the somewhat "clipped" response of the cubic prediction

near the peak. It might well be that small variations in the cubic parameters could result in a smoother distribution. In addition, no correction was made to the interaction parameter F_{12} due to the presence of the F_{122} and F_{122} terms. Again, this may lead to a different response.

7. COMPARISON OF PREDICTED STRENGTH WITH TEST DATA

This section of the report presents the analysis required to compute both the principal lamina stresses and the failure stresses as a function of ply orientation. The purpose here is to test the validity of the cubic approximation of the tensor polynomial by comparing predicted failure loads with the test data contained in Section 5.

7.1 CALCULATION OF LAMINA PRINCIPAL STRESSES

In order to utilize the failure equation, one is first confronted with the calculation of the lamina principal stresses. Assuming linear elastic behaviour, the lamina inplane stresses corresponding to the structural axes (x,y) can be determined for any ply orientation (θ) from Eqs. (19). This relation further assumes that for a given external load system, the structural strains define the laminae strains. Hence, based on known applied loads, the strain matrix can be determined from

$$\begin{bmatrix} \varepsilon_x \\ \varepsilon_y \\ \gamma_{xy} \end{bmatrix} = \begin{bmatrix} A_{ij} \end{bmatrix}^{-1} \begin{bmatrix} N_x \\ N_y \\ N_{xy} \end{bmatrix} \tag{31}$$

where the load matrix represents forces/unit length and each of the A_{ij} terms is given by

$$A_{ij} = \sum_{k=1}^{n} \bar{Q}_{ij} \, (t_k - t_{k-1}) \tag{32}$$

where k = 1, 2, ... n defines the laminae . For specially orthotropic construction (which exists for a symmetric laminate), then

$$A_{16} = A_{26} = 0 \tag{33}$$

Consequently,

$$[A_{ij}]^{-1} = \begin{bmatrix} \frac{A_{22}}{A} & -\frac{A_{12}}{A} & 0 \\ -\frac{A_{12}}{A} & \frac{A_{11}}{A} & 0 \\ 0 & 0 & \frac{1}{A_{66}} \end{bmatrix} \tag{34}$$

where $A = A_{11} A_{22} - A_{12}^2$. Substituting Eqs. (31) and (34) into Eq. (19) yields the lamina stresses

$$\begin{bmatrix} \sigma_x \\ \sigma_y \\ \tau_{xy} \end{bmatrix}_\theta = \begin{bmatrix} \bar{Q}_{11} & \bar{Q}_{12} & \bar{Q}_{16} \\ \bar{Q}_{21} & \bar{Q}_{22} & \bar{Q}_{26} \\ \bar{Q}_{61} & \bar{Q}_{62} & \bar{Q}_{66} \end{bmatrix} \begin{bmatrix} A_{22}/A & -A_{12}/A & 0 \\ -A_{12}/A & A_{11}/A & 0 \\ 0 & 0 & 1/A_{66} \end{bmatrix} \begin{bmatrix} N_x \\ N_y \\ N_{xy} \end{bmatrix} \tag{35}$$

The final step in the analysis is the transformation from the structural axes (x,y) to the principal lamina axes (1,2) for each ply having an orientation θ with respect to the structural axes. This yields the in-plane principal lamina stresses,

$$\begin{bmatrix}\sigma_1\\ \sigma_2\\ \sigma_6\end{bmatrix}_\theta = [T]\ [\bar{Q}_{ij}]\ [A_{ij}]^{-1}[N] \tag{36}$$

where

$$[T]_{\pm\theta} = \begin{bmatrix} m^2 & n^2 & \pm 2mn \\ n^2 & m^2 & \mp 2mn \\ \mp mn & \pm mn & (m^2 - n^2) \end{bmatrix} \quad \begin{matrix} \text{where } m = \cos\theta \\ n = \sin\theta \end{matrix} \tag{37}$$

7.2 CALCULATION OF FAILURE STRESSES FOR A LAMINATED STRUCTURE

Using the failure criterion defined by Eq. (26) where the sign of the shear stress (σ_6) is assumed not to affect the strength prediction, simultaneous failure of all laminae can occur for certain load conditions (such as internal pressure for example) if the structure is of special orthotropic construction ($A_{16} = A_{26} = 0$). In general however, for arbitrary loading (such as internal pressure and torsion for example), the individual laminae will have different principal stress distributions even if the configuration is specially orthotropic. For these cases, each lamina must be analyzed separately and the failure criterion applied to determine which lamina (or pairs of laminae) will fail first. Subsequently, the stresses must be adjusted due to partial structural failure and the failure condition applied again. This multi-mode type of failure analysis should then provide an estimate of the overall failure loads.

7.3 FAILURE PREDICTIONS FOR THE INTERNAL PRESSURE TESTS ON SYMMETRIC LAMINATED TUBES

Using the mean values of the orthotropic elastic constants listed in Table VI,

$$
\begin{aligned}
E_{11} &= 0.477 \times 10^7 \text{ psi} \\
E_{22} &= 0.121 \times 10^7 \text{ psi} \\
G_{12} &= 0.420 \times 10^6 \text{ psi} \\
\nu_{12} &= 0.336 \\
\nu_{21} &= 0.0855
\end{aligned} \tag{38}
$$

the orthotropic stiffness parameters can be calculated,

$$
\begin{aligned}
Q_{11} &= E_{11}/(1 - \nu_{12}\nu_{21}) = 0.491 \times 10^7 \text{ psi} \\
Q_{22} &= E_{22}/(1 - \nu_{12}\nu_{21}) = 0.125 \times 10^7 \text{ psi} \\
Q_{12} &= Q_{21} = \nu_{21} E_{11}/(1 - \nu_{12}\nu_{21}) = 0.042 \times 10^7 \text{ psi} \\
Q_{16} &= Q_{61} = 0 \\
Q_{66} &= G_{12} = 0.042 \times 10^7 \text{ psi}
\end{aligned} \tag{39}
$$

Hence the general orthotropic stiffness coefficients can be readily determined as a function of θ using Eqs. (20) and (21).

For the case of internal pressure loading with the ends free to expand axially, the generalized load matrix is given by

$$
\begin{bmatrix} N_x \\ N_y \\ N_{xy} \end{bmatrix} \cong pR \begin{bmatrix} 1/2 \\ 1 \\ 0 \end{bmatrix} \tag{40}
$$

Thus, substituting Eq. (40) and the appropriate $\overline{Q}_{ij}$, A_{ij} terms into Eq. (35) yields the lamina in-plane stresses which will take the following form;

$$\begin{bmatrix} \sigma_x \\ \sigma_y \\ \tau_{xy} \end{bmatrix}_\theta = \frac{pR}{t} \begin{bmatrix} 0.1250 \\ 0.2500 \\ \tau_{xy}(\theta) \end{bmatrix} \tag{41}$$

where t = lamina thickness. It is assumed that the laminate is comprised of four equal thickness laminae. Hence the σ_x and σ_y stresses are identical for each ply orientation θ and only the shear stress τ_{xy} varies with θ. The final step in the analysis once $\tau_{xy}(\theta)$ is known is the multiplication by the transformation matrix $[T]_{\pm\theta}$ given by Eq. (37).

Based on this method of analysis, a computer programme was written to determine the lamina principal stresses and solve the cubic equation (26) defining the failure condition (see Appendix D). The appropriate tensor strength components given by Eqs. (27) and (28) were used as the coefficients of Eq. (26). The actual failure pressures are recorded in Table VIII and a graphical comparison with the experimental values is presented in Fig. 35 as a function of ply orientation θ. Although the cubic terms were obtained from solutions of the polynomial matched to the 45^o and 60^o data, the remaining test results are also in reasonable agreement with the predicted response. Figure 36 presents the variation in principal failure stresses with fiber angle. These stresses can then be compared with the linear elastic limit values shown in Figs. 9, 14 and 15. It can be seen that the shear stress (σ_6) is only slightly in the nonlinear range and thus the assumption of linear elastic behaviour is acceptable. Moreover, it would appear that the failure mode

throughout the whole range of configurations was defined by a matrix tensile fracture.

7.4 FAILURE PREDICTIONS FOR THE COMBINED LOADING TESTS (INTERNAL PRESSURE AND TORSION) ON SYMMETRIC LAMINATED TUBES

Although the tube configurations studied here are similar to those described previously (4 ply symmetric laminates), the load condition has been complicated by the addition of a constant torque (= 500 in-lbs) to the internal pressure loads. For pure torsion (T) and constant shear stress across the laminate thickness $\bar{t}$ (= 4t), then the following equation holds,

$$T = 2 N_{xy} A \tag{42}$$

where A = enclosed area

$$N_{xy} = \tau \bar{t}$$

$$\therefore \quad N_{xy} = \frac{T}{2\pi R^2} \tag{43}$$

$$= 0.0765 \text{ kips/in}$$

Thus the generalized load matrix for this case is given by

$$\begin{bmatrix} N_x \\ N_y \\ N_{xy} \end{bmatrix} = \begin{bmatrix} pR/2 \\ pR \\ .0765 \end{bmatrix} \tag{44}$$

It can readily be shown that with the addition of the torque term, the principal stresses in the $+\theta$ and $-\theta$ laminae differ significantly. Consequently, a failure prediction must be made for both sets of laminae at each fiber orientation to determine which laminae will fail first (see computer programme in Appendix D). The results of these calculations are shown in Fig. 37 where both lower bound and median response curves have been indicated. Of some interest is the fact that initial failure conditions can occur in different laminae, depending on the fiber orientation. The lower bound curve can be used as a conservative estimate of the overall failure load if one assumes that once a set of laminae have fractured, the remaining structure cannot withstand the resulting load and thus coincident failure results. However, one can expect that some residual strength remains even after initial matrix failure in the first set of laminae and coupled with the other laminae, the ultimate structural failure stress should be somewhat higher than the lower bound predictions. Consequently, the median response curve can be used as a first approximation for comparison with the experimental failure loads. This was done in Fig. 38 where once again, general agreement was obtained.

Based on this failure analysis, the predicted principal stresses are shown for both $\pm\theta$ laminae in Fig. 39. Again it can be seen that the assumption of linear elastic behaviour was reasonable and the failure mode was one of matrix tensile fracture.

8. CONCLUSIONS

High quality laminated tubular specimens have been manu-

factured using a belt wrapper apparatus and subjected to the following load conditions: uniaxial tension and compression, pure torsion, internal pressure and combined torsion and internal pressure. Failure loads were obtained to evaluate the principal tensor strength parameters (F_i, F_{ii}; $i = 1,2,6$) and the quadratic interaction term F_{12}. It was then shown that a quadratic failure formulation was too conservative and a cubic polynomial can in fact be used to predict with reasonable confidence the failure loads for arbitrary fiber orientations. This was done on the basis of estimating four cubic parameters (F_{122}, F_{122}, F_{166}, F_{266}) using test data at $\theta = 45^{\circ}$ and 60°. Consequently, it is highly desirable to not only obtain more test data for comparison purposes but refine the estimates of these cubic terms. In addition, various failure modes of the tubes were considered. The case of internal pressure loading of symmetric laminated tubes resulted in simultaneous failure of all laminae. However, the addition of torsion to the loading indicated that failure of some laminae should precede overall structural failure.

Experiments were also performed to assess the effects of ambient temperature and post cure time on the orthotropic properties as well as on the failure parameters. Although only limited data were obtained, it was demonstrated how these effects can be interpreted and some results were presented for two strength parameters.

REFERENCES

1. Strength Theories of Failure for Anisotropic Materials by B. E. Kaminski and R. B. Lantz, Composite Materials: Testing and Design, ASTM STP 460, 1969.

2. A Survey of Failure Theories of Isotropic and Anisotropic Materials by R. S. Sandhu, AFFDL Tech. Rept. AFFDL-TR-72-71,

3. A Brief Survey of Empirical Multiaxial Strength for Composites by G. P. Sendeckyi, Composite Materials: Testing and Design ASTM STP 497, 1972.

4. Phenomenological Anisotropic Failure Criterion by E. M. Wu, Treatise on Composite Materials, Broutman, Krock and Sendeckyj, Eds., Academic Press, 1973.

5. Failure Criteria to Fracture Mode Analysis of Composite Laminates by E. M. Wu, 39th Meeting, AGARD Structures & Materials Panel (Failure Modes of Composite Materials), Munich, Germany, October 1974.

6. Laminate Strength - A Direct Characterization Procedure by E. M. Wu and J. K. Scheublein, Composite Materials: Testing and Design (Third Conference), ASTM STP 546, June 1974.

7. A General Theory of Strength for Anisotropic Materials by S. W. Tsai and E. M. Wu, J. Composite Materials, Vol. 5, Jan. 1971.

8. Optimal Experimental Measurements of Anisotropic Failure Tensors by E. M. Wu, J. Composite Materials, Vol. 6, Oct. 1972.

9. Ultimate Strength Analysis of Symmetric Laminates by R. S. Sandhu, AFFDL-TR-73-137, Feb. 1974.

10. Anisotropic Strength of Composites by V. D. Azzi and S. W. Tsai, Experimental Mechanics J., Sept. 1965.

11. Strength of Laminated Composite Materials by S. W. Tsai and V. D. Azzi, AIAA J., Vol. 4, No. 2, 1966.

12. On the Off-Axis Strength Test for Anisotropic Materials by R. B. Pipes and B. W. Cole, J. Composite Materials, Vol. 7, April 1973.

13. Characterizing Strength of Unidirectional Composites by O. Ishai and R. E. Lavengood, Comp. Mat: Testing and Design, ASTM STP460, 1969.

14. Influence of the Free Edge Upon the Strength of Angle-Ply Laminates by R. B. Pipes, B. E. Kaminski and N. J. Pagano, Test Methods for High Modulus Fibers and Composites ASTM STP 521, 1973.

15. Geometric Design of Composite Cylindrical Characterization Specimens by N. J. Pagano and J. M. Whitney, J. Composite Materials, Vol. 4, July 1970.

16. Design and Fabrication of Tubular Specimens for Composite Characterization by J. M. Whitney, N. J. Pagano and R. B. Pipes, Comp. Materials: Testing and Design, ASTM STP497, 1972.

17. Effect of End Attachment on the Strength of Fiber-Reinforced Composite Cylinders by J. M. Whitney, G. C. Grimes and P. C. Francis, J. Experimental Mechanics, May 1973.

18. Some Important Aspects in Testing High-Modulus Fiber Composite Tubes in Axial Tension by T. L. Sullivan and C. C. Chamis, Test Methods for High Modulus Fibers and Composites, ASTM STP 521, 1973.

19. Static Testing Techniques for Filament-Wound Composite Materials by C. W. Bert, Composites, Jan. 1974.

20. Laminate Tubular Specimens Subjected to Biaxial Stress States (Glass-Epoxy) by R. S. Sandhu, J. B. Monfort, F. E. Hussong et al., AFFDL-TR-73-7, Vol. 1, Feb. 1973.

21. Computer-Aided Mechanical Testing of Composites by E. M. Wu and K. L. Jerina, Materials Research and Standards, Vol. 12, Feb. 1972.

22. Fracture Strength of Helical-Wound Composite Cylinders by M. Vemura and K. Yamawaki.

23. An Experimental Study to Determine Failure Envelope of Composite Materials with Tubular Specimens under Combined Loads and Comparison Between Several Classical Criteria by V. Hotter, H. Schelling and H. Krauss.

24. Stresses in Shells by W. Flügge, Springer-Verlag Pub., Berlin, 1962.

25. Stability of Heterogeneous Aeolotropic Cylindrical Shells Under Combined Loading by S. Cheng and B. P. C. Ho, AIAA J., Vol. 1, No. 4, 1963.

26. Buckling of Fiber-Reinforced Circular Cylinders Under Axial Compression by R. C. Tennyson, D. B. Muggeridge and K. H. Chan, AFFDL-TR-72-102, Aug. 1972.

TABLE I

TENSILE, COMPRESSIVE, AND SHEAR FRACTURE DATA

SPECIMEN NO.		ULTIMATE STRENGTH (P.S.I.)
Longitudinal Tensile Strength Tests		
2a	0°	131,158
2b	0°	111,004
3a	0°	119,735
3b	0°	121,336
Mean Value		120,808
Longitudinal Compressive Strength Tests		
7a	0°	83,784
7b	0°	89,491
8a	0°	86,013
9a	0°	86,885
9b	0°	91,629
18a	0°	88,676
19a	0°	87,091
Mean Value		88,081
Transverse Tensile Strength Tests		
1a	90° (I)	2,980
1a	90° (II)	3,520
3a	90°	3,204
5a	90° (I)	3,150
5a	90° (II)	3,338
6b	90°	3,418
8b	90°	3,109
Mean Value		3,246

TABLE I (cont'd.)

TENSILE, COMPRESSIVE AND SHEAR FRACTURE DATA

SPECIMEN NO.		ULTIMATE STRENGTH (P.S.I.)
Transverse Compressive Strength Tests		
2a	90°	13,158
3b	90°	14,035
4b	90°	14,246
7b	90°	12,218
8c	90°	13,819
16b	90°	13,431
17a	90°	14,114
Mean Value		13,574
Shear Strength Tests		
2b	90°	6,737
4a	90°(I)	6,777
4a	90°(II)	6,851
5b	90°	6,864
6a	90°	6,765
7a	90°	6,497
17b	90°	7,336
Mean Value		6,832

TABLE II

STRENGTH TENSORS

F_1	$= -3.076 \times 10^{-3}$	K.S.I.$^{-1}$
F_2	$= 2.344 \times 10^{-1}$	K.S.I.$^{-1}$
F_6	$= 0.0$	K.S.I.$^{-1}$
F_{11}	$= 9.398 \times 10^{-5}$	K.S.I.$^{-2}$
F_{22}	$= 2.270 \times 10^{-2}$	K.S.I.$^{-2}$
F_{66}	$= 2.142 \times 10^{-2}$	K.S.I.$^{-2}$
$\lvert F_{12} \rvert$	$\leq 1.460 \times 10^{-3}$	K.S.I.$^{-2}$
$\lvert F_{16} \rvert$	$\leq 1.419 \times 10^{-3}$	K.S.I.$^{-2}$
$\lvert F_{26} \rvert$	$\leq 2.205 \times 10^{-2}$	K.S.I.$^{-2}$

TABLE III

INTERACTION STRENGTH TENSORS

TENSOR	OPTIMAL STRESS STATE	RANGE OF OPTIMAL B
$F_{12} \geqslant -0.5$	$\sigma_1 > 0,\ \sigma_2 < 0$	$-14.4 \geqslant \sigma_1/\sigma_2 \geqslant -15.6$
$F_{12} \leqslant 0.5$	$\sigma_1 < 0,\ \sigma_2 < 0$	$15.5 \geqslant \sigma_1/\sigma_2 \geqslant 13.3$
$F_{16} \geqslant 0$	$\sigma_1 > 0,\ \sigma_6 < 0$	$-15.65 \geqslant \sigma_1/\sigma_6 \geqslant -16.35$
$F_{16} \leqslant 0$	$\sigma_1 > 0,\ \sigma_6 > 0$	$16.35 \geqslant \sigma_1/\sigma_6 \geqslant 15.65$
$F_{26} \geqslant 0$	$\sigma_2 < 0,\ \sigma_6 > 0$	$-0.89 \geqslant \sigma_6/\sigma_2 \geqslant -1.0$
$F_{26} \leqslant 0$	$\sigma_2 < 0,\ \sigma_6 < 0$	$1.0 \geqslant \sigma_6/\sigma_2 \geqslant -0.89$

F_{12} TENSOR TESTS

SPECIMEN NUMBER	PREDICTED 1/2	MEASURED 1/2	ULTIMATE STRESS (K.S.I.)	COMPUTED F_{12} (K.S.I.$^{-2}$)	
10a 90°	-8.00	-8.69	$\sigma_1 = 108.8$ $\sigma_2 = -12.88$	1.869×10^{-4}	
10b 90°	-14.50	-15.49	$\sigma_1 = 103.4$ $\sigma_2 = -6.392$	-6.690×10^{-4}	*
11a 90°	-13.80	-13.33	$\sigma_1 = 100.0$ $\sigma_2 = -6.911$	-6.539×10^{-4}	*
13b 90°	-13.90	-15.13	$\sigma_1 = 105.4$ $\sigma_2 = -6.669$	-5.933×10^{-4}	*

* Mean Value of $F_{12} = -6.387 \times 10^{-4}$ K.S.I.$^{-2}$

TABLE IV ELASTIC CONSTANTS AND TRANSVERSE BURST STRENGTH FOR SCOTCHPLY (1002) TUBES AT VARIOUS TEST TEMPERATURES

TEST TEMPERATURE	TUBE DESIGNATION	E_{11}/β (psi)	E_{22}/β (psi)	E_{11} (psi)	E_{22} (psi)	ν_{12}	ν_{21}	$\sigma_2$burst (psi) (Mode 1)
- 80°F	24b 90°	6.23×10^6	1.59×10^6	5.86×10^6	1.50×10^6	0.482	0.123	4346
- 75°F	23c 90°							4399
- 45°F	23b 90°	6.43×10^6	1.76×10^6	6.32×10^6	1.73×10^6	0.250	0.068	4186
- 20°F	23a 90°	5.76×10^6	1.39×10^6	5.04×10^6	1.22×10^6	0.721	0.173	4110
- 20°F	22b 90°	5.99×10^6	1.51×10^6	5.80×10^6	1.46×10^6	0.356	0.089	4200
- 20°F	22c 90°							4224
70°F	12c 90°							3411
70°F	13c 90°	5.86×10^6	1.32×10^6	5.61×10^6	1.26×10^6	0.437	0.098	3369
70°F	11c 90°	6.01×10^6	1.29×10^6	5.66×10^6	1.22×10^6	0.520	0.112	3545
158°F	19b 90°	6.40×10^6	1.18×10^6	6.11×10^6	1.13×10^6	0.495	0.092	3216
158°F	16a 90°	6.35×10^6	1.15×10^6	6.07×10^6	1.10×10^6	0.495	0.090	2876
200°F	19a 90°	6.08×10^6	0.98×10^6	5.78×10^6	0.93×10^6	0.552	0.089	2300
200°F	14a 90°							2450
250°F	14b 90°	6.30×10^6	0.57×10^6	5.87×10^6	0.53×10^6	0.875	0.079	1405
250°F	14c 90°	6.08×10^6	0.66×10^6	5.91×10^6	0.65×10^6	0.511	0.056	1280
250°F	15a 90°							1325

TABLE V ELASTIC CONSTANTS AND TRANSVERSE BURST STRENGTH FOR SCOTCHPLY (1002) TUBES HAVING DIFFERENT LENGTHS OF POST CURE

LENGTH OF POST CURE	TUBE DESIG-NATION	E_{11}/β (psi)	E_{22}/β (psi)	E_{11} (psi)	E_{22} (psi)	ν_{12}	ν_{21}	σ_2 (psi) (Mode 1)
0 HRS.	18a 90°	5.896×10^6	1.307×10^6	5.591×10^6	1.239×10^6	0.4832	0.1071	3058
0 HRS.	18b 90°	6.049×10^6	1.417×10^6	5.670×10^6	1.328×10^6	0.5176	0.1212	2948
0 HRS.	18c 90°							3329
7 HRS.	21a 90°							3523
7 HRS.	21b 90°	6.054×10^6	1.329×10^6	5.599×10^6	1.229×10^6	0.5852	0.1285	3490
7 HRS.	21c 90°	5.855×10^6	1.260×10^6	5.543×10^6	1.193×10^6	0.4974	0.1071	3279
16.75 HRS.	11c 90°	6.013×10^6	1.297×10^6	5.663×10^6	1.222×10^6	0.5199	0.1122	3545
16.75 HRS.	12c 90°							3411
16.75 HRS.	13c 90°	5.865×10^6	1.319×10^6	5.612×10^6	1.262×10^6	0.4374	0.0984	3369
24 HRS.	20a 90°	5.978×10^6	1.283×10^6	5.743×10^6	1.233×10^6	0.4280	0.0982	3653
24 HRS.	20b 90°	5.908×10^6	1.273×10^6	5.426×10^6	1.169×10^6	0.6152	0.1326	3972
24 HRS.	20c 90°							3903

TABLE VI

MATERIAL PROPERTIES

SPECIMEN NUMBER	E_{11} (10^6 P.S.I.)	E_{22} (10^6 P.S.I.)	G_{12} (10^6 P.S.I.)	ν_{12}	ν_{21}
Calculated Directly From Stress-Strain Curves					
2b 0°	4.74				
3b 0°	4.79				
Mean Value	4.765				
3a 90°		1.245			
5a 90°(I)		1.157			
5a 90°(II)		1.284			
6b 90°		1.157			
Mean Value		1.211			
2b 90°			0.431		
4a 90°(I)			0.408		
7a 90°			0.420		
Mean Value			0.420		
Calculated Using the Characterization Computer Program*					
1c 0°	4.945	1.170	0.4888	0.3043	0.0720
6b 0°	4.676	1.226	0.4645	0.2827	0.07412
2b ∓ 30°	5.107	1.426	0.4574	0.2676	0.07473
7b ∓ 30°	5.447	1.174	0.5216	0.4165	0.08978
4b ∓ 60°	5.081	1.645	0.4082	0.2230	0.07221
9b ∓ 60°	5.125	1.420	0.4733	0.2377	0.0659
5c 90°	4.669	1.248	0.4215	0.4074	0.1089
10b 90°	4.876	1.416	0.4844	0.4313	0.1252
Mean Values	4.991	1.341	0.465	0.3213	0.08536

* 4 ply cylinders (−, +, +, −)

TABLE VI (cont'd)

MATERIAL PROPERTIES

SPECIMEN NUMBER	E_{11} (10^6 P.S.I.)	E_{22} (10^6 P.S.I.)	G_{12} (10^6 P.S.I.)	ν_{12}	ν_{21}
Manufacturer's Values					
	5.7	1.4			

TABLE VII

GEOMETRY OF TUBES USED IN BIAXIAL STRENGTH TESTS

TUBE DESIGNATION	R (IN)	$\bar{t}$ (IN)
6a 0	1.017	.0400
6b 0	1.017	.0406
6c 0	1.017	.0407
7a $\overline{+}$ 30°	1.018	.0397
7b $\overline{+}$ 30°	1.018	.0408
7c $\overline{+}$ 30	1.018	.0405
8a $\overline{+}$ 45	1.021	.0406
8b $\overline{+}$ 45	1.021	.0408
8c $\overline{+}$ 45	1.020	.0397
9a $\overline{+}$ 60°	1.021	.0401
9b $\overline{+}$ 60°	1.021	.0410
9c $\overline{+}$ 60°	1.021	.0404
10a 90°	1.021	.0410
10b 90°	1.021	.0400
10c 90°	1.021	.0404

TABLE VIII

BIAXIAL STRENGTH TEST DATA*

SPECIMEN NUMBER	MEASURED BURST PRESSURE (P.S.I.)
6a 0°	131.0
6b 0°	135.0
6c 0°	108.0
Mean Value	124.7
7a $\mp 30^{\circ}$	241.0
7b $\mp 30^{\circ}$	260.0
7c $\mp 30^{\circ}$	240.0
Mean Value	247.0
8a $\mp 45^{\circ}$	557.5
8b $\mp 45^{\circ}$	582.0
8c $\mp 45^{\circ}$	630.0
Mean Value	589.8
9a $\mp 60^{\circ}$	675.0
9b $\mp 60^{\circ}$	643.0
9c $\mp 60^{\circ}$	665.0
Mean Value	661.0
10a 90°	250.0
10b 90°	242.0
10c 90°	289.0
Mean Value	260.3

*4 Ply Cylinders ($-\theta$, $+\theta$, $+\theta$, $-\theta$)

TABLE IX

GEOMETRY OF LAMINATED TUBES FOR COMBINED LOADING TESTS

TUBE DESIGNATION	θ 1	2	3	4 *	L in.	R in.	$\bar{t}$ in.
1a 0°	0°	0°	0°	0°	9.5	1.016	0.0399
1b 0°	0°	0°	0°	0°	9.5	1.016	0.0404
1c 0°	0°	0°	0°	0°	9.5	1.016	0.0401
2a $\bar{+}$ 30°	-30°	30°	30°	-30°	9.5	1.019	0.0408
2b $\bar{+}$ 30°	-30°	30°	30°	-30°	9.5	1.020	0.0410
2c $\bar{+}$ 30°	-30°	30°	30°	-30°	9.5	1.019	0.0406
3a $\bar{+}$ 45°	-45°	45°	45°	-45°	9.5	1.022	0.0409
3b $\bar{+}$ 45°	-45°	45°	45°	-45°	9.5	1.022	0.0410
3c $\bar{+}$ 45°	-45°	45°	45°	-45°	9.5	1.022	0.0404
4a $\bar{+}$ 60°	-60°	60°	60°	-60°	9.5	1.022	0.0405
4b $\bar{+}$ 60°	-60°	60°	60°	-60°	9.5	1.022	0.0414
4c $\bar{+}$ 60°	-60	60°	60°	-60°	9.5	1.022	0.0410
5a 90°	90°	90°	90°	90°	9.5	1.022	0.0410
5b 90°	90°	90°	90°	90°	9.5	1.022	0.0417
5c 90°	90°	90°	90°	90°	9.5	1.021	0.0410

*1st lamina is innermost lamina

TABLE X

FAILURE PRESSURES UNDER COMBINED LOADING
OF CONSTANT TORQUE AND INCREASING INTERNAL PRESSURE*

TUBE DESIGNATION	FAILURE PRESSURE (p.s.i.)
1a 0°	112
1b 0°	145
2b $\mp 30^{\circ}$	245
2c $\mp 30^{\circ}$	276
3a $\mp 45^{\circ}$	623
3b $\mp 45^{\circ}$	597
4a $\mp 60^{\circ}$	675
4c $\mp 60^{\circ}$	597
5a 90°	276
5b 90°	256
5c 90°	273

*4 ply cylinders (-, +, +, -)

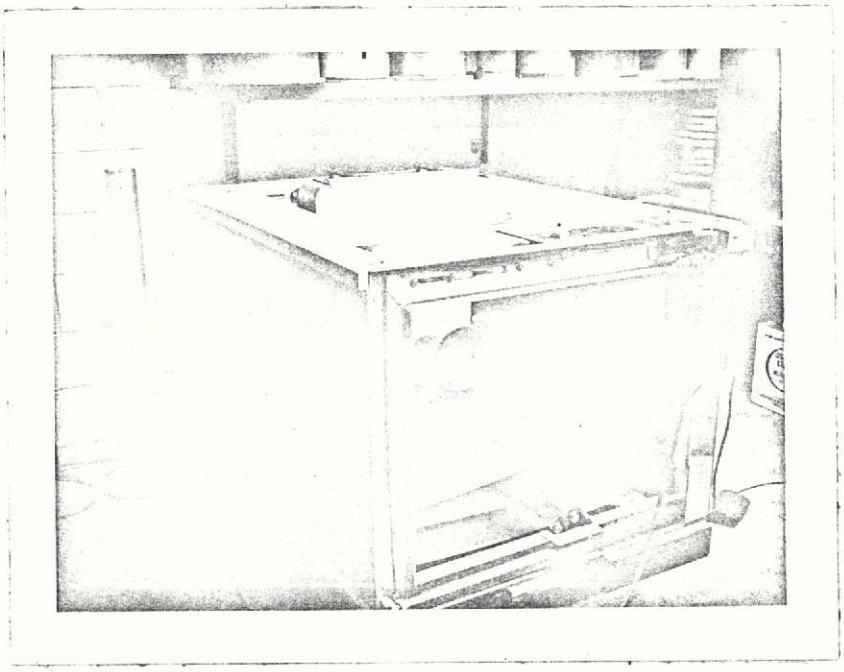

FIG. 1 BELT WRAPPING APPARATUS

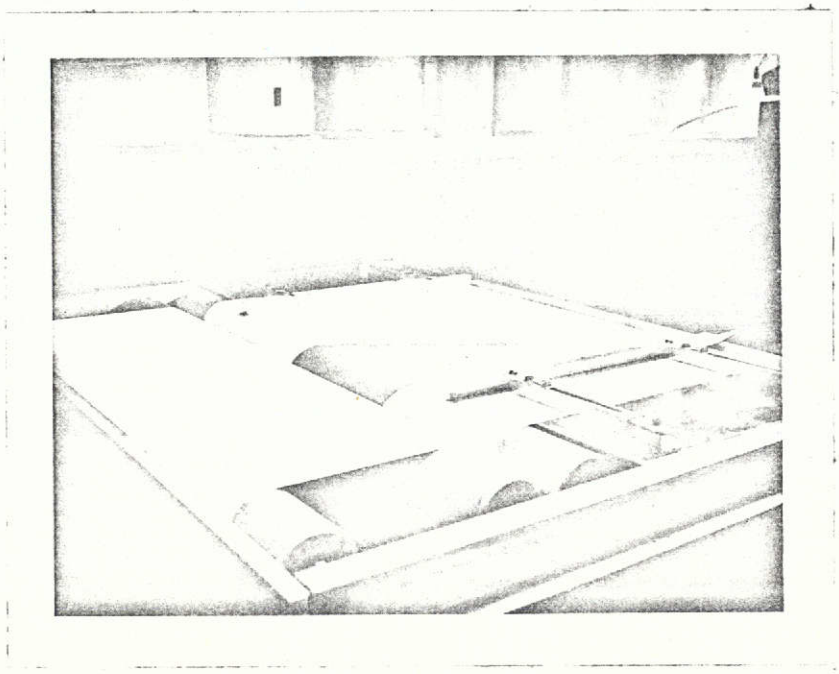

FIG. 2 SPECIMEN FABRICATION

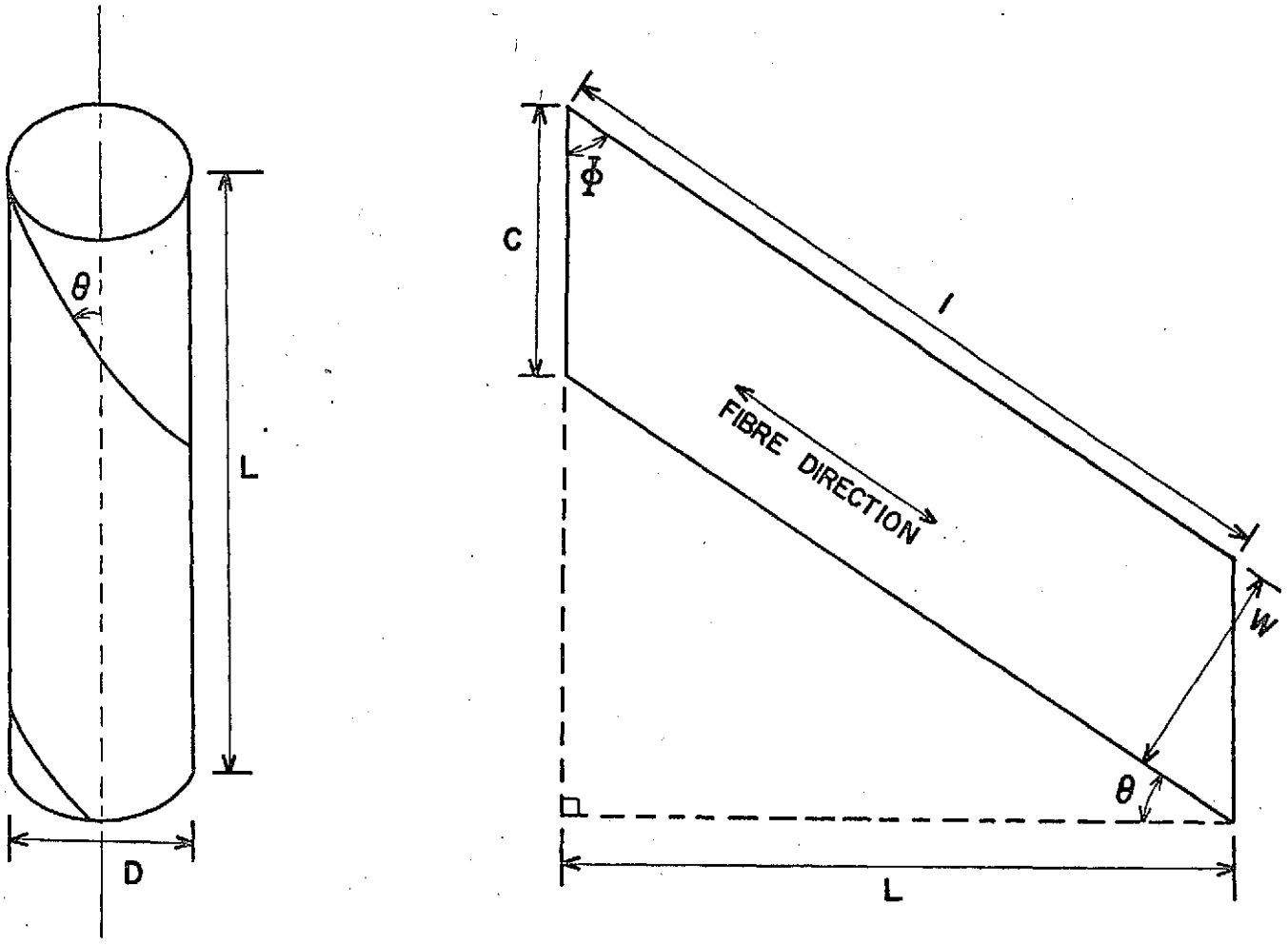

FIG. 3 LAMINA GEOMETRY

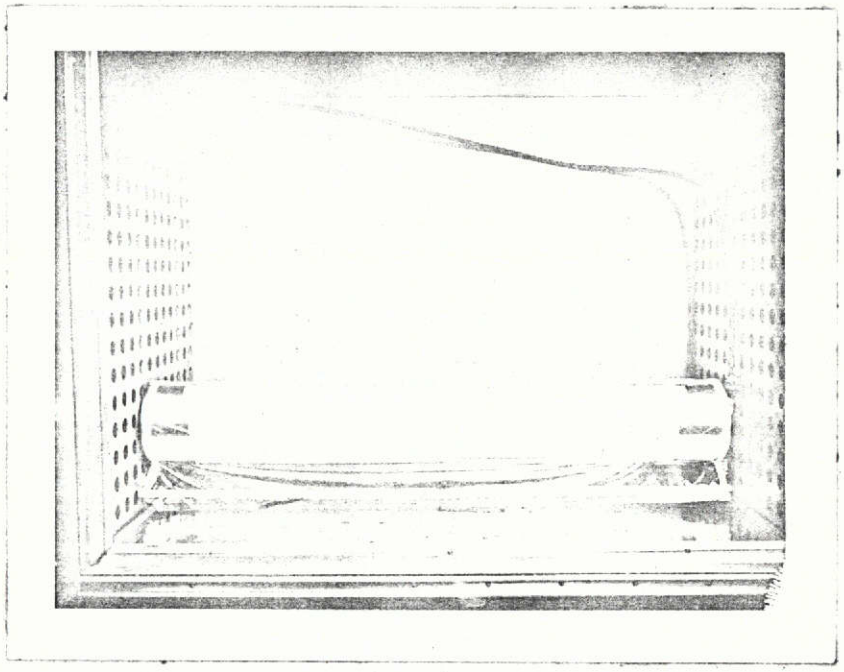

FIG. 4 SPECIMEN IN VACUUM BAG READY FOR CURING

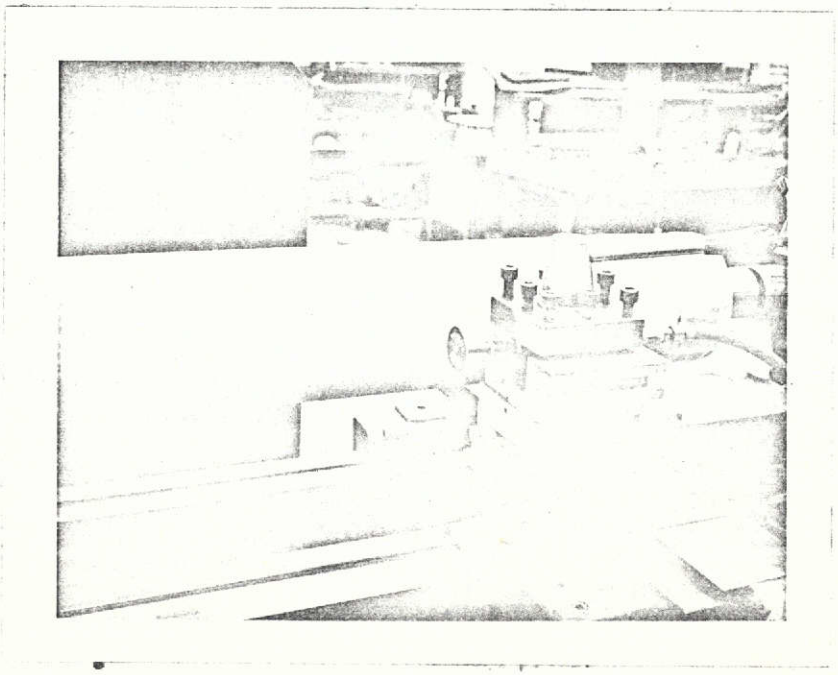

FIG. 5 APPARATUS FOR CUTTING SPECIMENS

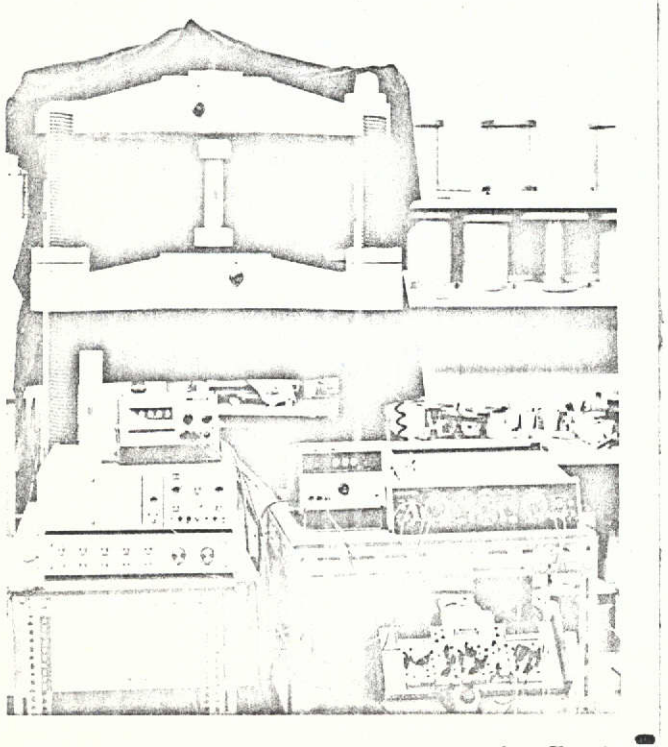

FIG. 6 LONGITUDINAL TENSILE STRENGTH TEST SET-UP

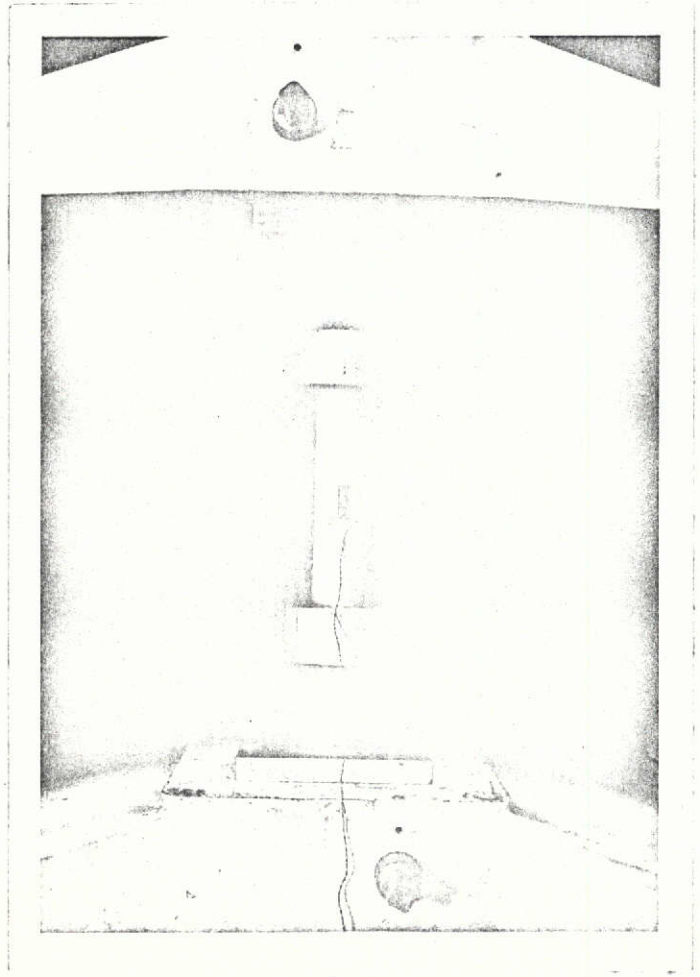

FIG. 7 ONSET OF FAILURE

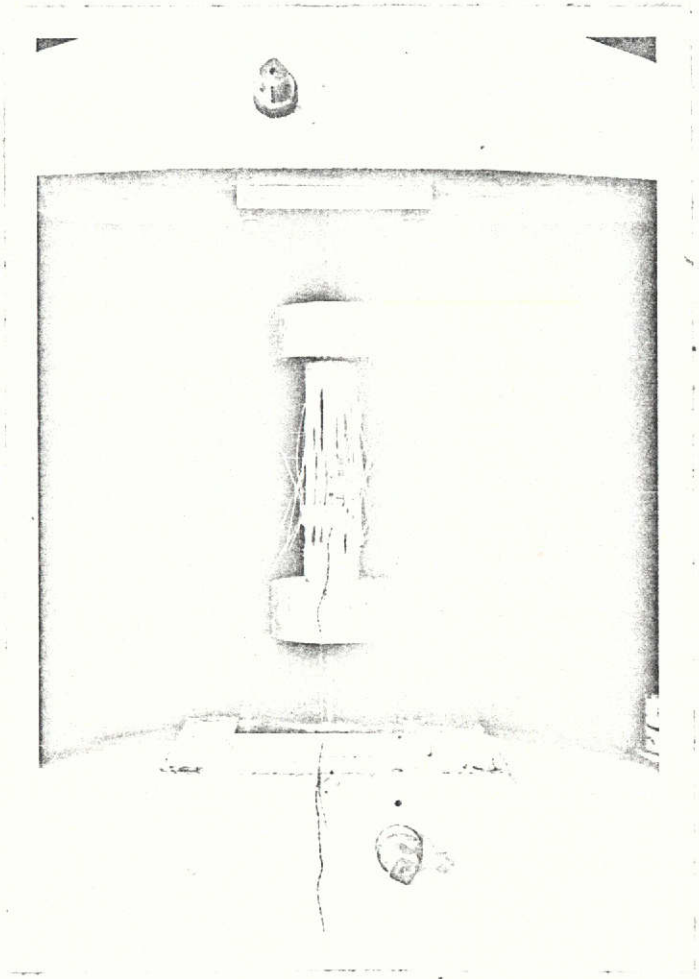

FIG. 8 COMPLETE FAILURE

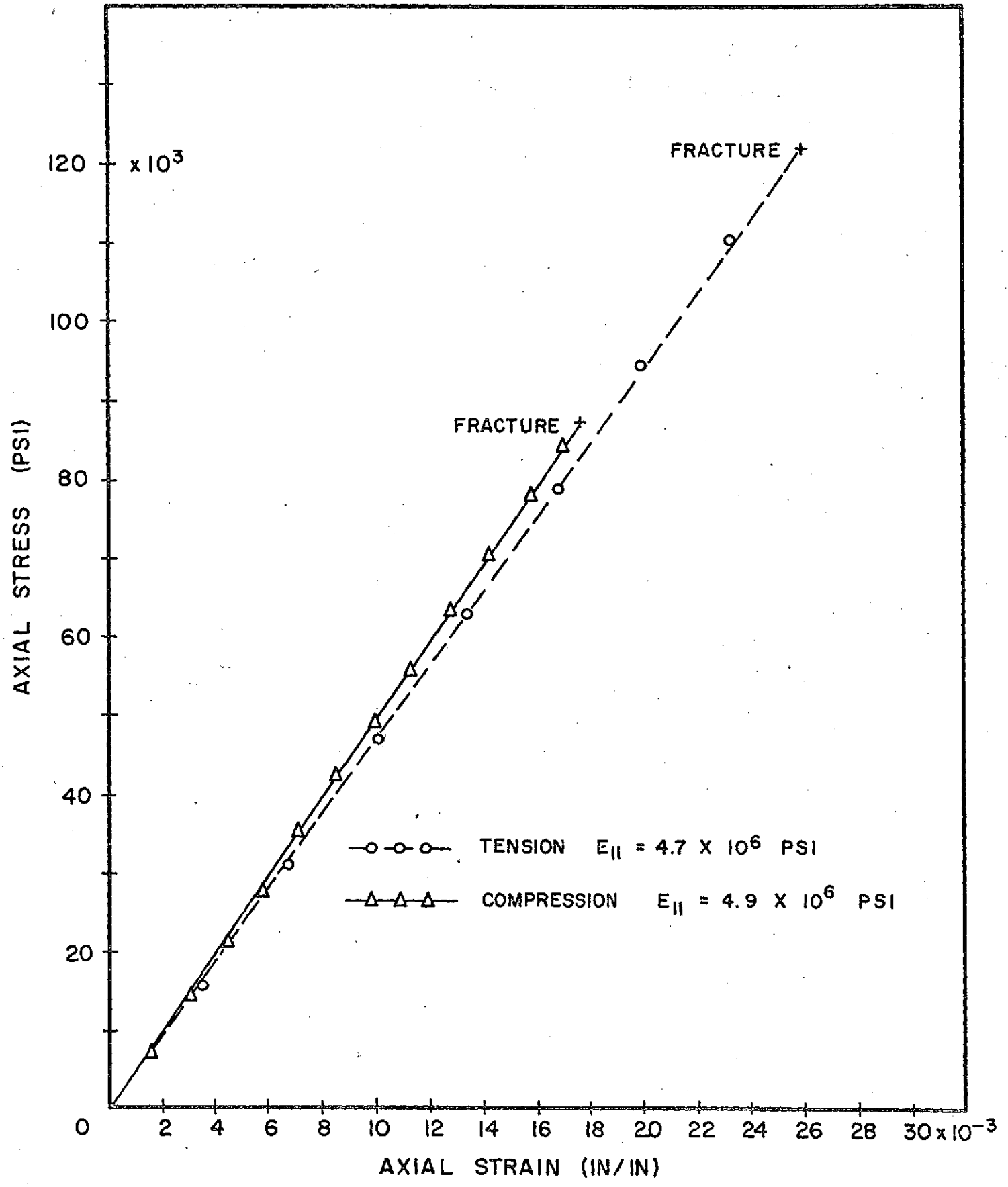

FIG. 9 STRESS – STRAIN CURVES FOR SCOTCHPLY (1002) LOADED PARALLEL TO FIBER DIRECTION

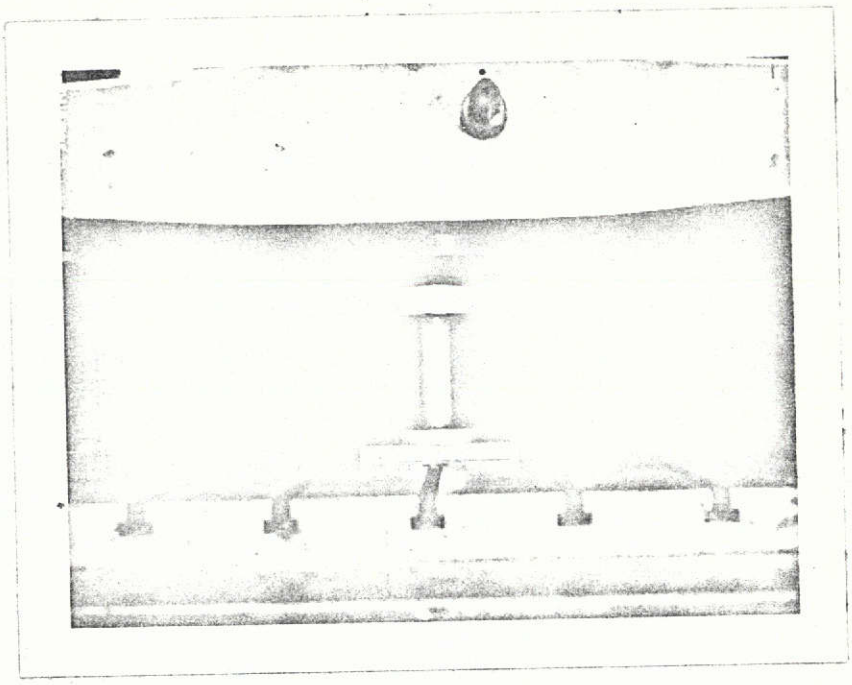

FIG. 10 LONGITUDINAL COMPRESSIVE STRENGTH TEST SPECIMEN

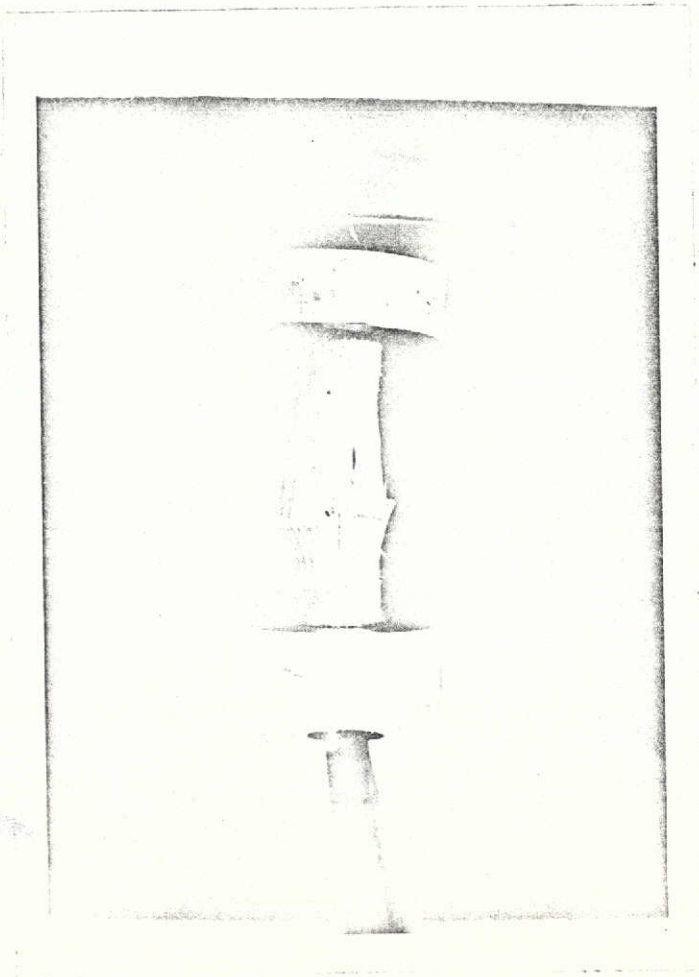

FIG. 11 AFTER FAILURE

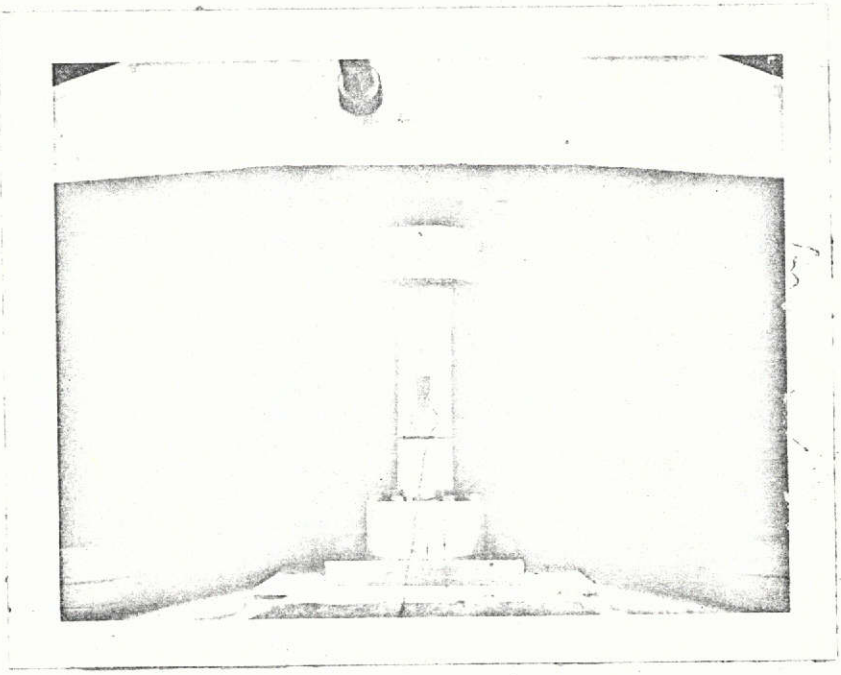

FIG. 12 TRANSVERSE TENSILE FAILURE

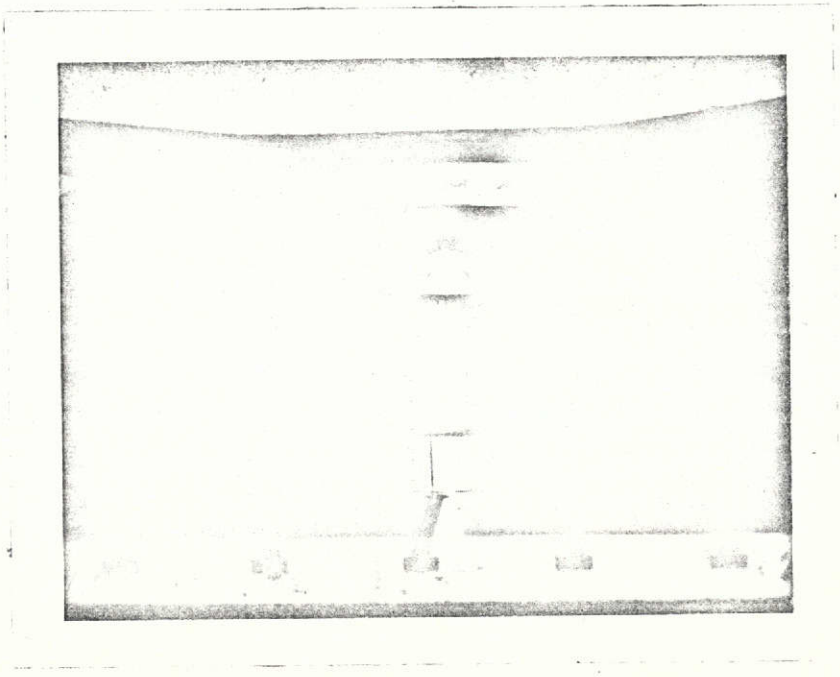

FIG. 13 TRANSVERSE COMPRESSIVE FAILURE

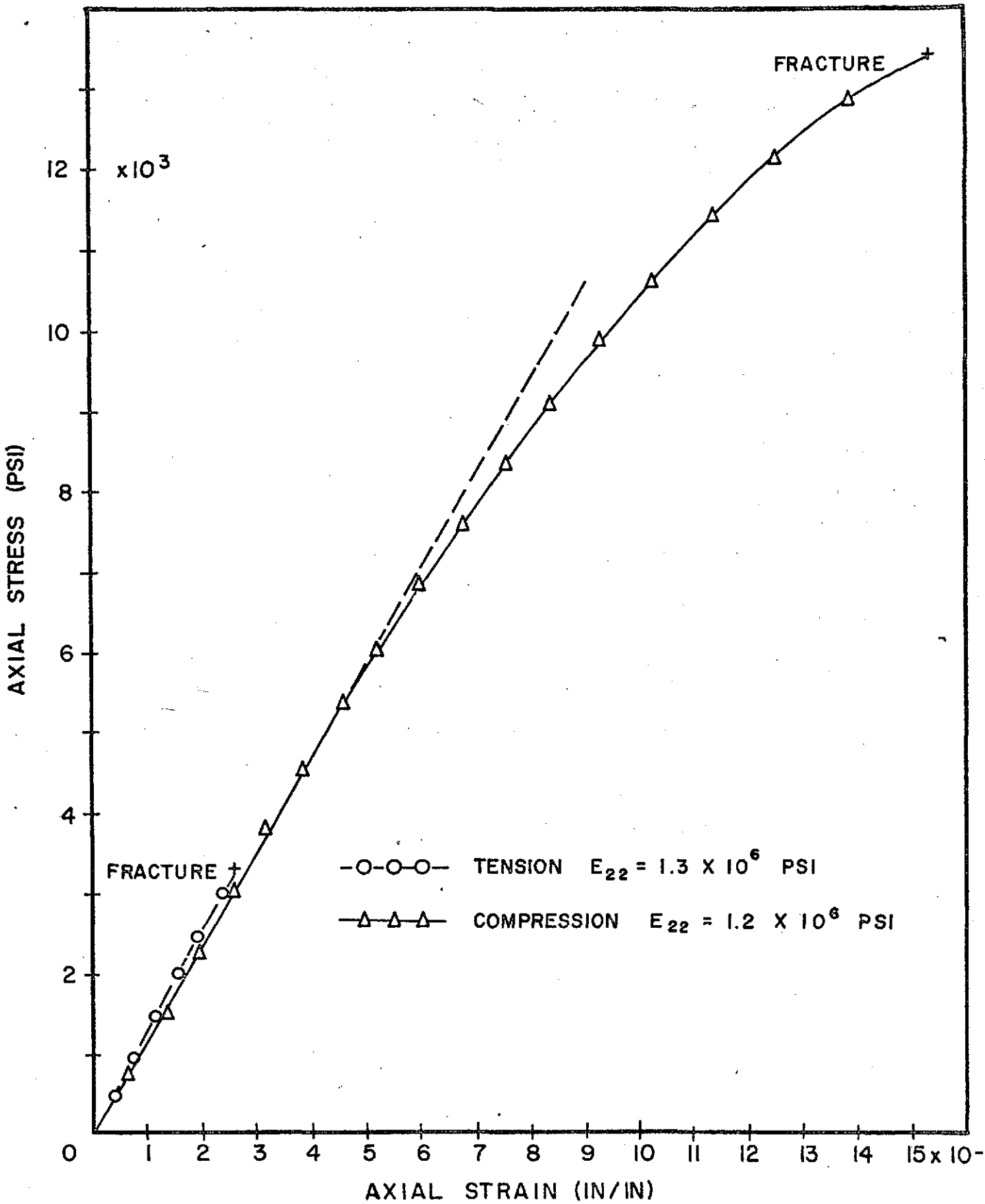

FIG. 14 STRESS-STRAIN CURVES FOR SCOTCHPLY (1002) LOADED PERPENDICULAR TO FIBER DIRECTION

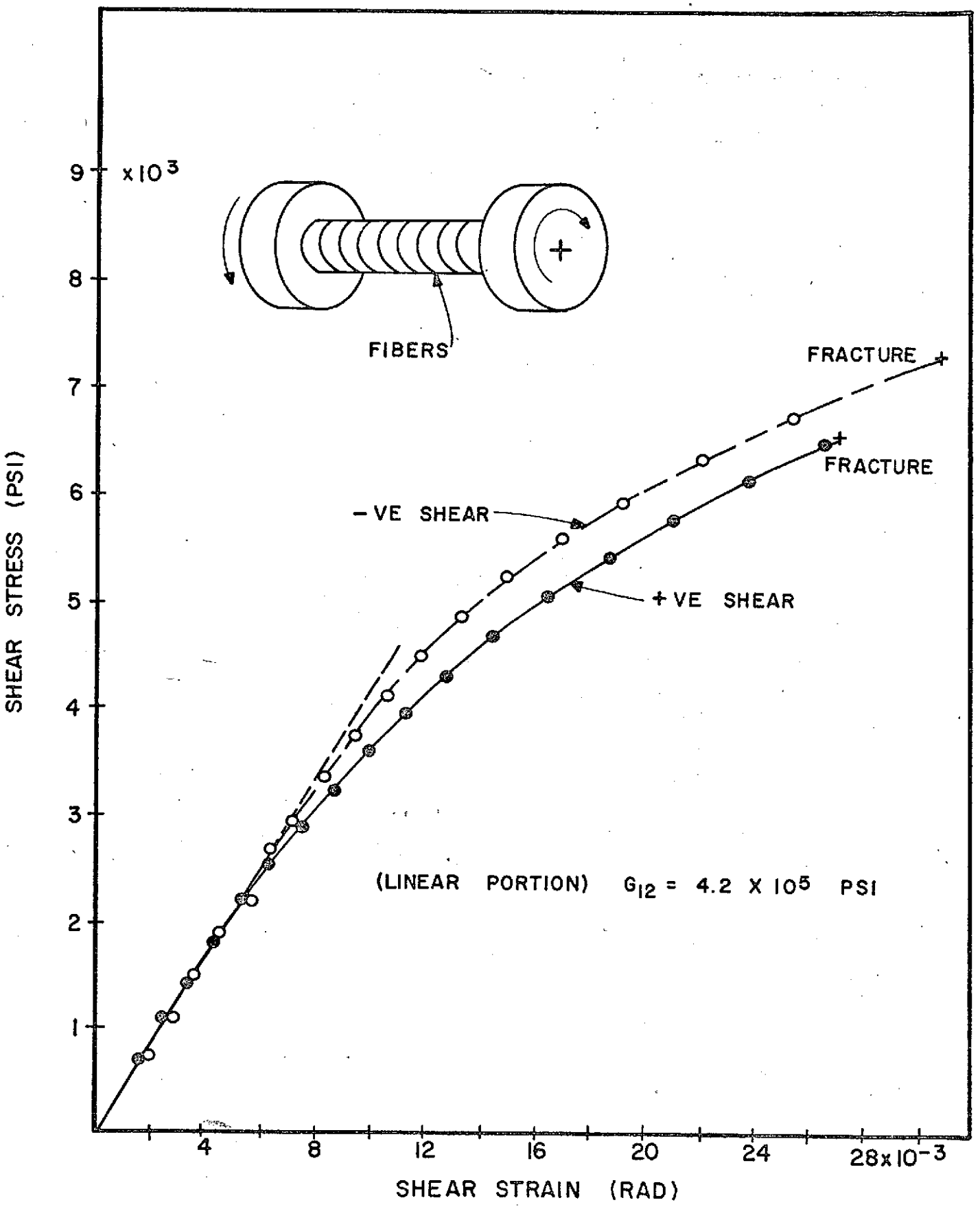

FIG. 15 STRESS-STRAIN CURVES FOR SCOTCHPLY (1002) IN PURE SHEAR

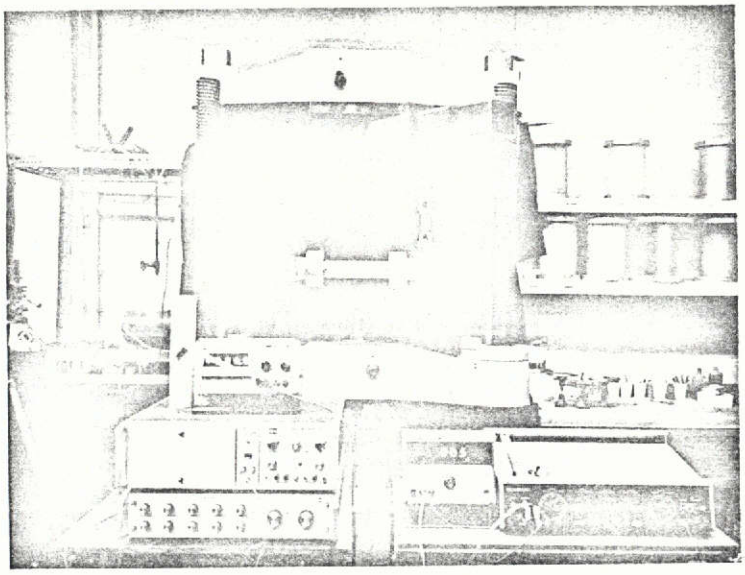

FIG. 16 SHEAR STRENGTH TEST SET-UP

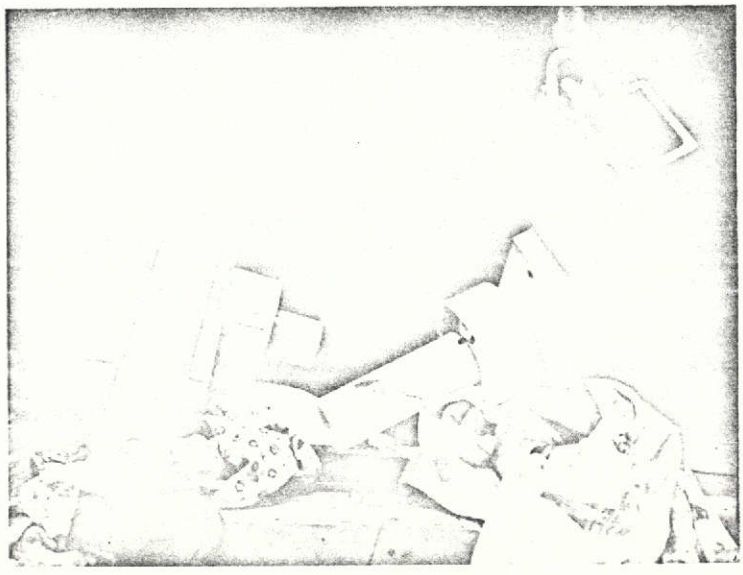

FIG. 17 SHEAR FAILURE OF A SPECIMEN LOADED UNDER PURE TORSION

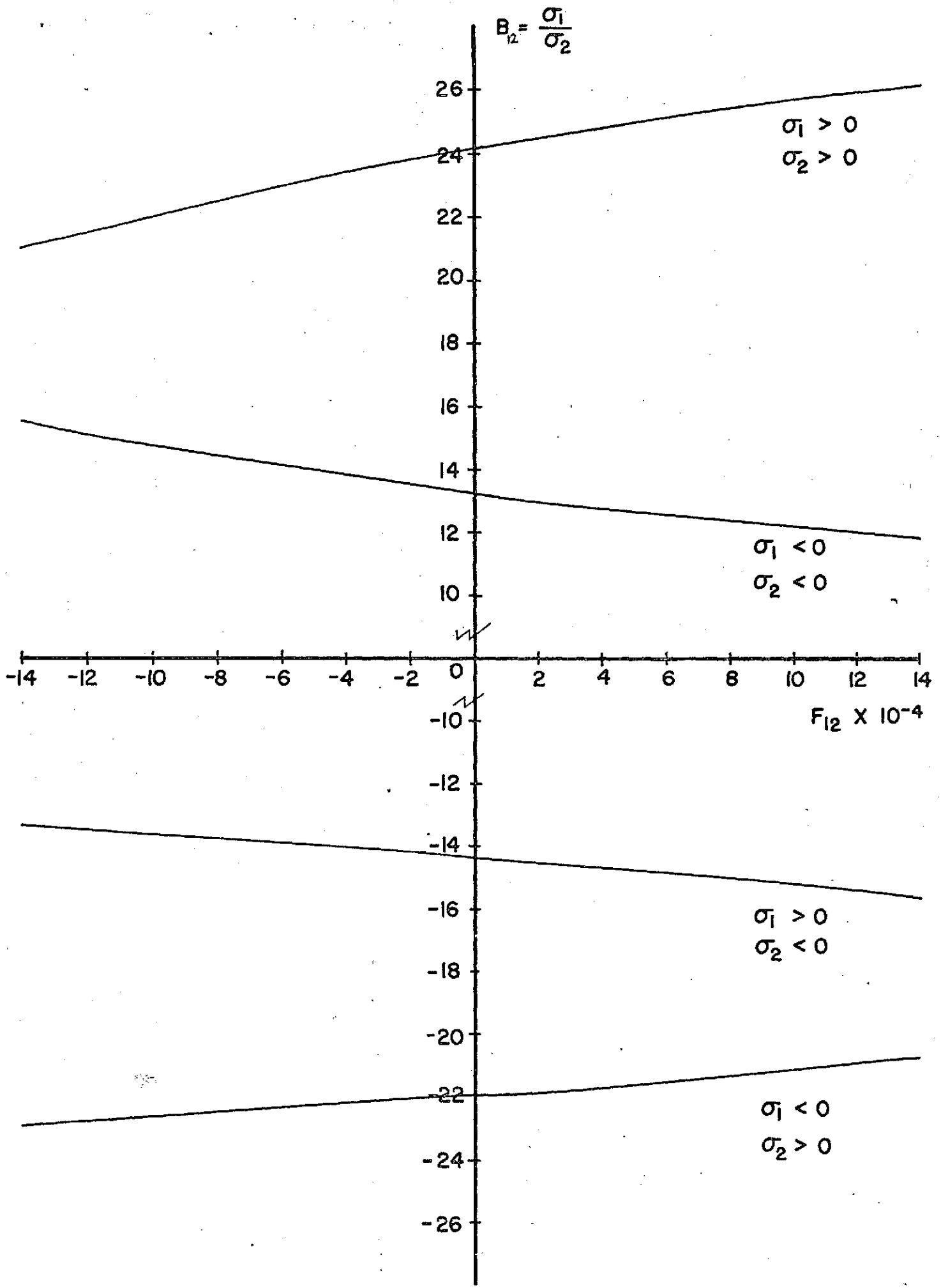

FIG. 18 OPTIMUM BIAXIAL STRESS RATIO, B_{12}, FOR THE DETERMINATION OF F_{12}

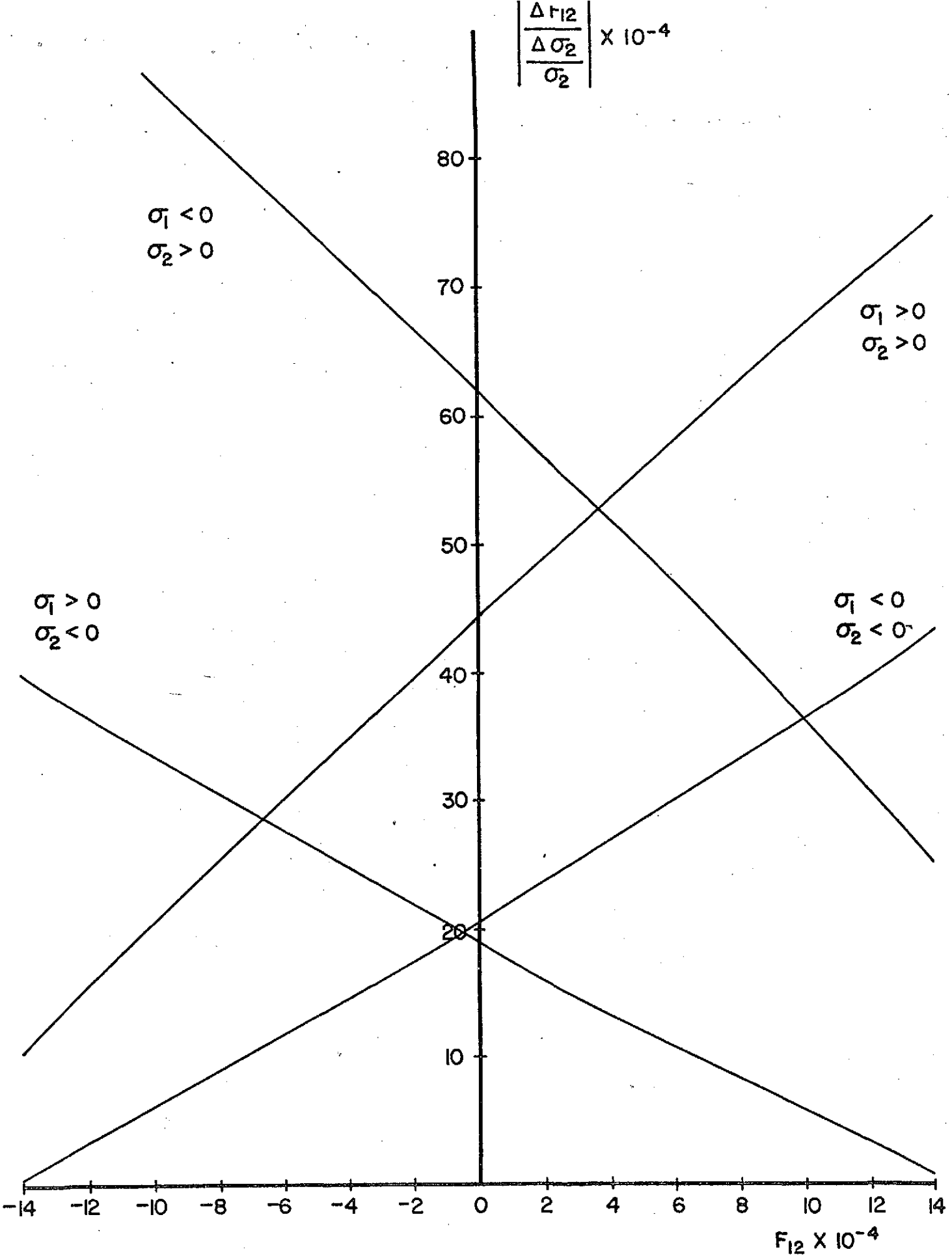

FIG. 19 ATTAINABLE RESOLUTION OF F_{12} FOR OPTIMAL RATIOS, $B_{12} = \frac{\sigma_1}{\sigma_2}$

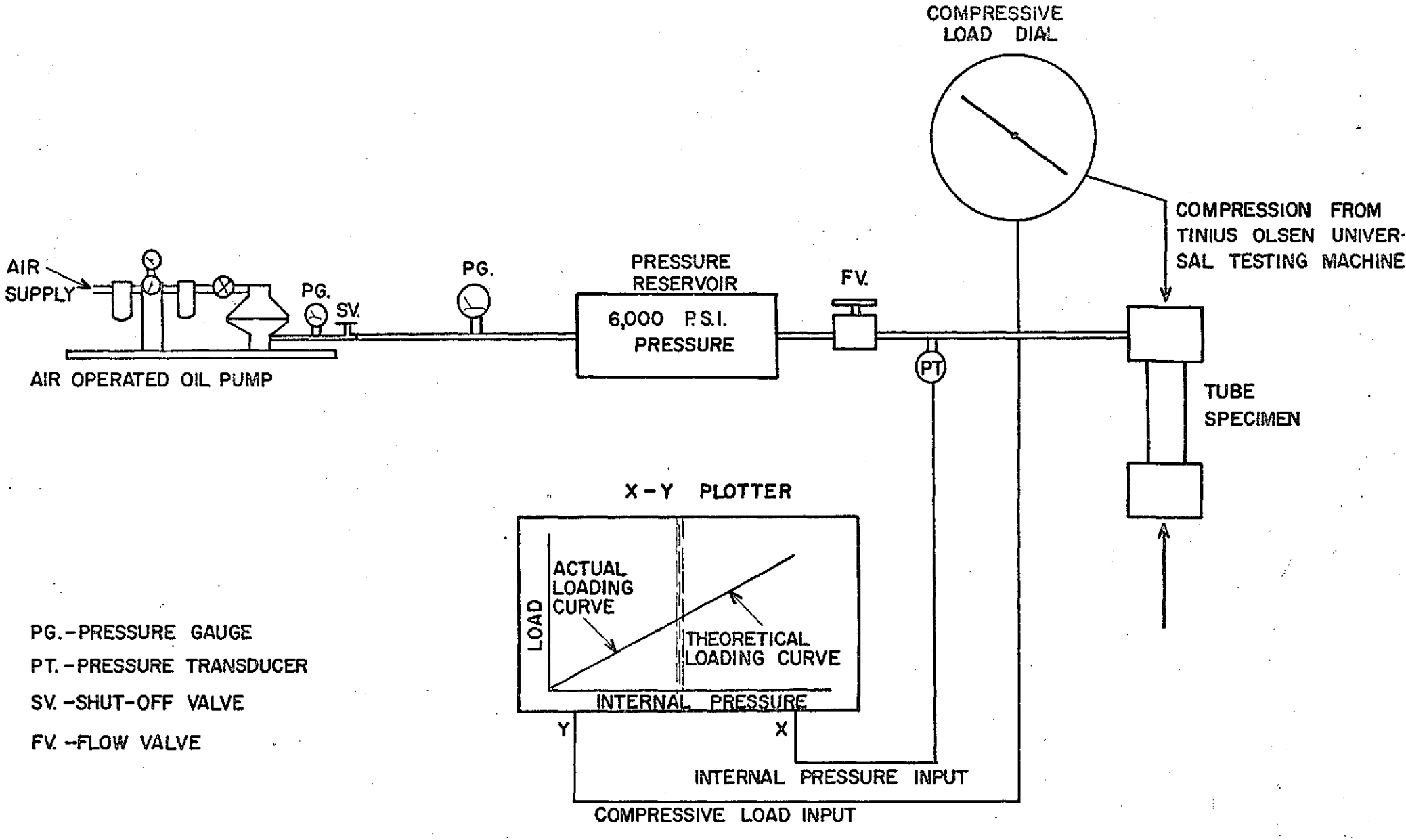

FIG. 20 SCHEMATIC DIAGRAM OF THE TEST SET-UP FOR THE DETERMINATION OF THE F_{12} INTERACTION TENSOR

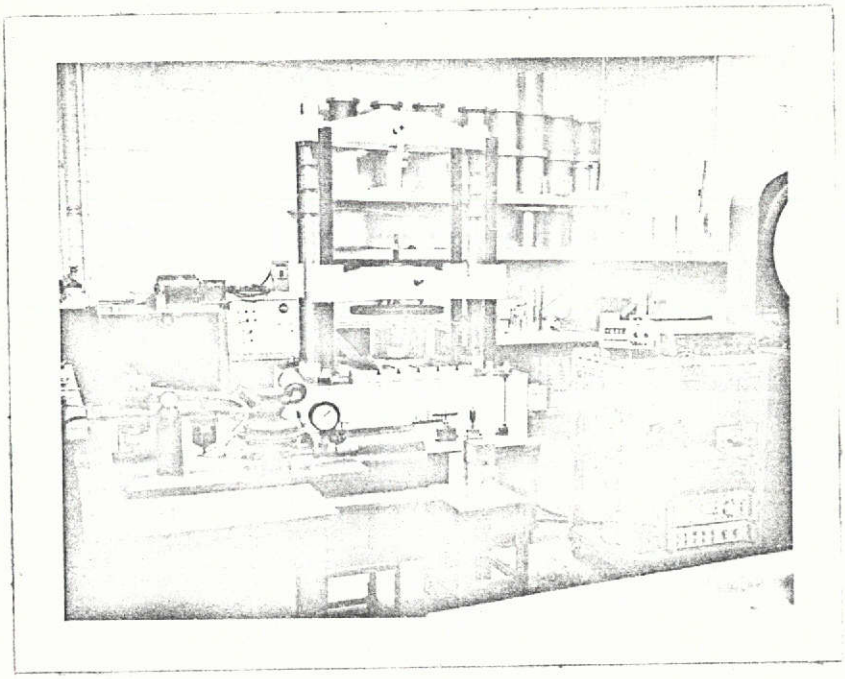

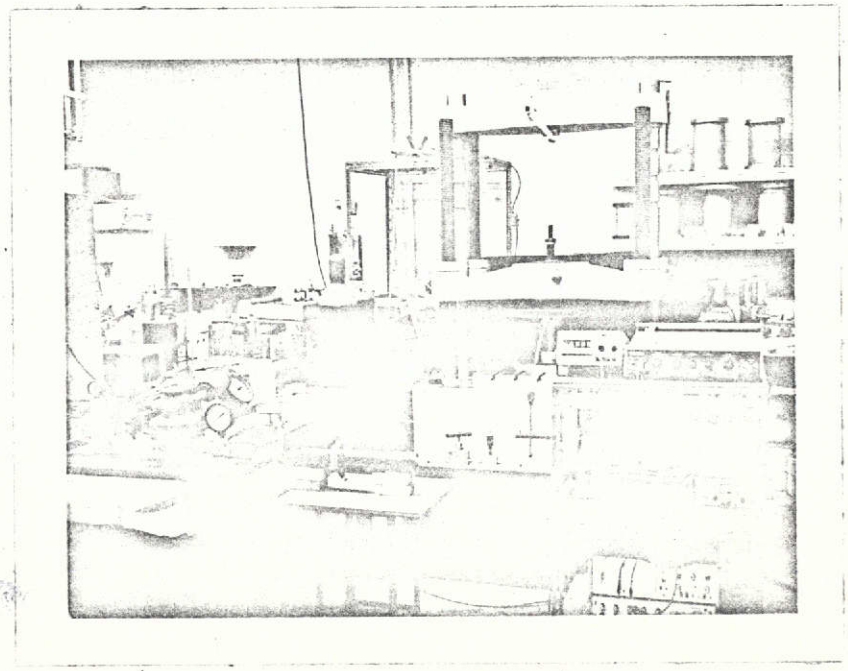

FIG. 21 TEST SET-UP FOR THE DETERMINATION OF THE F_{12} INTERACTION TENSOR

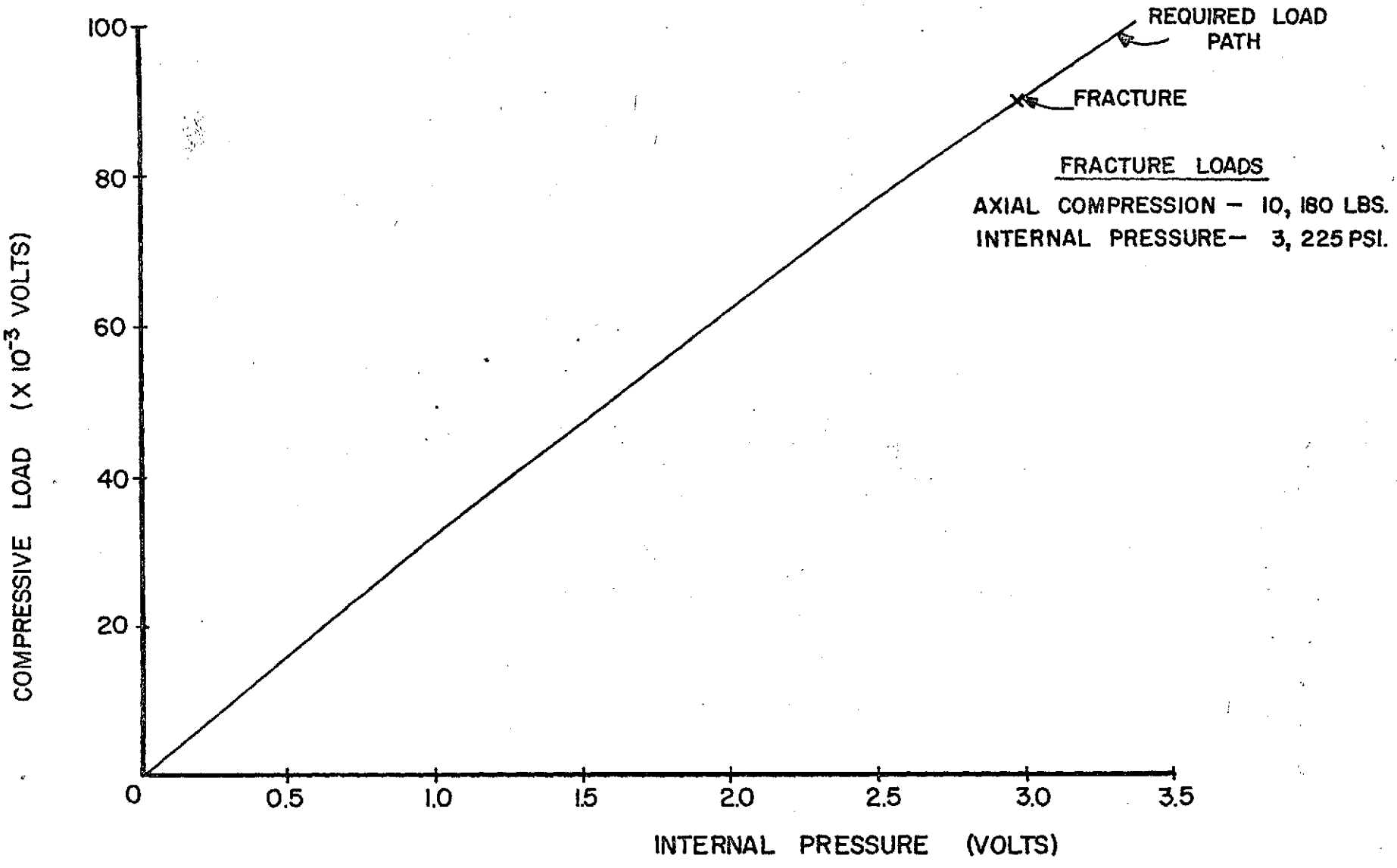

FIG. 22 COMBINED LOADING CURVE FOR F_{12} TEST (TUBE 13b 90°)

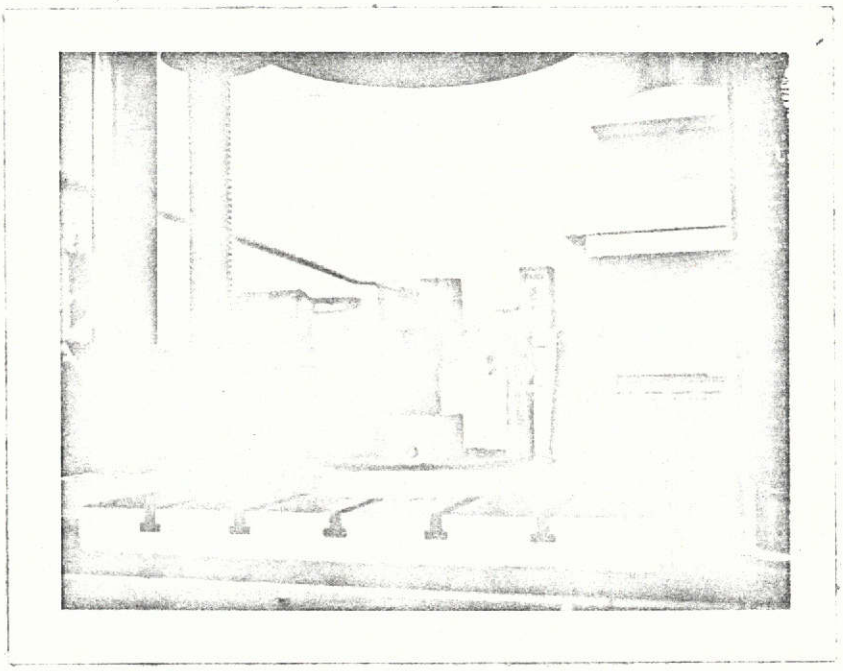

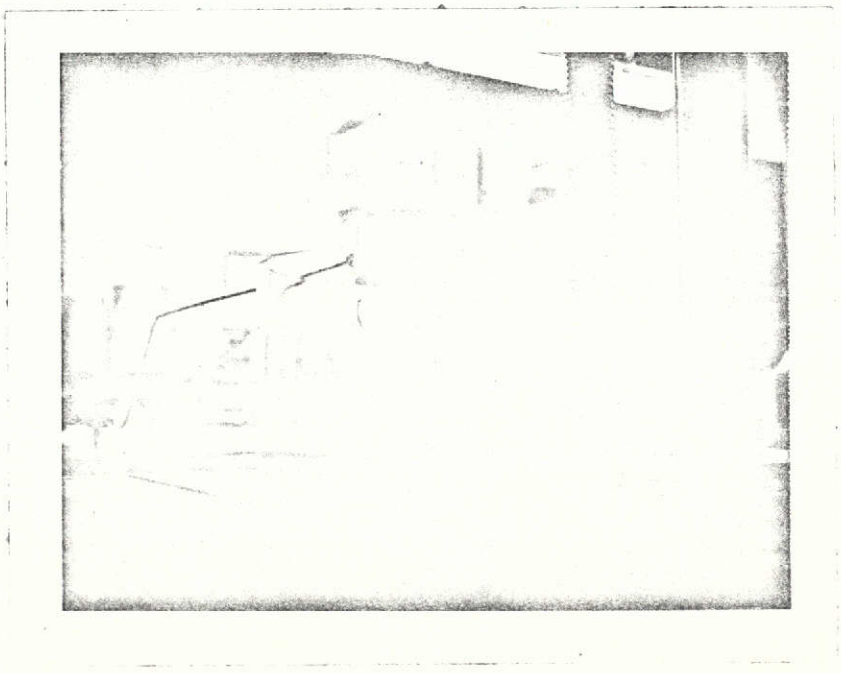

FIG. 23 SPECIMEN FAILURE IN F_{12} TESTING

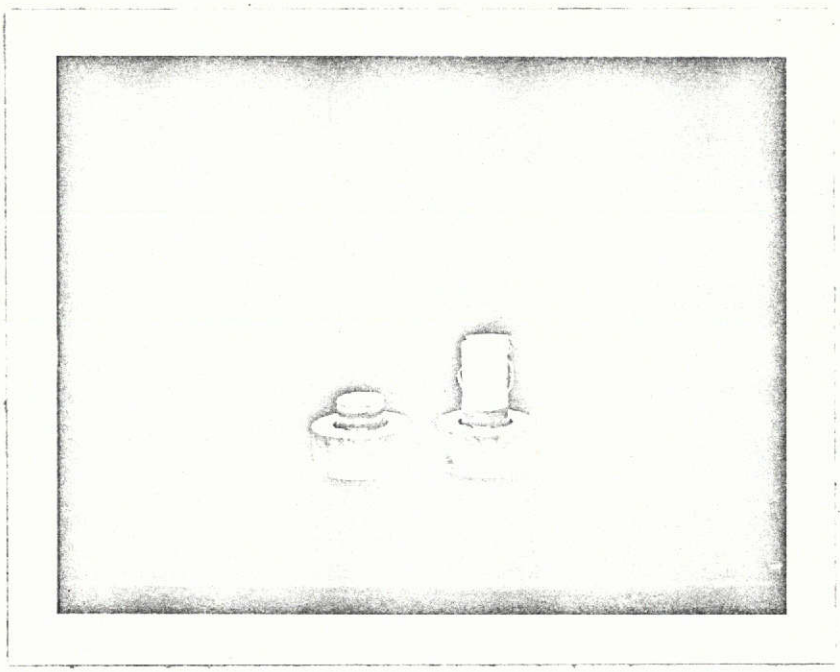

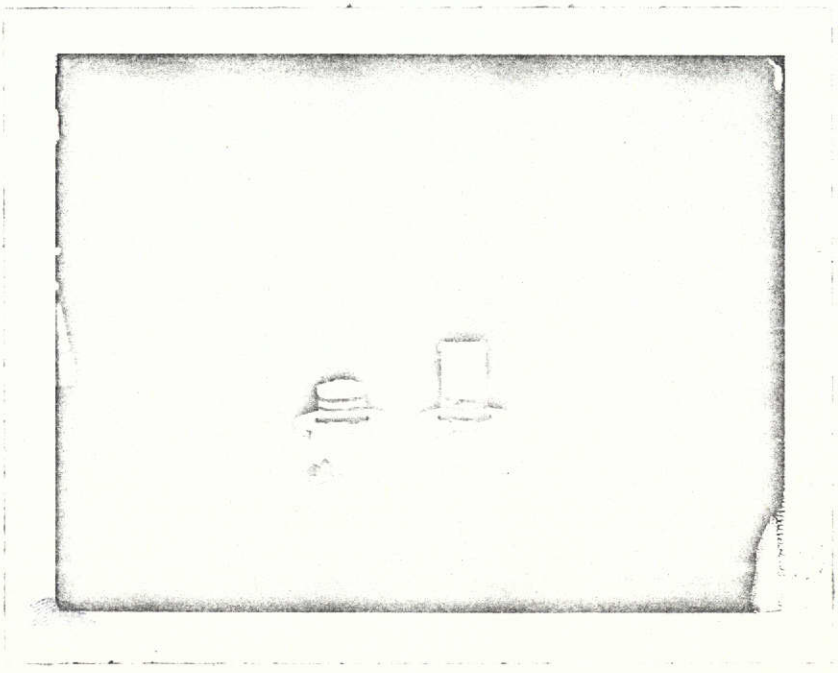

FIG. 24 FAILED SPECIMENS FROM THE F_{12} TESTING

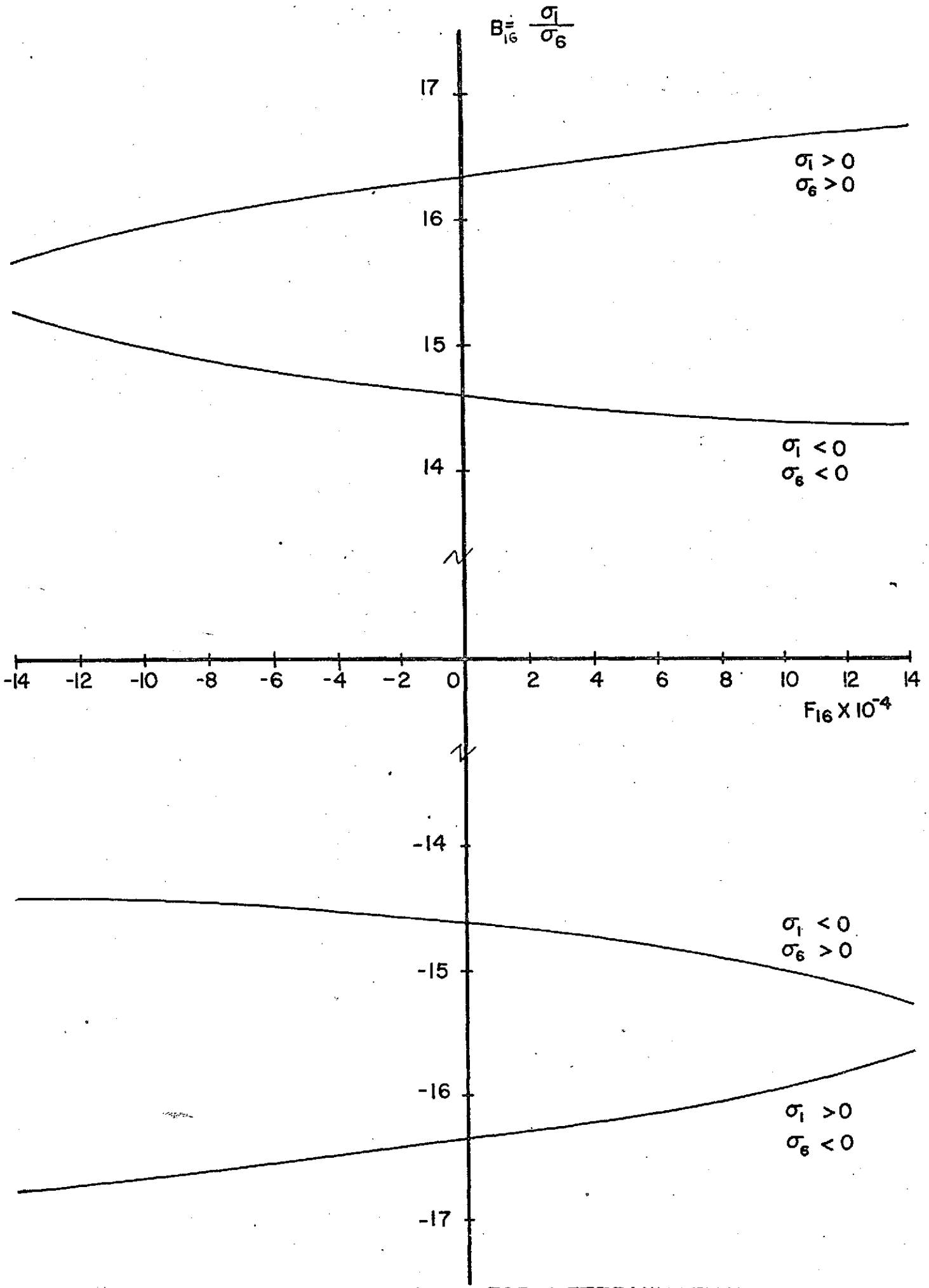

FIG 2.5 OPTIMUM BIAXIAL RATIO B_{16} FOR DETERMINATION OF F_{16}

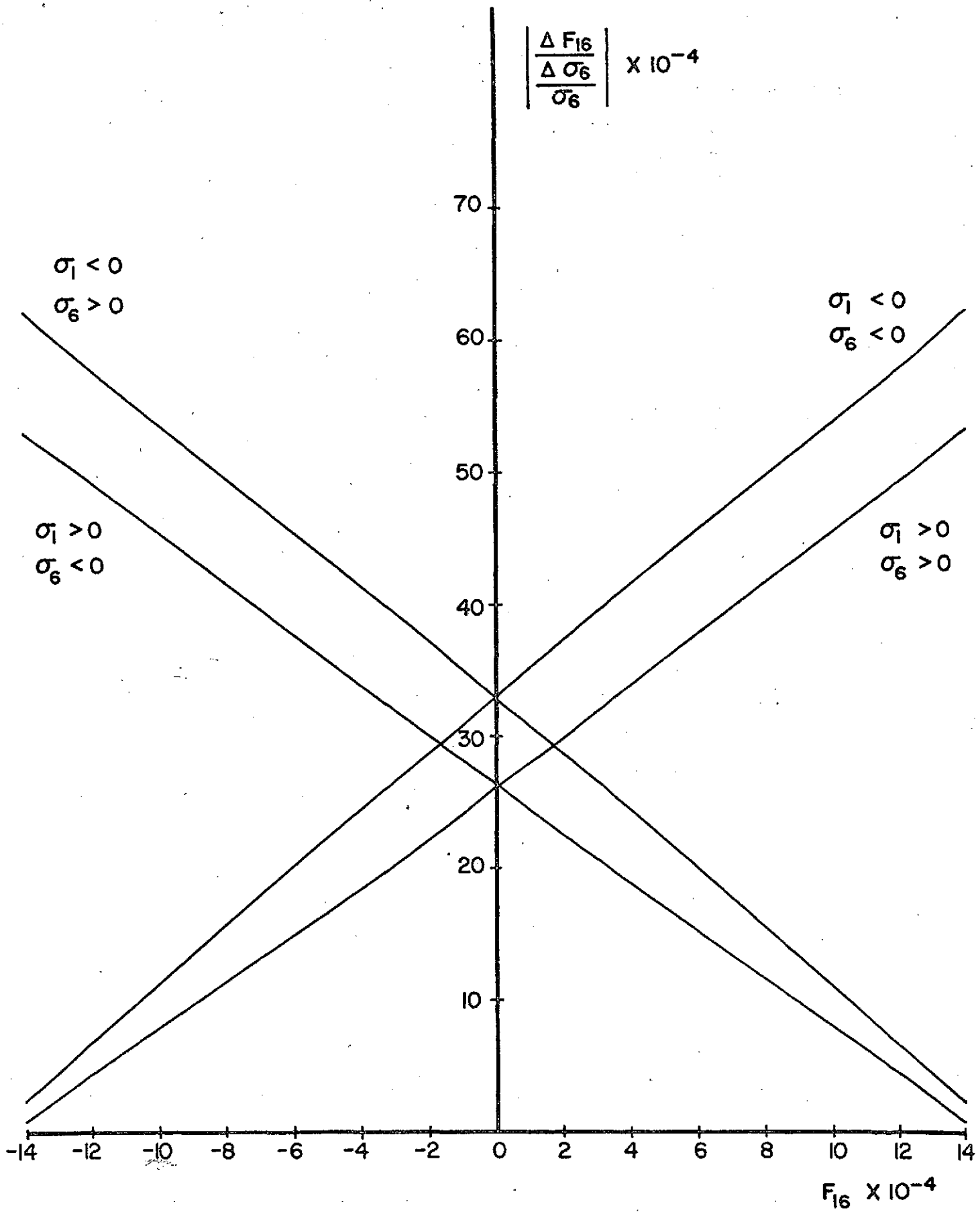

FIG. 2.6 ATTAINABLE RESOLUTION OF F_{16} FOR OPTIMAL RATIOS, $B_{16} = \frac{\sigma_1}{\sigma_6}$

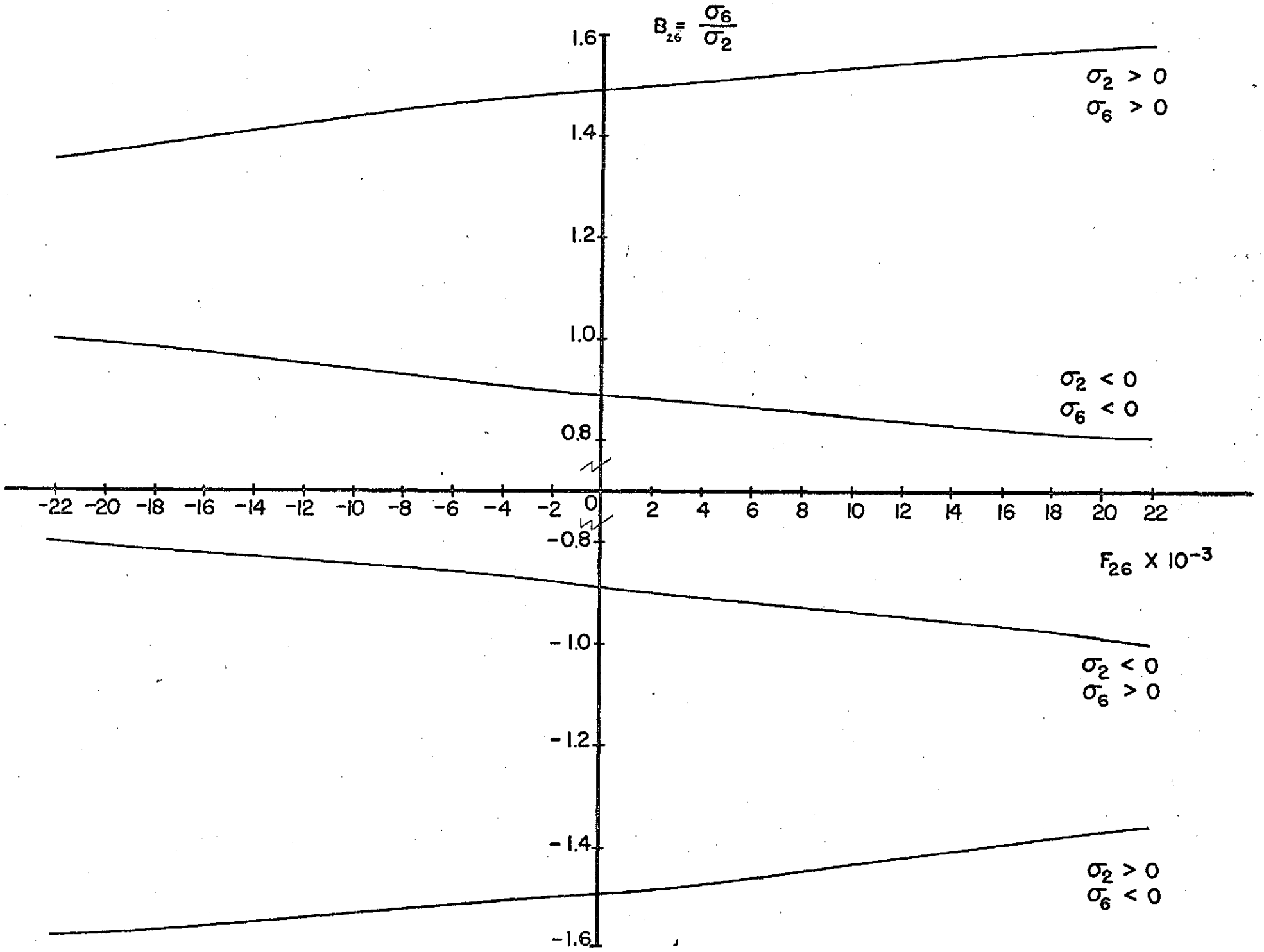

FIG. 27 OPTIMUM BIAXIAL RATIO B_{26} FOR DETERMINATION OF F_{26}

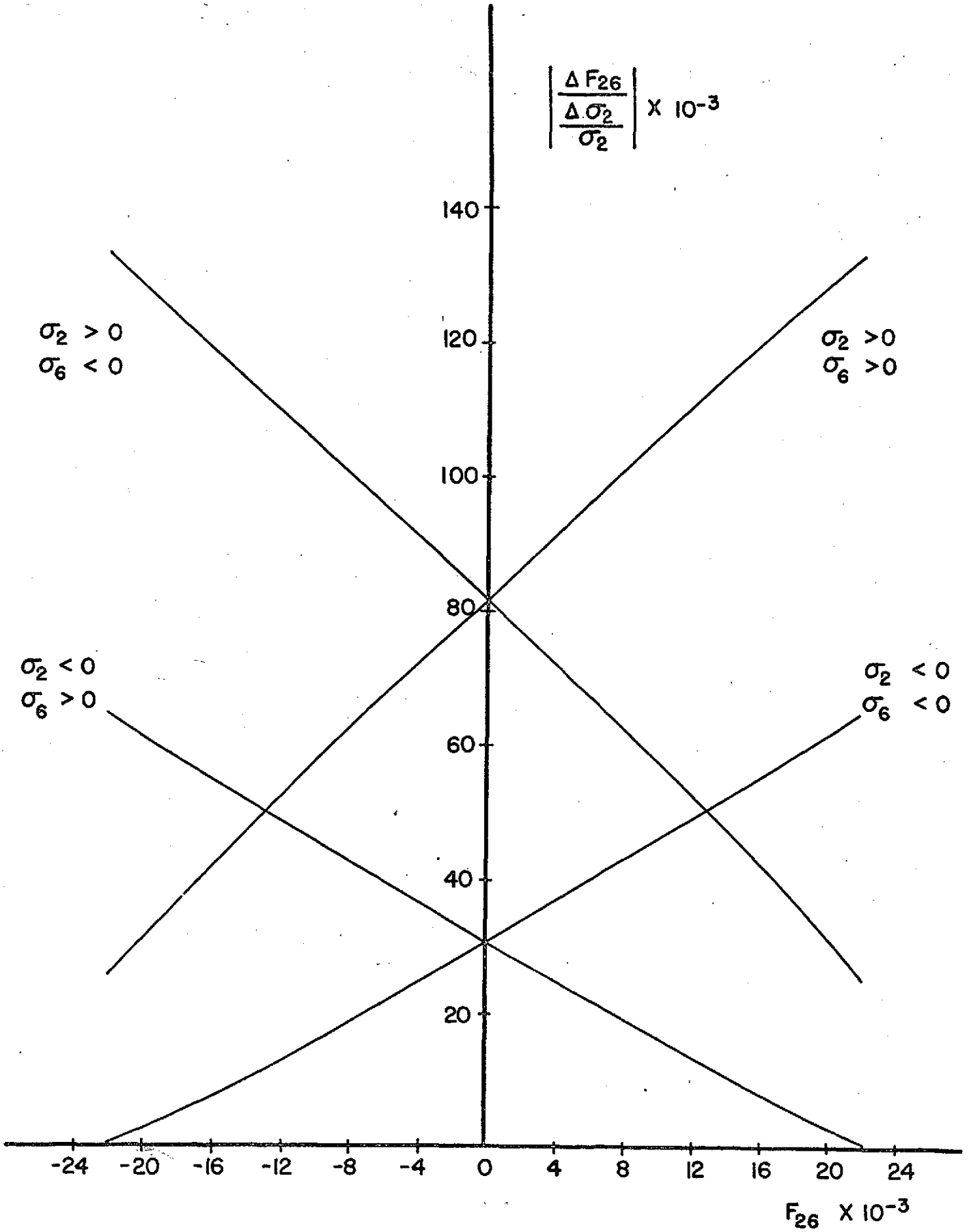

FIG. 28 ATTAINABLE RESOLUTION OF F_{26} FOR OPTIMAL RATIOS, $B_{26} = \frac{\sigma_6}{\sigma_2}$

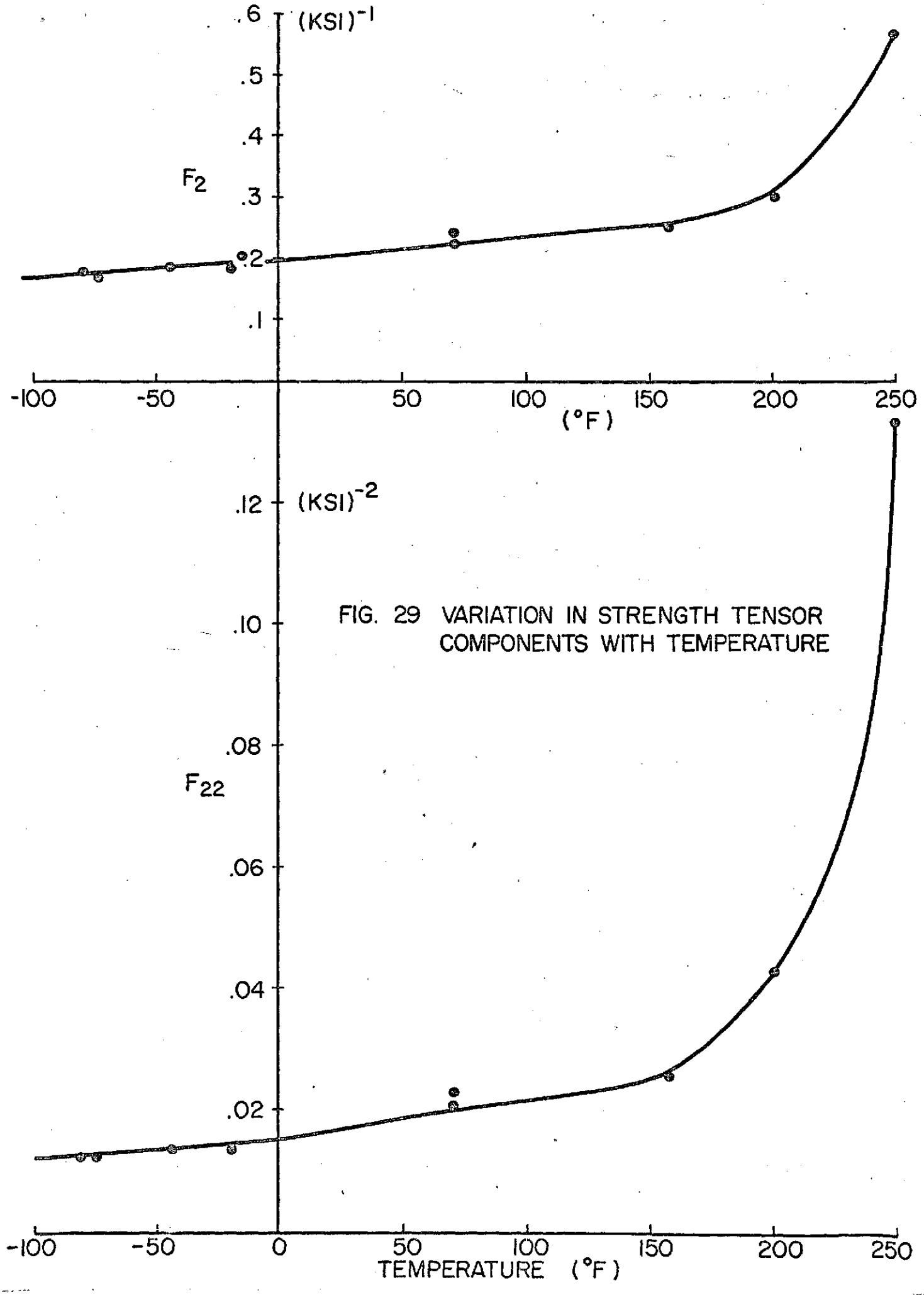

FIG. 29 VARIATION IN STRENGTH TENSOR COMPONENTS WITH TEMPERATURE

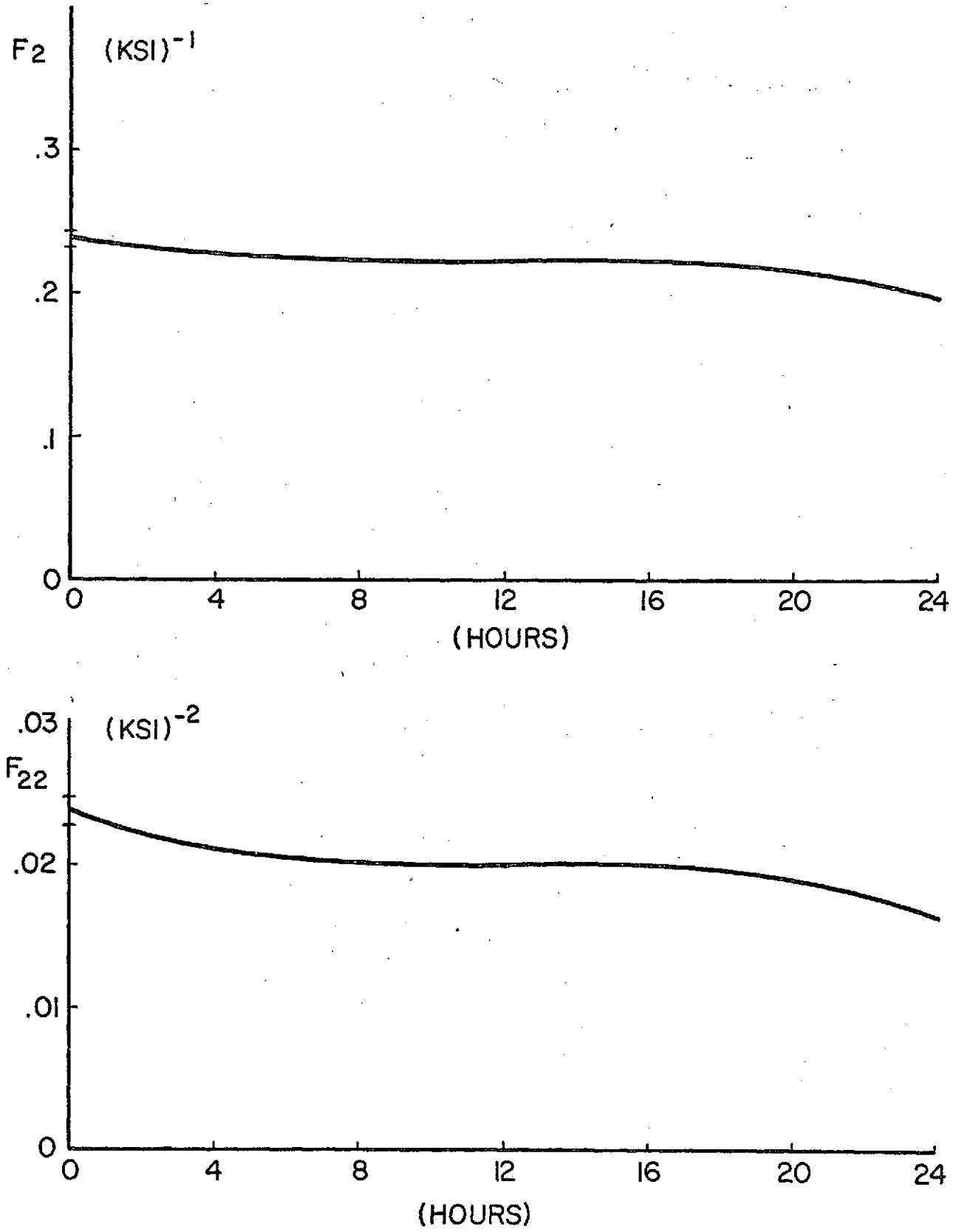

FIG. 30 THE VARIATION IN STRENGTH TENSOR COMPONENT WITH POST CURE TIME

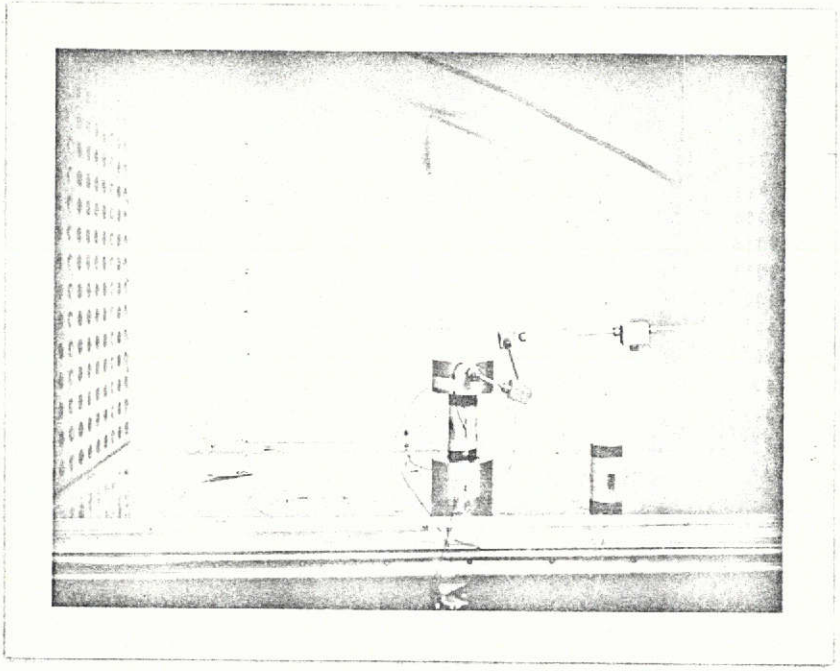

FIG. 31 INTERNAL PRESSURE TEST SET-UP

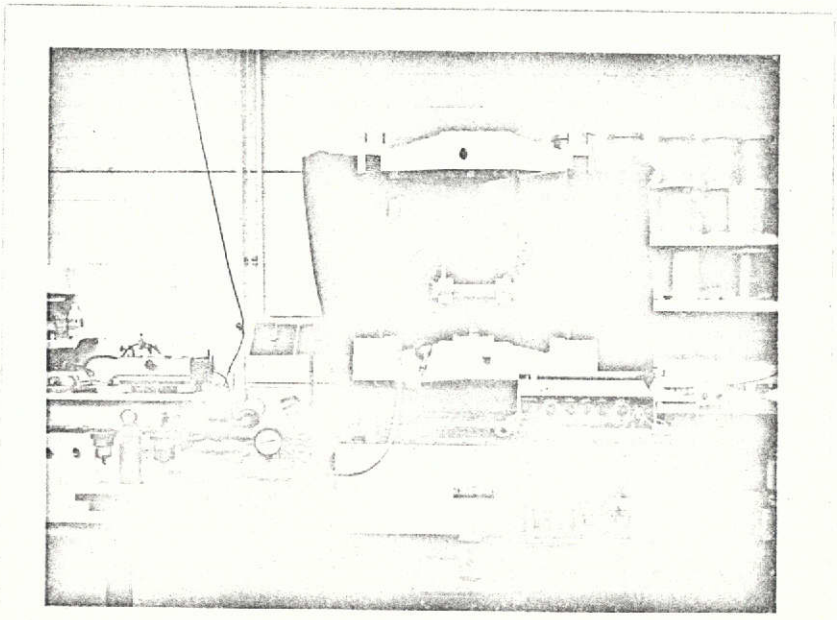

FIG. 32 COMBINED LOADING OF TORSION AND INTERNAL PRESSURE

FIG. 33 PLOT OF CUBIC FAILURE POLYNOMIAL TO DETERMINE ROOTS

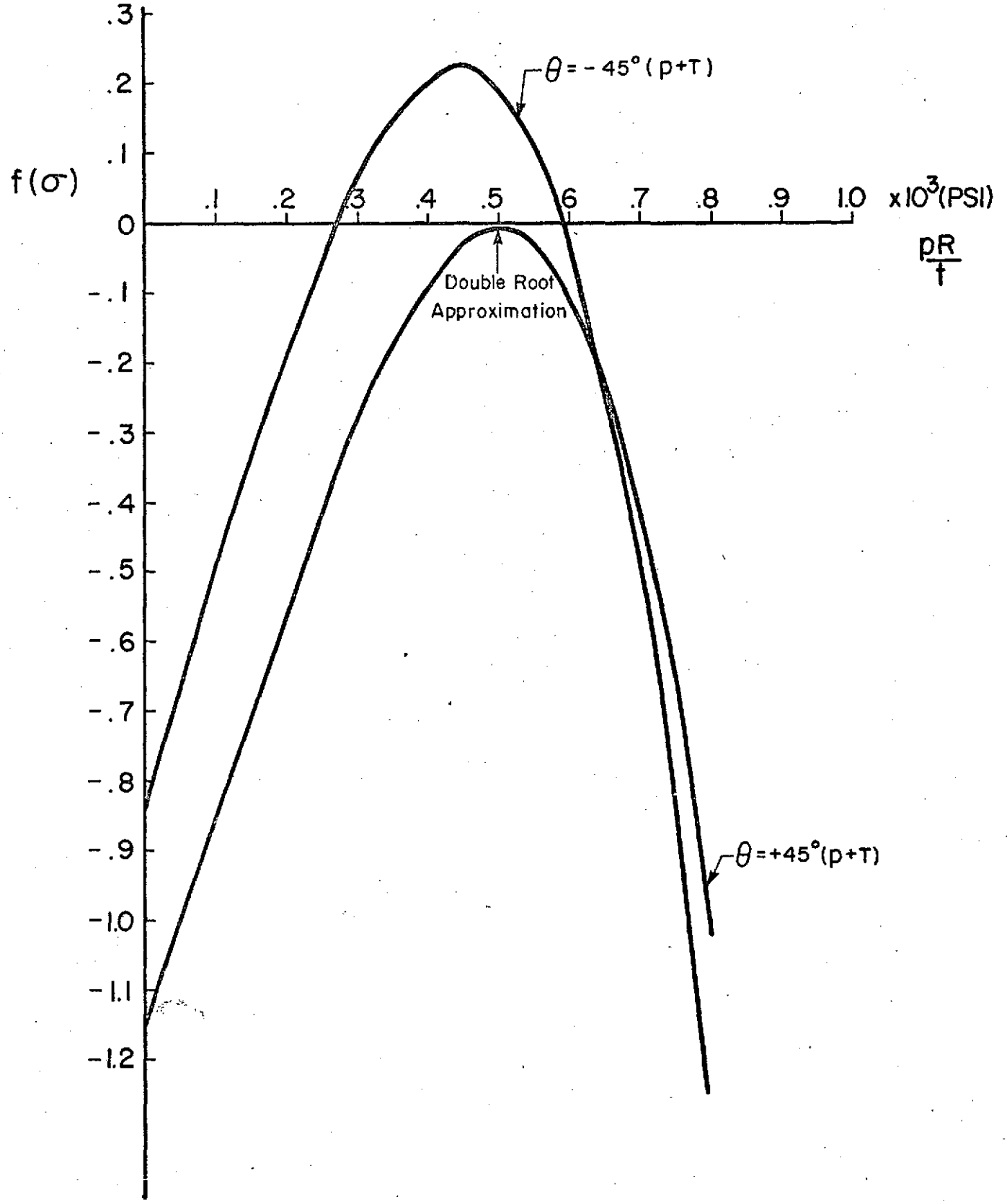

FIG. 34 COMPARISON OF QUADRATIC AND CUBIC TENSOR POLYNOMIAL STRENGTH PREDICTIONS (ALL ODD-ORDER TERMS IN σ_6 SET TO ZERO) FOR SYMMETRIC LAMINATED TUBES UNDER INTERNAL PRESSURE

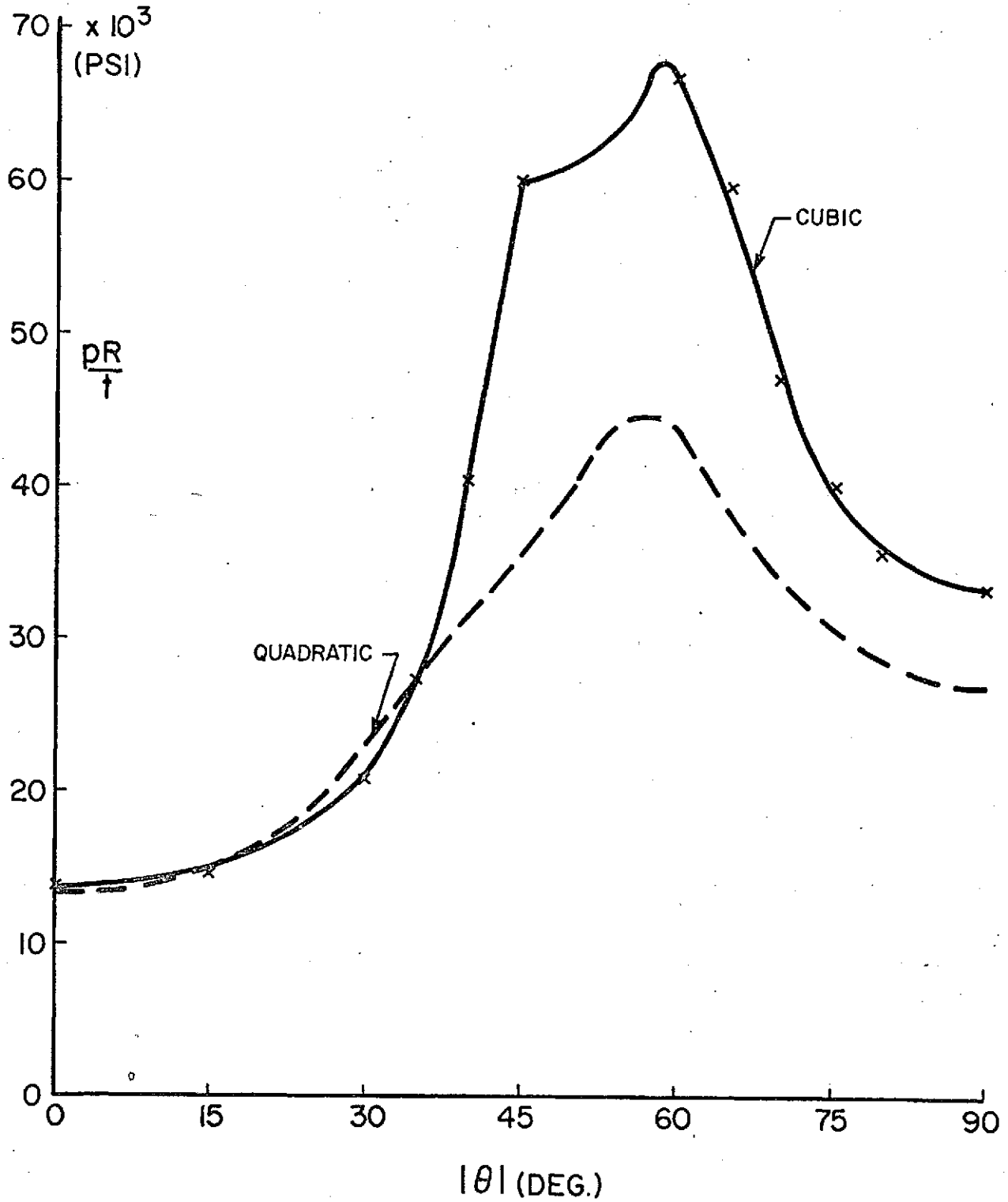

FIG. 35 COMPARISON OF FAILURE PREDICTION WITH EXPERIMENTS FOR SYMMETRIC LAMINATED TUBES UNDER INTERNAL PRESSURE

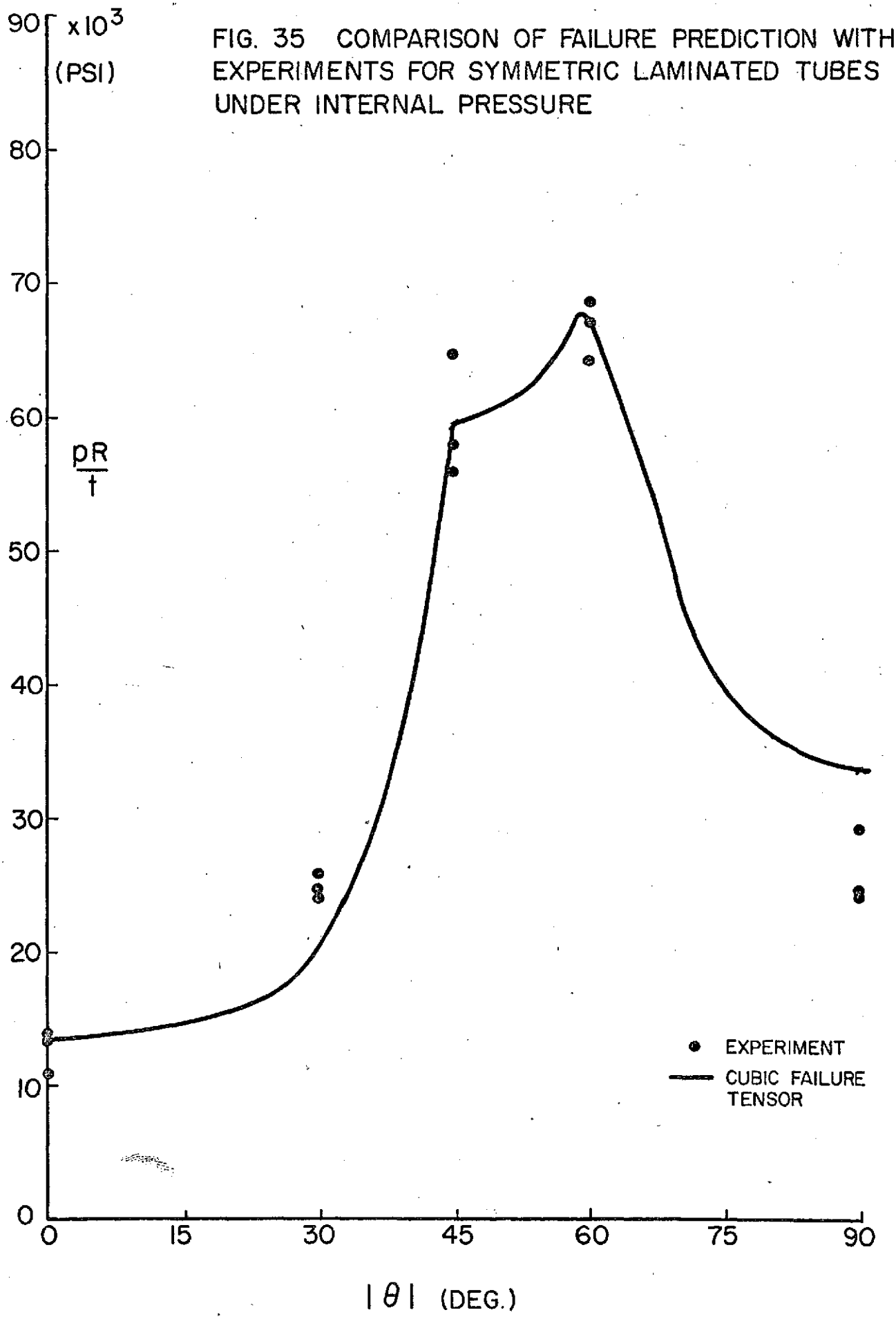

FIG. 36 VARIATION IN PRINCIPAL FAILURE STRESSES WITH FIBER ORIENTATION FOR SYMMETRIC LAMINATED TUBES UNDER INTERNAL PRESSURE

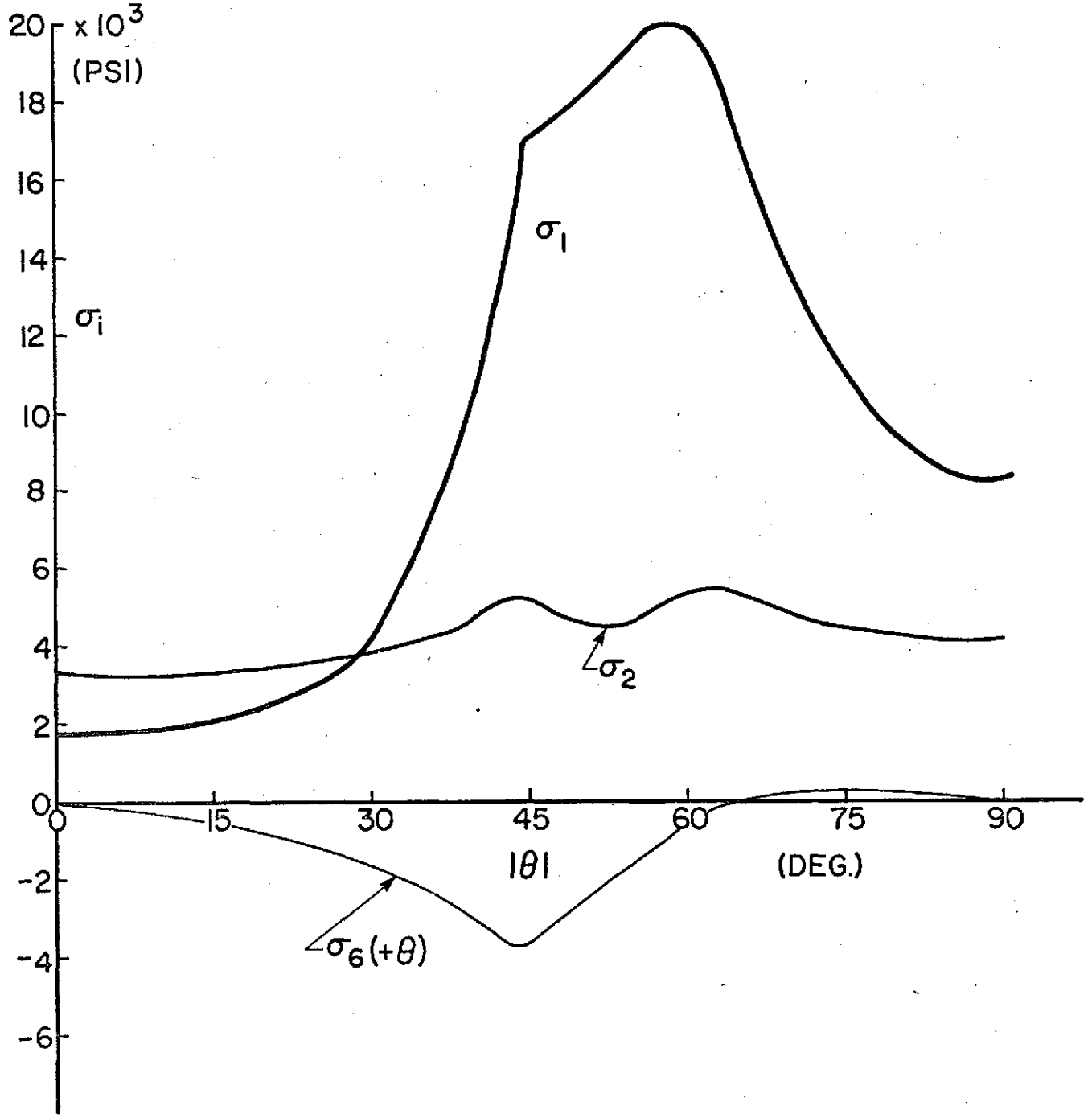

FIG. 37 COMPARISON OF PREDICTED FAILURE LOADS FOR $\pm\theta$ LAMINATED TUBES UNDER INTERNAL PRESSURE WITH TORQUE USING CUBIC FAILURE TENSOR

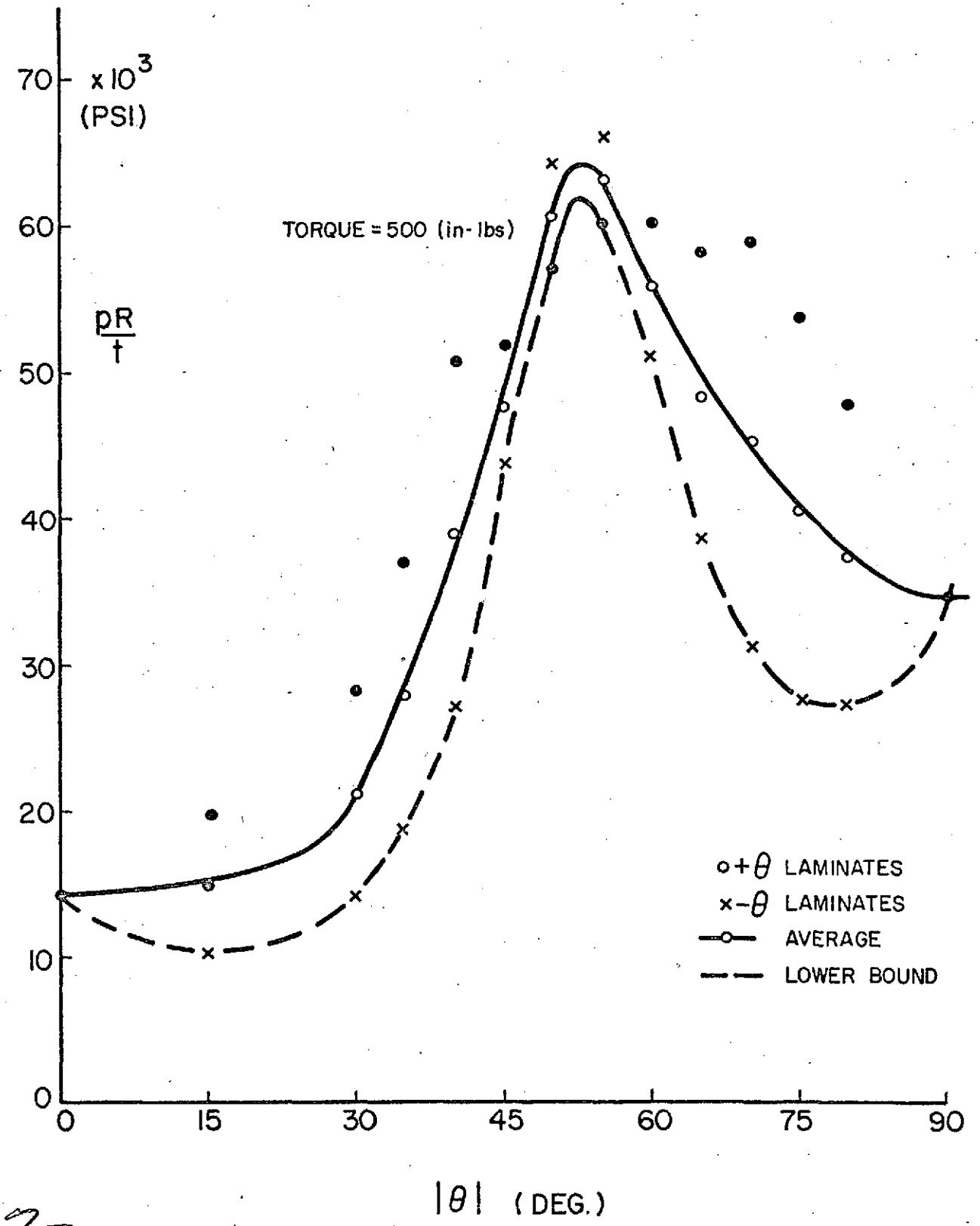

C-2

FIG. 38 COMPARISON OF MEAN CUBIC TENSOR POLYNOMIAL FAILURE PREDICTION WITH EXPERIMENT FOR SYMMETRIC LAMINATED TUBES UNDER INTERNAL PRESSURE AND CONSTANT TORQUE

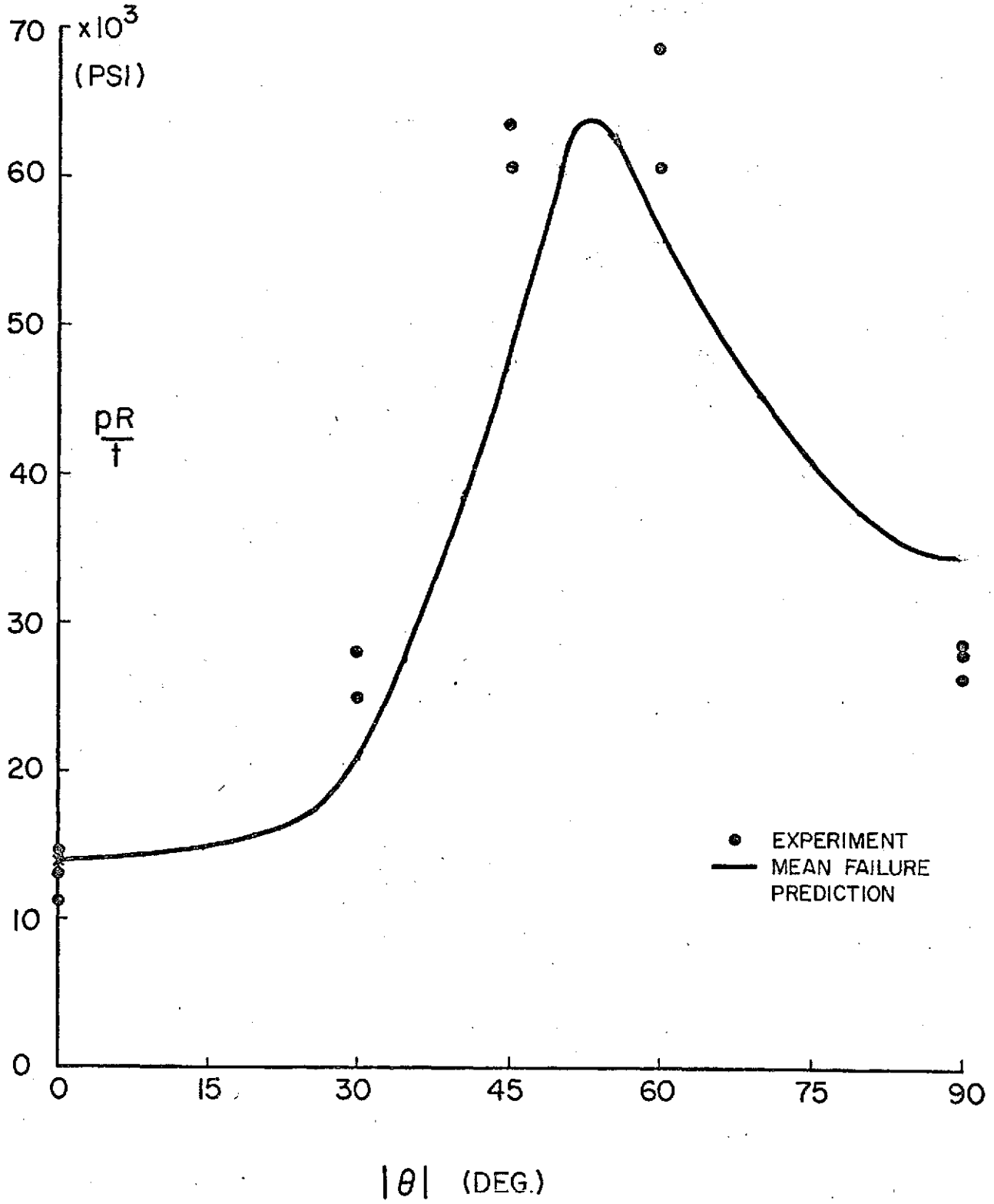

FIG. 39 PLOT OF THE PRINCIPAL MEMBRANE STRESSES AT FAILURE FOR SYMMETRIC LAMINATED TUBES UNDER INTERNAL PRESSURE AND CONSTANT TORQUE

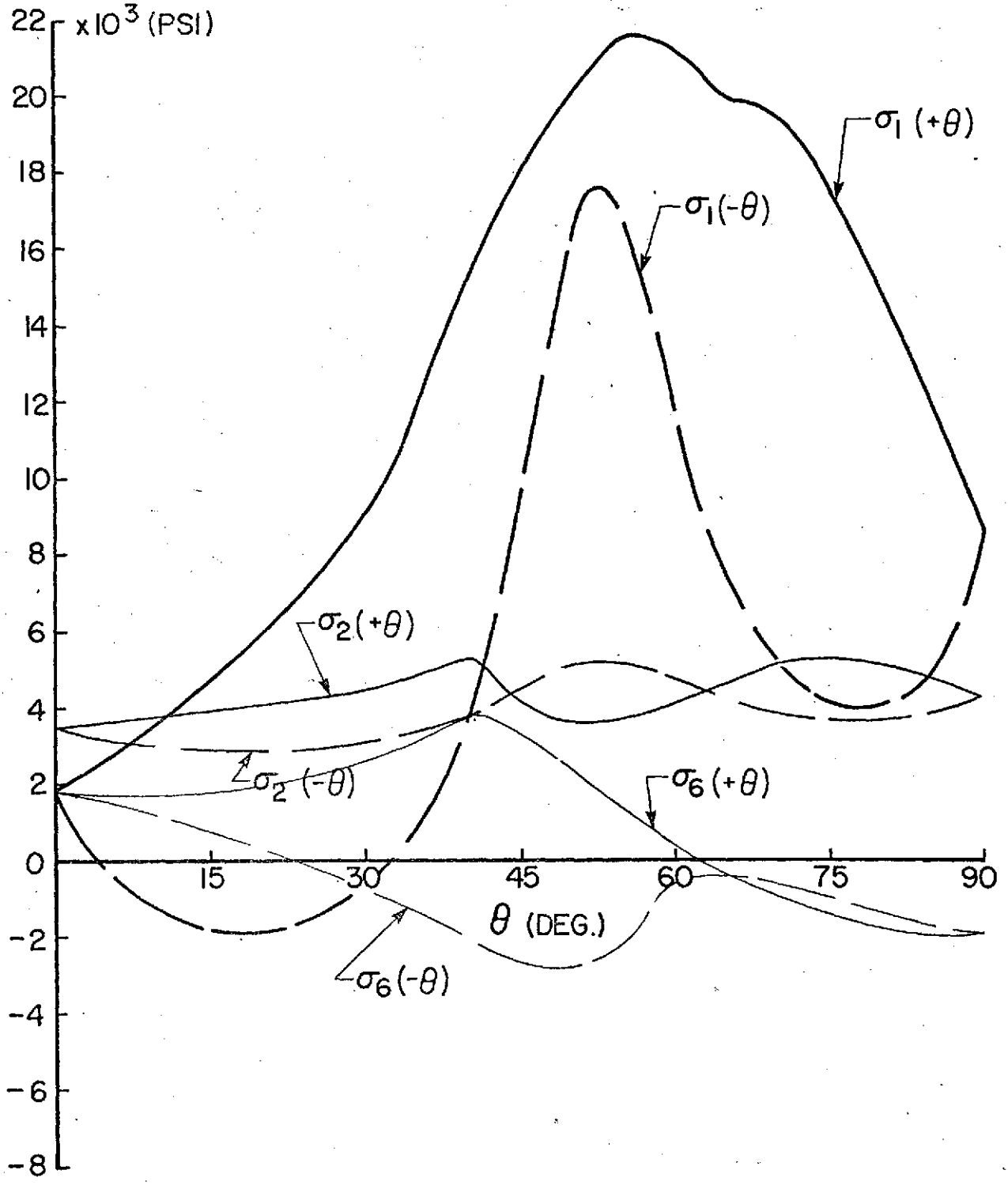

APPENDIX A

DETERMINATION OF STRESSES IN FIBRE-REINFORCED CYLINDERS UNDER COMBINED LOADING

A.1 Anisotropic Shell Theory

1. Equilibrium Equations

Let the mid-surface of the circular cylindrical shell be the reference surface with x, θ, and z measured with respect to that surface in the axial, circumferential, and radial directions respectively (Fig. A.1). The components of displacement u, v, and w of a point on the mid-surface are the displacements in the x, θ, and z directions due to the externally applied loadings. The thickness, h, of the tube is assumed to be uniform. Differentiation is denoted by a comma.

For a cylindrical element, the strains are given in the following form:

$$\epsilon_x = \epsilon_x^\circ + zK_x$$

$$\epsilon_\theta = \epsilon_\theta^\circ + z[1 - z/R]\, K_\theta \tag{A1}$$

$$\epsilon_{x\theta} = [1 + z^2/2R^2]\,\epsilon_{x\theta}^\circ + z[1 - z/2R]\, K_{x\theta}$$

where

$$\begin{aligned}
\epsilon_x^\circ &= u,_x \\
\epsilon_\theta^\circ &= (1/R)\,(v,_\theta + w) \\
\epsilon_{x\theta}^\circ &= (u,_\theta/R) + v,_x \\
K_x &= -w,_{xx} \\
K_\theta &= -(1/R^2)\,(w,_{\theta\theta} + w) \\
K_x &= -(2/R)\,[w,_{x\theta} + (u,_\theta/2R) - (v,_x/2)]
\end{aligned} \tag{A2}$$

are the mid-plane strains and curvatures.

Under axisymmetric loading differentiation with respect to the θ coordinate is assumed to be zero. Substituting this and equation (A2) into equation (A1) gives the strain-displacement relations in the following form:

$$\epsilon_x = u,_x - z\, w,_{xx}$$

$$\epsilon_\theta = \frac{w}{R}\left[1 - \frac{z}{R} + \frac{z^2}{R^2}\right] \tag{A3}$$

$$\epsilon_{x\theta} = v,_x \left[1 + \frac{z}{R}\right]$$

The force and moment resultants are related to the middle-plane strains and curvatures in the following manner

(Ref. 25):

$$\begin{bmatrix} N_x \\ N_\theta \\ N_{x\theta} \\ M_x \\ M_\theta \\ M_{x\theta} \end{bmatrix} = \begin{bmatrix} A_{11} & A_{12} & D_{16}/2R^2 & D_{11}/R & 0 & D_{16}/2R \\ A_{12} & A_{22} & D_{26}/2R^2 & 0 & -D_{22}/R & -D_{26}/2R \\ 0 & 0 & A_{66}+D_{66}/2R^2 & D_{16}/R & 0 & D_{66}/2R \\ D_{11}/R & D_{12}/R & D_{16}/R & D_{11} & D_{12} & D_{16} \\ 0 & 0 & 0 & D_{12} & D_{22} & D_{26} \\ D_{16}/R & D_{26}/R & D_{66}/R & D_{16} & D_{26} & D_{66} \end{bmatrix} \begin{bmatrix} \epsilon_x^\circ \\ \epsilon_\theta^\circ \\ \epsilon_{x\theta}^\circ \\ K_x \\ K_\theta \\ K_{x\theta} \end{bmatrix} \quad (A4$$

$$\text{where } (A_{ij}, D_{ij},) = \int_{-h/2}^{h/2} Q_{ij}\ (1, z^2)dz \qquad (i,j = 1,2,6) \quad (A5$$

The equilibrium equations are obtained by considering the forces and moments acting on an infinitesimal element of the mid-plane of the shell (Fig.A.2). These are

$$N_{x,x} = 0$$

$$N_{x\theta,x} + \frac{1}{R} M_{x\theta,x} = 0 \qquad (A6)$$

$$M_{x,xx} - \frac{N_\theta}{R} + p = 0$$

where p is the internal pressure applied to the tube.

2. The Governing Differential Equation

The first part of equation (A6) gives, upon integration, that

$$N_x = \text{constant} = N_o \qquad (A7)$$

by substituting the constitutive equations (A4) into the second and third parts of equation (A6) and using equation

(A7) the following differential equation in w can be derived.

$$\lambda_1 w,_{xxxx} + \frac{\lambda_2}{R^2} w,_{xx} + \frac{\lambda_3 w}{R^2} = p - \frac{A_{12}\bar{A}_{66}}{RD} N_o + \frac{A_{12}\bar{A}_{16}}{2\pi R^2 D} T \qquad (A8)$$

where $\lambda_1 = \left[D_{11} - \frac{1}{R^2 D} \left(D_{11}^2 \bar{A}_{66} - 4\bar{A}_{16} D_{16} D_{11} + 4A_{11} D_{16}^2 \right) \right]$

$$\lambda_2 = \frac{2}{D} \left(\bar{A}_{66} A_{12} D_{11} - 2A_{12} D_{16} \bar{A}_{16} \right)$$

$$\lambda_3 = \bar{A}_{22} - \frac{A_{12}^2 \bar{A}_{66}}{D}$$

$$\bar{A}_{22} = A_{22} + \frac{D_{22}}{R^2}$$

$$\bar{A}_{66} = A_{66} + \frac{3D_{66}}{R^2}$$

$$\bar{A}_{16} = \frac{D_{16}}{R^2}$$

$$D = A_{11} \bar{A}_{66} - \bar{A}_{16}^2$$

3. Solution of the Governing Differential Equation

The differential equation (A8) can be solved by rewriting it in the form:

$$w,_{xxxx} + \frac{\lambda_2}{R^2 \lambda_1} w,_{xx} + \frac{\lambda_3}{R^2 \lambda_1} w = \frac{1}{\lambda_1} \left(p - \frac{A_{12} \bar{A}_{66}}{RD} N_o + \frac{A_{12} \bar{A}_{16}}{2\pi R^2 D} T \right) \qquad (A9)$$

The solution to this equation is composed of a particular

solution, w_o, and the solution to the homogeneous equation, w_h. For this case, the particular solution is

$$w_o = \frac{R^2}{\lambda_3}\left(p - \frac{A_{12}\,\bar{A}_{66}}{RD}N_o + \frac{A_{12}\,\bar{A}_{16}}{2\pi R^2 D}T\right) \qquad (A10)$$

and the solution of the homogeneous differential equation is of the form

$$w_h = k\,e^{mx} \qquad (A11)$$

where k and m are either real or complex constants. Substituting equation (A11) into the homogeneous differential equation and solving for m gives

$$m^2 = \frac{-b \pm \sqrt{b^2-4d}}{2} \qquad (A12)$$

where $b = \dfrac{\lambda_2}{R^2\lambda_1}$ and $d = \dfrac{\lambda_3}{R^2\lambda_1}$

There are three possible cases that could be solved for, namely, $4d > b^2$, $4d = b^2$, and $4d < b^2$, however, only the first case will be solved in detail in this paper.

When $4d > b^2$, than equation (A12) becomes

$$m^2 = \tfrac{1}{2}(-b \pm i\sqrt{4d-b^2}) \qquad (A13)$$
$$= \theta \pm i\phi$$

where $i = \sqrt{-1}$

$\theta = -b/2$

$\phi = \pm \tfrac{1}{2}\sqrt{4d-b^2}$

Therefore, m can be written as

$$m = \pm \alpha \pm i\beta \tag{A14}$$

and $$m^2 = \alpha^2 - \beta^2 \pm i2\alpha\beta \tag{A15}$$

so that $$\Theta = \alpha^2 - \beta^2 = -b/2 \tag{A16}$$

and $$\phi = 2\alpha\beta = \tfrac{1}{2}\sqrt{4d-b^2} \tag{A17}$$

Solving equation (A16) and (A17) gives that

$$\alpha = \tfrac{1}{2}\,(2\sqrt{d} - b)^{\frac{1}{2}} \tag{A18}$$

and $$\beta = \tfrac{1}{2}\,(2\sqrt{d} + b)^{\frac{1}{2}} \tag{A19}$$

Substituting these into equation (A14) and then into equation (A11) gives the following expression for the solution of the homogeneous differential equation

$$w_h = e^{\alpha x}\,(A\cos\beta x + B\sin\beta x) + e^{-\alpha x}\,(C\cos\beta x + D\sin\beta x) \tag{A20}$$

and $$w = w_h + w_o \tag{A21}$$

The constants A, B, C, and D can be solved for through the use of the boundary conditions.

Once the expression for w is known, its derivations can be calculated quite easily. In order to determine the stresses and strains in the tube, the only other quantities needed are $u_{,x}$ and $v_{,x}$, which can be calculated from the following relations

$$u_{,x} = \frac{\bar{A}_{66}}{D}\left[N_o - \frac{\bar{A}_{16}}{\bar{A}_{66}}\frac{T}{2\pi R} - \frac{A_{12}}{R}\,w + w_{,xx}\left(\frac{D_{11}}{R} - \frac{2\bar{A}_{16}D_{16}}{R\bar{A}_{66}}\right)\right] \tag{A22}$$

$$v_{,x} = \frac{A_{11}}{2\pi RD} - \frac{\bar{A}_{16}}{D} No + \frac{A_{12}\,\bar{A}_{16}}{RD} w + w_{,xx}\left[\frac{2D_{16}D - \bar{A}_{16}D_{11}\bar{A}_{66} + 2\bar{A}_{16}^2 D_{16}}{RD\bar{A}_{66}}\right.$$

The stresses in each ply are calculated from Hooke's law for plane stress,

$$\begin{bmatrix}\sigma_x\\ \sigma_\theta\\ \sigma_{x\theta}\end{bmatrix}^k = \begin{bmatrix}\bar{Q}_{11} & \bar{Q}_{12} & \bar{Q}_{16}\\ \bar{Q}_{12} & \bar{Q}_{22} & \bar{Q}_{26}\\ \bar{Q}_{16} & \bar{Q}_{26} & \bar{Q}_{66}\end{bmatrix}^k \begin{bmatrix}\epsilon_x\\ \epsilon_\theta\\ \epsilon_{x\theta}\end{bmatrix}^k \qquad (A24)$$

where $\bar{Q}_{ij}$ is the lamina stiffness matrix referred to an arbitrary set of axes.

A.2 Conclusions

In this paper is presented a method derived from the extension of Flugge's shell theory to anisotropic materials by which the stress variations along the length as well as across the thickness of a symmetrically laminated orthotropic cylinder can be calculated. A computer program has been written to perform this task and is listed in the following section. The results for a four ply circumferentially wrapped cylinder loaded under a combination of axial compression and internal pressure are also listed and plotted there. As can be readily seen from these results, the effects of the end contraints are confined to relatively small regions near the ends of the cylinder.

This analysis allows the researcher to more optimally design composite cylinders so that the test section is sufficiently far from the ends of the cylinder where the large

bending stresses are induced and the thickness of the tube can be chosen so that the stress variation across it remains very small. Also, other types of end attachments (boundary conditions) could be designed that might relieve these large bending stresses caused by rigidly clamping the ends of the cylinder.

A.3 Computer Program to Calculate Shell Stresses

Purpose: To calculate σ_x, σ_θ, $\sigma_{x\theta}$ as functions of x, the position along the length of the tube, and z, the position across the thickness, for circumferentially wrapped tubes.

Method: Calculate the mid-plane strains and curvatures and then determine the stresses from the Hooke's law relations.

Input: The data card contains the loading applied to the tube.

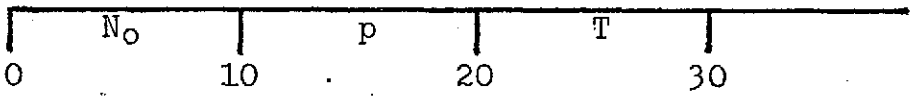

Output: Position along the length of the tube, x (tube end at x=0); position across the thickness of the tube, z (mid-plane reference surface at z=0); applied loadings, N_o, p, T; stresses σ_x, σ_θ, $\sigma_{x\theta}$; radial displacement and derivatives, w, $w_{,x}$, $w_{,xx}$.

```
// JOB    0001

LOG DRIVE   CART SPEC   CBRT AVAIL  PHY DRIVE
  0000        0001        0001        0000

V2 M11   ACTUAL  8K  CONFIG  8K

// FOR
*LIST SOURCE PROGRAM
*ONE WORD INTEGERS
*IOCS(1132PRINTER,PLOTTER,CARD)
C
C     THIS PROGRAM CALCULATES AS A FUNCTION OF X(THE POSITION ALONG THE
C     LENGTH OF THE TUBE) AND AS A FUNCTION OF Z(THE POSITION ACROSS THE
C     THICKNESS OF THE TUBE) THE AXIAL STRESS, THE RADIAL STRESS, AND
C     THE SHEARING STRESS RESULTING FROM ANY GIVEN COMBINATION OF AXIAL
C     FORCE, INTERNAL PRESSURE, AND TORQUE
C
      REAL NO,H,L1,L2,L3,LN,K(4)
      DIMENSION Q(3,3),E(3),STR(3),COF(4,4),WOM(4),N1(4),N2(4)
      PI=3.14159                                                    W
      R=1.020
      H=0.040
      Z=H/2.0
C
C     THE NEXT FIVE CARDS GIVE THE ELASTIC CONSTANTS OF THE COMPOSITE
C
      E11=0.4765E7
      E22=0.1211E7
      G12=0.4230E6
      V12=0.3363
      V21=0.0855
      VV=1.0-V12*V21
C
C     THE Q-MATRIX IS THE STIFFNESS MATRIX
C
      Q(1,1)=E22/VV
      Q(2,2)=E11/VV
      Q(1,2)=E11*V21/VV
      Q(2,1)=Q(1,2)
      Q(3,3)=G12
      Q(1,3)=0.0
      Q(2,3)=0.0
      Q(3,1)=Q(1,3)
      Q(3,2)=Q(2,3)
      A11=Q(1,1)*H
      A12=Q(1,2)*H
      A16=Q(1,3)*H
      A22=Q(2,2)*H
      A26=Q(2,3)*H
      A66=Q(3,3)*H
      D11=Q(1,1)*H**3.0/12.0
      D12=Q(1,2)*H**3.0/12.0
      D22=Q(2,2)*H**3.0/12.0
      D16=Q(1,3)*H**3.0/12.0
      D26=Q(2,3)*H**3.0/12.0
      D66=Q(3,3)*H**3.0/12.0
C
```

STIPULATE SHELL RADIUS AND THICKNESS

MATERIAL PROPERTIES

CALCULATE $\bar{Q}_{ij}$ MATRIX

CALCULATE A_{ij} MATRIX

CALCULATE D_{ij} MATRIX

ORIGINAL PAGE IS
OF POOR QUALITY

FOLDOUT FRAME 1

FOLDOUT FRAME 2

```
      THE NEXT 11 CARDS GIVE THE CONSTANTS USED IN THE DIFF. EQN.

      F22=A22+D22/R**2.0
      F66=A66+3.0*D66/R**2.0
      F16=D16/R**2.0
      D=A11*F66-F16**2.0
      L1=D11-(D11**2.0*F66-4.0*D11*D16*F16+4.0*D16**2.0*A11)/(D*R**2.0)
      L2=2.0*(F66*A12*D11-2.0*A12*F16*D16)/D
      L3=F22-A12**2.0*F66/D
      C1=SQRT(L3/(R**2.0*L1))
      C2=L2/(R**2.0*L1)
      D2=4.0*C1**2.0
      B2=C2**2.0
      WRITE(3,500)B2,D2
  500 FORMAT(1H ,'B2= ',E10.4,5X,'4D2= ',E10.4,///)
      ALF=SQRT(2.0*C1-C2)/2.0
      BET=SQRT(2.0*C1+C2)/2.0
      LN=5.0
      CO=COS(BET*LN)
      SI=SIN(BET*LN)
      EX=EXP(ALF*LN)
      EXM=EXP(-ALF*LN)

      THE COF-MATRIX IS FOUND BY APPLYING THE B.C.'S TO THE SOLUTION OF
      THE DIFF. EQN. FOR W.  IT IS THE MATRIX USED TO DETERMINE THE
      CONSTANTS A,B,C,D.

      THESE ARE FOR THE RIGIDLY CLAMPED CASE

      COF(1,1)=1.0
      COF(1,2)=0.0
      COF(1,3)=1.0
      COF(1,4)=0.0
      COF(2,1)=ALF
      COF(2,2)=BET
      COF(2,3)=-ALF
      COF(2,4)=BET
      COF(3,1)=CO*EX
      COF(3,2)=SI*EX
      COF(3,3)=CO*EXM
      COF(3,4)=SI*EXM
      COF(4,1)=(ALF*CO-BET*SI)*EX
      COF(4,2)=(BET*CO+ALF*SI)*EX
      COF(4,3)=(-ALF*CO-BET*SI)*EXM
      COF(4,4)=(BET*CO-ALF*SI)*EXM
      WRITE(3,600)COF
  600 FORMAT(4E14.4,/)

      NOW FIND THE INVERSE OF COF TO FIND A,B,C,D

      CALL MINV(COF,4,DET,N1,N2)
      WRITE(3,700)COF
  700 FORMAT(4E14.4,/)
      READ(2,100) NO,P,T
  100 FORMAT(3F10.2)
      CALL SCALF(6.0,0.10,0.0,-50.0)
      CALL FGRID(1,0.0,-50.0,1.0,100)
      CALL FGRID(0,0.0,0.0,0.0,0.10,25)
```

```
      CALL FCHAR(2.55,-1.0,0.20,0.20,0.0)
      WRITE(7,10)
   10 FORMAT('X (IN.)')
      CALL FCHAR(-0.15,10.0,0.20,0.20,PI/2.0)
      WRITE(7,11)
   11 FORMAT(' STRESS X (K.S.I.)')
      AX=0.50
      DO 12 I=1,5
      CALL FCHAR(AX-0.05/6.0,-2.50,0.10,0.10,3.0*PI/2.0)
      WRITE(7,13)AX
   13 FORMAT(F3.1)
      AX=AX+0.50
   12 CONTINUE
      AY=-50.0
      DO 14 I=1,11
      CALL FCHAR(-0.7/6.0,AY-0.50,0.10,0.10,0.0)
      WRITE(7,15)AY
   15 FORMAT(F6.1)
      AY=AY+10.0
   14 CONTINUE
      CALL FCHAR(1.25,-45.0,0.20,0.20,0.0)
      WRITE(7,81)
   81 FORMAT('STRESS X AS A FUNCTION OF X FOR')
      CALL FCHAR(1.25,-48.0,0.20,0.20,0.0)
      WRITE(7,82)
   82 FORMAT('RIGIDLY CLAMPED ENDS')
      CALL FCHAR(1.00,-51.0,0.20,0.20,0.0)
      WRITE(7,83)NO,P,T
   83 FORMAT('NO=',F8.2,' LB./IN.',',' P=',F7.1,' P.S.I.',',' T=',F4.1,' ',' I
     1N.-LB.')
      WO=R**2.0*P-1.0*(A12*F66*NO)/(R*D)+(A12*F16*T)/(2.0*PI*8*R*D))/L3/L3
      WOM(1)=-WO
      WOM(2)=0.0
      WOM(3)=-WO
      WOM(4)=0.0
      DO 3 II=1,4
      K(II)=0.0
      DO 3 JJ=1,4
      K(II)=K(II)+COF(II,JJ)*WOM(JJ)
    3 CONTINUE
      WRITE(3,800)K
  800 FORMAT(4E14.4)
      DO 21 L=1,3
      WRITE(3,200)
  200 FORMAT(1H1,3X,'X',5X,'Z',5X,'NO',7X,'P',9X,'T',5X,'STRESS X',5X,'(,'S
     7TRESS Y',5X,'STRESS XY',8X,'W',12X,'WX',11X,'WXX',/)
      X=0.0
      DO 1 N=1,51
      CS=COS(BET*X)
      SN=SIN(BET*X)
      W=(K(1)*CS+K(2)*SN)*EXP(ALF*X)+(K(3)*CS+K(4)*SN)*EXP(-ALF*X)+WO
      WX=((K(1)*ALF+K(2)*BET)*CS+(K(2)*ALF-K(1)*BET)*SN)*EXP(ALF*X)+((K(K(
     84)*BET-K(3)*ALF)*CS-(K(3)*BET+K(4)*ALF)*SN)*EXP(-ALF*X)
      WXX=((K(1)*ALF**2.0+2.0*K(2)*ALF*BET-K(1)*BET**2.0)*CS+(K(2)*ALF*.F**
     12.0-2.0*K(1)*ALF*BET-K(2)*BET**2.0)*SN)*EXP(ALF*X)+((K(3)*ALF**2.'2.0
     2-2.0*K(4)*ALF*BET-K(3)*BET**2.0)*CS +(K(4)*ALF**2.0+2.0*K(3)*ALF*.F*B
     3ET-K(4)*BET**2.0)*SN)*EXP(-ALF*X)                              B
      UX=F66*(NO+D11*WXX/R-A12*W/R-F16*T/(F66*2.0*PI*R)-2.0*F16*D16*WXX/XX/
```

PLOTTER SECTION

CALCULATE THE CONSTANTS A, B, C, D

FOLDOUT FRAME /

FOLDOUT FRAME 2

```
     1(R*F66))/D
      VX=(T*A11/(2.0*PI*R)-F16*NO+WXX*(2.0*D16*D-F16*D11*F66+2.0*D16*F16
     1**2.0)/(R*F66)+W*A12*F16/R)/D
      E(1)=UX-Z*WXX
      E(2)=(1.0-Z/R+(Z/R)**2.0)*W/R
      E(3)=(1.0+Z/R)*VX
      DO 2 I=1,3
      STR(I)=0.0
      DO 2 J=1,3
      STR(I)=STR(I)+Q(I,J)*E(J)
    2 CONTINUE
      WRITE(3,300)X,Z,NO,P,T,STR(1),STR(2),STR(3),W,WX,WXX
  300 FORMAT(1H ,F5.2,1X,F6.3,1X,F7.1,2X,F7.1,2X,F7.1,2X,E11.4,2X,E11.4,
     52X,E11.4,2X,E11.4,2X,E11.4,2X,E11.4)
      X=FLOAT(N)*2.5/50.0
    1 CONTINUE
      CALL FPLOT(-2,0.0,0.0)
      X=0.0
      DO 31 N=1,201
      CS=COS(BET*X)
      SN=SIN(BET*X)
      W=(K(1)*CS+K(2)*SN)*EXP(ALF*X)+(K(3)*CS+K(4)*SN)*EXP(-ALF*X)+WO
      WX=((K(1)*ALF+K(2)*BET)*CS+(K(2)*ALF-K(1)*BET)*SN)*EXP(ALF*X)+((K(
     84)*BET-K(3)*ALF)*CS-(K(3)*BET+K(4)*ALF)*SN)*EXP(-ALF*X)
      WXX=((K(1)*ALF**2.0+2.0*K(2)*ALF*BET-K(1)*BET**2.0)*CS+(K(2)*ALF**
     12.0-2.0*K(1)*ALF*BET-K(2)*BET**2.0)*SN)*EXP(ALF*X)+((K(3)*ALF**2.0
     2-2.0*K(4)*ALF*BET-K(3)*BET**2.0)*CS +(K(4)*ALF**2.0+2.0*K(3)*ALF*B
     3ET-K(4)*BET**2.0)*SN)*EXP(-ALF*X)                              B
      UX=F66*(NO+D11*WXX/R-A12*W/R-F16*T/(F66*2.0*PI*R)-2.0*F16*D16*WXX/
     1(R*F66))/D
      VX=(T*A11/(2.0*PI*R)-F16*NO+WXX*(2.0*D16*D-F16*D11*F66+2.0*D16*F16
     1(R*F66))/D
      VX=(T*A11/(2.0*PI*R)-F16*NO+WXX*(2.0*D16*D-F16*D11*F66+2.0*D16*F16
     1**2.0)/(R*F66)+W*A12*F16/R)/D
      E(1)=UX-Z*WXX
      E(2)=(1.0-Z/R+(Z/R)**2.0)*W/R
      E(3)=(1.0+Z/R)*VX
      DO 32 I=1,3
      STR(I)=0.0
      DO 32 J=1,3
      STR(I)=STR(I)+Q(I,J)*E(J)
   32 CONTINUE
      DO 73 I=1,3
      STR(I)=STR(I)/1000.0
   73 CONTINUE
      CALL FPLOT(0,X,STR(1))
      X=FLOAT(N)*2.5/200.0
   31 CONTINUE
      CALL FPLOT(1,0.0,0.0)
      Z=Z-0.02
   21 CONTINUE
      CALL EXIT
      END
```

CALCULATE THE STRAINS $\epsilon_x, \epsilon_\theta, \epsilon_{x\theta}$

CALCULATE THE STRESSES $\sigma_x, \sigma_\theta, \sigma_{x\theta}$

PLOTTER SECTION

The tube considered in this example was a circumferentially wrapped tube loaded to failure in simple axial compression. The expression used to calculate the ultimate failure stress was simply

$$\sigma_{ult.} = \frac{P_{ult.}}{A}$$

and this gave a value for σ_x of -13,158 psi. The computer program was then used to calculate the stress distribution in the tube using the ultimate load as input and it gave the same results in the test section of the tube. It also showed that the tube had been reinforced sufficiently at the ends to overcome the large stresses that were induced there. As can be seen from the printout, the stress distribution across the thickness was also fairly uniform.

X	Z	NO	P	T	STRESS X	STRESS Y	STRESS XY	W	WX	WXX
0.00	-0.020	-538.0	0.0	0.0	-0.9207E 04	-0.3097E 04	0.0000E 00	0.1164E-09	0.2677E-08	0.1537E 00
0.05	-0.020	-538.0	0.0	0.0	-0.1198E 05	-0.3359E 04	0.0000E 00	0.1409E-03	0.4738E-02	0.4562E-01
0.10	-0.020	-538.0	0.0	0.0	-0.1341E 05	-0.2573E 04	0.0000E 00	0.4069E-03	0.5439E-02	-0.1015E-01
0.15	-0.020	-538.0	0.0	0.0	-0.1392E 05	-0.1563E 04	0.0000E 00	0.6550E-03	0.4317E-02	-0.3021E-01
0.20	-0.020	-538.0	0.0	0.0	-0.1393E 05	-0.7247E 03	0.0000E 00	0.8316E-03	0.2744E-02	-0.3055E-01
0.25	-0.020	-538.0	0.0	0.0	-0.1373E 05	-0.1721E 03	0.0000E 00	0.9334E-03	0.1394E-02	-0.2278E-01
0.30	-0.020	-538.0	0.0	0.0	-0.1349E 05	0.1209E 03	0.0000E 00	0.9785E-03	0.4849E-03	-0.1373E-01
0.35	-0.020	-538.0	0.0	0.0	-0.1331E 05	0.2328E 03	0.0000E 00	0.9889E-03	-0.1035E-04	-0.6499E-02
0.40	-0.020	-538.0	0.0	0.0	-0.1319E 05	0.2420E 03	0.0000E 00	0.9824E-03	-0.2090E-03	-0.1876E-02
0.45	-0.020	-538.0	0.0	0.0	-0.1313E 05	0.2070E 03	0.0000E 00	0.9708E-03	-0.2358E-03	0.4887E-03
0.50	-0.020	-538.0	0.0	0.0	-0.1311E 05	0.1632E 03	0.0000E 00	0.9601E-03	-0.1856E-03	0.1324E-02
0.55	-0.020	-538.0	0.0	0.0	-0.1311E 05	0.1271E 03	0.0000E 00	0.9525E-03	-0.1172E-03	0.1321E-02
0.60	-0.020	-538.0	0.0	0.0	-0.1312E 05	0.1034E 03	0.0000E 00	0.9482E-03	-0.5909E-04	0.9783E-03
0.65	-0.020	-538.0	0.0	0.0	-0.1313E 05	0.9102E 02	0.0000E 00	0.9463E-03	-0.2016E-04	0.5857E-03
0.70	-0.020	-538.0	0.0	0.0	-0.1314E 05	0.8635E 02	0.0000E 00	0.9459E-03	0.8874E-06	0.2745E-03
0.75	-0.020	-538.0	0.0	0.0	-0.1314E 05	0.8604E 02	0.0000E 00	0.9462E-03	0.9217E-05	0.7702E-04
0.80	-0.020	-538.0	0.0	0.0	-0.1314E 05	0.8759E 02	0.0000E 00	0.9467E-03	0.1021E-04	-0.2323E-04
0.85	-0.020	-538.0	0.0	0.0	-0.1314E 05	0.8950E 02	0.0000E 00	0.9471E-03	0.7983E-05	-0.5799E-04
0.90	-0.020	-538.0	0.0	0.0	-0.1314E 05	0.9105E 02	0.0000E 00	0.9475E-03	0.5008E-05	-0.5712E-04
0.95	-0.020	-538.0	0.0	0.0	-0.1314E 05	0.9206E 02	0.0000E 00	0.9476E-03	0.2503E-05	-0.4199E-04
1.00	-0.020	-538.0	0.0	0.0	-0.1314E 05	0.9259E 02	0.0000E 00	0.9477E-03	0.8371E-06	-0.2497E-04
1.05	-0.020	-538.0	0.0	0.0	-0.1314E 05	0.9279E 02	0.0000E 00	0.9477E-03	-0.5706E-07	-0.1159E-04
1.10	-0.020	-538.0	0.0	0.0	-0.1314E 05	0.9280E 02	0.0000E 00	0.9477E-03	-0.4059E-06	-0.3155E-05
1.15	-0.020	-538.0	0.0	0.0	-0.1314E 05	0.9273E 02	0.0000E 00	0.9477E-03	-0.4427E-06	0.1093E-05
1.20	-0.020	-538.0	0.0	0.0	-0.1314E 05	0.9264E 02	0.0000E 00	0.9477E-03	-0.3431E-06	0.2538E-05
1.25	-0.020	-538.0	0.0	0.0	-0.1314E 05	0.9258E 02	0.0000E 00	0.9477E-03	-0.2139E-06	0.2469E-05
1.30	-0.020	-538.0	0.0	0.0	-0.1314E 05	0.9253E 02	0.0000E 00	0.9477E-03	-0.1060E-06	0.1802E-05
1.35	-0.020	-538.0	0.0	0.0	-0.1314E 05	0.9251E 02	0.0000E 00	0.9477E-03	-0.3471E-07	0.1064E-05
1.40	-0.020	-538.0	0.0	0.0	-0.1314E 05	0.9250E 02	0.0000E 00	0.9477E-03	0.3261E-08	0.4894E-06
1.45	-0.020	-538.0	0.0	0.0	-0.1314E 05	0.9250E 02	0.0000E 00	0.9477E-03	0.1785E-07	0.1289E-06
1.50	-0.020	-538.0	0.0	0.0	-0.1314E 05	0.9251E 02	0.0000E 00	0.9477E-03	0.1917E-07	-0.5105E-07
1.55	-0.020	-538.0	0.0	0.0	-0.1314E 05	0.9251E 02	0.0000E 00	0.9477E-03	0.1474E-07	-0.1110E-06
1.60	-0.020	-538.0	0.0	0.0	-0.1314E 05	0.9251E 02	0.0000E 00	0.9477E-03	0.9134E-08	-0.1066E-06
1.65	-0.020	-538.0	0.0	0.0	-0.1314E 05	0.9251E 02	0.0000E 00	0.9477E-03	0.4488E-08	-0.7732E-07
1.70	-0.020	-538.0	0.0	0.0	-0.1314E 05	0.9252E 02	0.0000E 00	0.9477E-03	0.1437E-08	-0.4538E-07
1.75	-0.020	-538.0	0.0	0.0	-0.1314E 05	0.9252E 02	0.0000E 00	0.9477E-03	-0.1747E-09	-0.2065E-07
1.80	-0.020	-538.0	0.0	0.0	-0.1314E 05	0.9252E 02	0.0000E 00	0.9477E-03	-0.7851E-09	-0.5253E-08
1.85	-0.020	-538.0	0.0	0.0	-0.1314E 05	0.9252E 02	0.0000E 00	0.9477E-03	-0.8302E-09	0.2367E-08
1.90	-0.020	-538.0	0.0	0.0	-0.1314E 05	0.9252E 02	0.0000E 00	0.9477E-03	-0.6337E-09	0.4853E-08
1.95	-0.020	-538.0	0.0	0.0	-0.1314E 05	0.9252E 02	0.0000E 00	0.9477E-03	-0.3899E-09	0.4608E-08
2.00	-0.020	-538.0	0.0	0.0	-0.1314E 05	0.9252E 02	0.0000E 00	0.9477E-03	-0.1899E-09	0.3316E-08
2.05	-0.020	-538.0	0.0	0.0	-0.1314E 05	0.9252E 02	0.0000E 00	0.9477E-03	-0.5949E-10	0.1933E-08
2.10	-0.020	-538.0	0.0	0.0	-0.1314E 05	0.9252E 02	0.0000E 00	0.9477E-03	0.8919E-11	0.8707E-09
2.15	-0.020	-538.0	0.0	0.0	-0.1314E 05	0.9252E 02	0.0000E 00	0.9477E-03	0.3442E-10	0.2138E-09
2.20	-0.020	-538.0	0.0	0.0	-0.1314E 05	0.9252E 02	0.0000E 00	0.9477E-03	0.3591E-10	-0.1075E-09
2.25	-0.020	-538.0	0.0	0.0	-0.1314E 05	0.9252E 02	0.0000E 00	0.9477E-03	0.2732E-10	-0.2085E-09
2.30	-0.020	-538.0	0.0	0.0	-0.1314E 05	0.9252E 02	0.0000E 00	0.9477E-03	0.1698E-10	-0.1929E-09
2.35	-0.020	-538.0	0.0	0.0	-0.1314E 05	0.9252E 02	0.0000E 00	0.9477E-03	0.8743E-11	-0.1336E-09
2.40	-0.020	-538.0	0.0	0.0	-0.1314E 05	0.9252E 02	0.0000E 00	0.9477E-03	0.3623E-11	-0.7312E-10
2.45	-0.020	-538.0	0.0	0.0	-0.1314E 05	0.9252E 02	0.0000E 00	0.9477E-03	0.1105E-11	-0.3170E-10
2.50	-0.020	-538.0	0.0	0.0	-0.1314E 05	0.9252E 02	0.0000E 00	0.9477E-03	0.2642E-18	-0.1729E-10
0.8938E-23		0.2916E-23		0.2307E-03		0.2302E-03				

X	Z	NO	P	T	STRESS X	S	STRESS Y	STRESS XY	W	WX	WXX
0.00	0.000	-538.0	0.0	0.0	-0.1312E 05	-	-0.4416E 04	0.0000E 00	0.1164E-09	0.2677E-08	0.1537E 00
0.05	0.000	-538.0	0.0	0.0	-0.1314E 05	-	-0.3764E 04	0.0000E 00	0.1409E-03	0.4738E-02	0.4562E-01
0.10	0.000	-538.0	0.0	0.0	-0.1315E 05	-	-0.2525E 04	0.0000E 00	0.4069E-03	0.5439E-02	-0.1015E-01
0.15	0.000	-538.0	0.0	0.0	-0.1316E 05	-	-0.1368E 04	0.0000E 00	0.6550E-03	0.4317E-02	-0.3021E-01
0.20	0.000	-538.0	0.0	0.0	-0.1316E 05	-	-0.5443E 03	0.0000E 00	0.8316E-03	0.2744E-02	-0.3055E-01
0.25	0.000	-538.0	0.0	0.0	-0.1315E 05	-	-0.6844E 02	0.0000E 00	0.9334E-03	0.1394E-02	-0.2278E-01
0.30	0.000	-538.0	0.0	0.0	-0.1315E 05		0.1426E 03	0.0000E 00	0.9785E-03	0.4849E-03	-0.1373E-01
0.35	0.000	-538.0	0.0	0.0	-0.1315E 05		0.1914E 03	0.0000E 00	0.9889E-03	-0.1035E-04	-0.6499E-02
0.40	0.000	-538.0	0.0	0.0	-0.1315E 05		0.1615E 03	0.0000E 00	0.9824E-03	-0.2090E-03	-0.1876E-02
0.45	0.000	-538.0	0.0	0.0	-0.1315E 05		0.1074E 03	0.0000E 00	0.9708E-03	-0.2358E-03	0.4887E-03
0.50	0.000	-538.0	0.0	0.0	-0.1315E 05		0.5751E 02	0.0000E 00	0.9601E-03	-0.1856E-03	0.1324E-02
0.55	0.000	-538.0	0.0	0.0	-0.1315E 05		0.2216E 02	0.0000E 00	0.9525E-03	-0.1172E-03	0.1321E-02
0.60	0.000	-538.0	0.0	0.0	-0.1315E 05		0.1900E 01	0.0000E 00	0.9482E-03	-0.5909E-04	0.9783E-03
0.65	0.000	-538.0	0.0	0.0	-0.1315E 05	-	-0.6992E 01	0.0000E 00	0.9463E-03	-0.2016E-04	0.5857E-03
0.70	0.000	-538.0	0.0	0.0	-0.1315E 05	-	-0.8955E 01	0.0000E 00	0.9459E-03	0.8874E-06	0.2745E-03
0.75	0.000	-538.0	0.0	0.0	-0.1315E 05	-	-0.7595E 01	0.0000E 00	0.9462E-03	0.9217E-05	0.7702E-04
0.80	0.000	-538.0	0.0	0.0	-0.1315E 05	-	-0.5236E 01	0.0000E 00	0.9467E-03	0.1021E-04	-0.2323E-04
0.85	0.000	-538.0	0.0	0.0	-0.1315E 05	-	-0.3078E 01	0.0000E 00	0.9471E-03	0.7983E-05	-0.5799E-04
0.90	0.000	-538.0	0.0	0.0	-0.1315E 05	-	-0.1564E 01	0.0000E 00	0.9475E-03	0.5008E-05	-0.5712E-04
0.95	0.000	-538.0	0.0	0.0	-0.1315E 05	-	-0.7009E 00	0.0000E 00	0.9476E-03	0.2503E-05	-0.4199E-04
1.00	0.000	-538.0	0.0	0.0	-0.1315E 05	-	-0.3262E 00	0.0000E 00	0.9477E-03	0.8371E-06	-0.2497E-04
1.05	0.000	-538.0	0.0	0.0	-0.1315E 05	-	-0.2477E 00	0.0000E 00	0.9477E-03	-0.5706E-07	-0.1159E-04
1.10	0.000	-538.0	0.0	0.0	-0.1315E 05	-	-0.3103E 00	0.0000E 00	0.9477E-03	-0.4059E-06	-0.3155E-05
1.15	0.000	-538.0	0.0	0.0	-0.1315E 05	-	-0.4126E 00	0.0000E 00	0.9477E-03	-0.4427E-06	0.1093E-05
1.20	0.000	-538.0	0.0	0.0	-0.1315E 05	-	-0.5056E 00	0.0000E 00	0.9477E-03	-0.3431E-06	0.2538E-05
1.25	0.000	-538.0	0.0	0.0	-0.1315E 05	-	-0.5689E 00	0.0000E 00	0.9477E-03	-0.2139E-06	0.2469E-05
1.30	0.000	-538.0	0.0	0.0	-0.1315E 05	-	-0.6072E 00	0.0000E 00	0.9477E-03	-0.1060E-06	0.1802E-05
1.35	0.000	-538.0	0.0	0.0	-0.1315E 05	-	-0.6232E 00	0.0000E 00	0.9477E-03	-0.3471E-07	0.1064E-05
1.40	0.000	-538.0	0.0	0.0	-0.1315E 05	-	-0.6256E 00	0.0000E 00	0.9477E-03	0.3261E-08	0.4894E-06
1.45	0.000	-538.0	0.0	0.0	-0.1315E 05	-	-0.6232E 00	0.0000E 00	0.9477E-03	0.1785E-07	0.1289E-06
1.50	0.000	-538.0	0.0	0.0	-0.1315E 05	-	-0.6186E 00	0.0000E 00	0.9477E-03	0.1917E-07	-0.5105E-07
1.55	0.000	-538.0	0.0	0.0	-0.1315E 05	-	-0.6146E 00	0.0000E 00	0.9477E-03	0.1474E-07	-0.1110E-06
1.60	0.000	-538.0	0.0	0.0	-0.1315E 05	-	-0.6123E 00	0.0000E 00	0.9477E-03	0.9134E-08	-0.1066E-06
1.65	0.000	-538.0	0.0	0.0	-0.1315E 05	-	-0.6106E 00	0.0000E 00	0.9477E-03	0.4488E-08	-0.7732E-07
1.70	0.000	-538.0	0.0	0.0	-0.1315E 05	-	-0.6095E 00	0.0000E 00	0.9477E-03	0.1437E-08	-0.4538E-07
1.75	0.000	-538.0	0.0	0.0	-0.1315E 05	-	-0.6095E 00	0.0000E 00	0.9477E-03	-0.1747E-09	-0.2065E-07
1.80	0.000	-538.0	0.0	0.0	-0.1315E 05	-	-0.6095E 00	0.0000E 00	0.9477E-03	-0.7851E-09	-0.5253E-08
1.85	0.000	-538.0	0.0	0.0	-0.1315E 05	-	-0.6100E 00	0.0000E 00	0.9477E-03	-0.8302E-09	0.2367E-08
1.90	0.000	-538.0	0.0	0.0	-0.1315E 05	-	-0.6100E 00	0.0000E 00	0.9477E-03	-0.6337E-09	0.4853E-08
1.95	0.000	-538.0	0.0	0.0	-0.1315E 05	-	-0.6100E 00	0.0000E 00	0.9477E-03	-0.3899E-09	0.4608E-08
2.00	0.000	-538.0	0.0	0.0	-0.1315E 05	-	-0.6100E 00	0.0000E 00	0.9477E-03	-0.1899E-09	0.3316E-08
2.05	0.000	-538.0	0.0	0.0	-0.1315E 05	-	-0.6106E 00	0.0000E 00	0.9477E-03	-0.5949E-10	0.1933E-08
2.10	0.000	-538.0	0.0	0.0	-0.1315E 05	-	-0.6106E 00	0.0000E 00	0.9477E-03	0.8919E-11	0.8707E-09
2.15	0.000	-538.0	0.0	0.0	-0.1315E 05	-	-0.6106E 00	0.0000E 00	0.9477E-03	0.3442E-10	0.2138E-09
2.20	0.000	-538.0	0.0	0.0	-0.1315E 05	-	-0.6106E 00	0.0000E 00	0.9477E-03	0.3591E-10	-0.1075E-09
2.25	0.000	-538.0	0.0	0.0	-0.1315E 05	-	-0.6106E 00	0.0000E 00	0.9477E-03	0.2732E-10	-0.2085E-09
2.30	0.000	-538.0	0.0	0.0	-0.1315E 05	-	-0.6106E 00	0.0000E 00	0.9477E-03	0.1698E-10	-0.1929E-09
2.35	0.000	-538.0	0.0	0.0	-0.1315E 05	-	-0.6100E 00	0.0000E 00	0.9477E-03	0.8743E-11	-0.1336E-09
2.40	0.000	-538.0	0.0	0.0	-0.1315E 05	-	-0.6100E 00	0.0000E 00	0.9477E-03	0.3623E-11	-0.7312E-10
2.45	0.000	-538.0	0.0	0.0	-0.1315E 05	-	-0.6100E 00	0.0000E 00	0.9477E-03	0.1105E-11	-0.3170E-10
2.50	0.000	-538.0	0.0	0.0	-0.1315E 05	-	-0.6100E 00	0.0000E 00	0.9477E-03	0.2642E-18	-0.1729E-10

FOLDOUT FRAME 1

FOLDOUT FRAME 2

X	Z	NO	P	T	STRESS X	STRESS Y	STRESS XY	W	WX	WXX
0.00	0.020	-538.0	0.0	0.0	-0.1705E 05	-0.5736E 04	0.0000E 00	0.1164E-09	0.2677E-08	0.1537E 00
0.05	0.020	-538.0	0.0	0.0	-0.1431E 05	-0.4169E 04	0.0000E 00	0.1409E-03	0.4738E-02	0.4562E-01
0.10	0.020	-538.0	0.0	0.0	-0.1290E 05	-0.2477E 04	0.0000E 00	0.4069E-03	0.5439E-02	-0.1015E-01
0.15	0.020	-538.0	0.0	0.0	-0.1239E 05	-0.1171E 04	0.0000E 00	0.6550E-03	0.4317E-02	-0.3021E-01
0.20	0.020	-538.0	0.0	0.0	-0.1238E 05	-0.3607E 03	0.0000E 00	0.8316E-03	0.2744E-02	-0.3055E-01
0.25	0.020	-538.0	0.0	0.0	-0.1258E 05	0.3890E 02	0.0000E 00	0.9334E-03	0.1394E-02	-0.2278E-01
0.30	0.020	-538.0	0.0	0.0	-0.1281E 05	0.1680E 03	0.0000E 00	0.9785E-03	0.4849E-03	-0.1373E-01
0.35	0.020	-538.0	0.0	0.0	-0.1299E 05	0.1537E 03	0.0000E 00	0.9889E-03	-0.1035E-04	-0.6499E-02
0.40	0.020	-538.0	0.0	0.0	-0.1311E 05	0.8490E 02	0.0000E 00	0.9824E-03	-0.2090E-03	-0.1876E-02
0.45	0.020	-538.0	0.0	0.0	-0.1317E 05	0.1162E 02	0.0000E 00	0.9708E-03	-0.2358E-03	0.4887E-03
0.50	0.020	-538.0	0.0	0.0	-0.1319E 05	-0.4448E 02	0.0000E 00	0.9601E-03	-0.1856E-03	0.1324E-02
0.55	0.020	-538.0	0.0	0.0	-0.1319E 05	-0.7909E 02	0.0000E 00	0.9525E-03	-0.1172E-03	0.1321E-02
0.60	0.020	-538.0	0.0	0.0	-0.1318E 05	-0.9601E 02	0.0000E 00	0.9482E-03	-0.5909E-04	0.9783E-03
0.65	0.020	-538.0	0.0	0.0	-0.1317E 05	-0.1013E 03	0.0000E 00	0.9463E-03	-0.2016E-04	0.5857E-03
0.70	0.020	-538.0	0.0	0.0	-0.1316E 05	-0.1006E 03	0.0000E 00	0.9459E-03	0.8874E-06	0.2745E-03
0.75	0.020	-538.0	0.0	0.0	-0.1316E 05	-0.9758E 02	0.0000E 00	0.9462E-03	0.9217E-05	0.7702E-04
0.80	0.020	-538.0	0.0	0.0	-0.1316E 05	-0.9441E 02	0.0000E 00	0.9467E-03	0.1021E-04	-0.2323E-04
0.85	0.020	-538.0	0.0	0.0	-0.1316E 05	-0.9200E 02	0.0000E 00	0.9471E-03	0.7983E-05	-0.5799E-04
0.90	0.020	-538.0	0.0	0.0	-0.1316E 05	-0.9052E 02	0.0000E 00	0.9475E-03	0.5008E-05	-0.5712E-04
0.95	0.020	-538.0	0.0	0.0	-0.1316E 05	-0.8981E 02	0.0000E 00	0.9476E-03	0.2503E-05	-0.4199E-04
1.00	0.020	-538.0	0.0	0.0	-0.1316E 05	-0.8958E 02	0.0000E 00	0.9477E-03	0.8371E-06	-0.2497E-04
1.05	0.020	-538.0	0.0	0.0	-0.1316E 05	-0.8962E 02	0.0000E 00	0.9477E-03	-0.5706E-07	-0.1159E-04
1.10	0.020	-538.0	0.0	0.0	-0.1316E 05	-0.8976E 02	0.0000E 00	0.9477E-03	-0.4059E-06	-0.3155E-05
1.15	0.020	-538.0	0.0	0.0	-0.1316E 05	-0.8989E 02	0.0000E 00	0.9477E-03	-0.4427E-06	0.1093E-05
1.20	0.020	-538.0	0.0	0.0	-0.1316E 05	-0.9000E 02	0.0000E 00	0.9477E-03	-0.3431E-06	0.2538E-05
1.25	0.020	-538.0	0.0	0.0	-0.1316E 05	-0.9006E 02	0.0000E 00	0.9477E-03	-0.2139E-06	0.2469E-05
1.30	0.020	-538.0	0.0	0.0	-0.1316E 05	-0.9009E 02	0.0000E 00	0.9477E-03	-0.1060E-06	0.1802E-05
1.35	0.020	-538.0	0.0	0.0	-0.1316E 05	-0.9010E 02	0.0000E 00	0.9477E-03	-0.3471E-07	0.1064E-05
1.40	0.020	-538.0	0.0	0.0	-0.1316E 05	-0.9010E 02	0.0000E 00	0.9477E-03	0.3261E-08	0.4894E-06
1.45	-0.020	-538.0	0.0	0.0	-0.1316E 05	-0.9009E 02	0.0000E 00	0.9477E-03	0.1785E-07	0.1289E-06
1.50	0.020	-538.0	0.0	0.0	-0.1316E 05	-0.9009E 02	0.0000E 00	0.9477E-03	0.1917E-07	-0.5105E-07
1.55	0.020	-538.0	0.0	0.0	-0.1316E 05	-0.9008E 02	0.0000E 00	0.9477E-03	0.1474E-07	-0.1110E-06
1.60	0.020	-538.0	0.0	0.0	-0.1316E 05	-0.9008E 02	0.0000E 00	0.9477E-03	0.9134E-08	-0.1066E-06
1.65	0.020	-538.0	0.0	0.0	-0.1316E 05	-0.9008E 02	0.0000E 00	0.9477E-03	0.4488E-08	-0.7732E-07
1.70	0.020	-538.0	0.0	0.0	-0.1316E 05	-0.9008E 02	0.0000E 00	0.9477E-03	0.1437E-08	-0.4538E-07
1.75	0.020	-538.0	0.0	0.0	-0.1316E 05	-0.9008E 02	0.0000E 00	0.9477E-03	-0.1747E-09	-0.2065E-07
1.80	0.020	-538.0	0.0	0.0	-0.1316E 05	-0.9008E 02	0.0000E 00	0.9477E-03	-0.7851E-09	-0.5253E-08
1.85	0.020	-538.0	0.0	0.0	-0.1316E 05	-0.9008E 02	0.0000E 00	0.9477E-03	-0.8302E-09	0.2367E-08
1.90	0.020	-538.0	0.0	0.0	-0.1316E 05	-0.9008E 02	0.0000E 00	0.9477E-03	-0.6337E-09	0.4853E-08
1.95	0.020	-538.0	0.0	0.0	-0.1316E 05	-0.9008E 02	0.0000E 00	0.9477E-03	-0.3899E-09	0.4608E-08
2.00	0.020	-538.0	0.0	0.0	-0.1316E 05	-0.9008E 02	0.0000E 00	0.9477E-03	-0.1899E-09	0.3316E-08
2.05	0.020	-538.0	0.0	0.0	-0.1316E 05	-0.9008E 02	0.0000E 00	0.9477E-03	-0.5949E-10	0.1933E-08
2.10	0.020	-538.0	0.0	0.0	-0.1316E 05	-0.9008E 02	0.0000E 00	0.9477E-03	0.8919E-11	0.8707E-09
2.15	0.020	-538.0	0.0	0.0	-0.1316E 05	-0.9008E 02	0.0000E 00	0.9477E-03	0.3442E-10	0.2138E-09
2.20	0.020	-538.0	0.0	0.0	-0.1316E 05	-0.9008E 02	0.0000E 00	0.9477E-03	0.3591E-10	-0.1075E-09
2.25	0.020	-538.0	0.0	0.0	-0.1316E 05	-0.9008E 02	0.0000E 00	0.9477E-03	0.2732E-10	-0.2085E-09
2.30	0.020	-538.0	0.0	0.0	-0.1316E 05	-0.9008E 02	0.0000E 00	0.9477E-03	0.1698E-10	-0.1929E-09
2.35	0.020	-538.0	0.0	0.0	-0.1316E 05	-0.9008E 02	0.0000E 00	0.9477E-03	0.8743E-11	-0.1336E-09
2.40	0.020	-538.0	0.0	0.0	-0.1316E 05	-0.9008E 02	0.0000E 00	0.9477E-03	0.3623E-11	-0.7312E-10
2.45	0.020	-538.0	0.0	0.0	-0.1316E 05	-0.9008E 02	0.0000E 00	0.9477E-03	0.1105E-11	-0.3170E-10
2.50	0.020	-538.0	0.0	0.0	-0.1316E 05	-0.9008E 02	0.0000E 00	0.9477E-03	0.2642E-18	-0.1729E-10

B2= 0.4175E 00 4D2= 0.1053E 06

COF

0.1000E 01	0.8998E 01	0.1573E 20	-0.1369E 21
0.0000E 00	0.9016E 01	0.3089E 20	0.4198E 21
0.1000E 01	-0.8998E 01	0.1308E-19	-0.3495E-18
0.0000E 00	0.9016E 01	0.2570E-19	-0.1132E-18

COF^{-1}

-0.1503E-38	0.0000E 00	0.1000E 01	0.9980E 00
0.0000E 00	0.0000E 00	0.0000E 00	0.1109E 00
0.3873E-19	0.1264E-19	-0.3873E-19	-0.8996E-19
-0.2850E-20	0.1451E-20	0.2850E-20	0.4238E-20
-0.3671E-22	-0.1197E-22	-0.9477E-03	-0.9458E-03
↑ A	↑ B	↑ C	↑ D

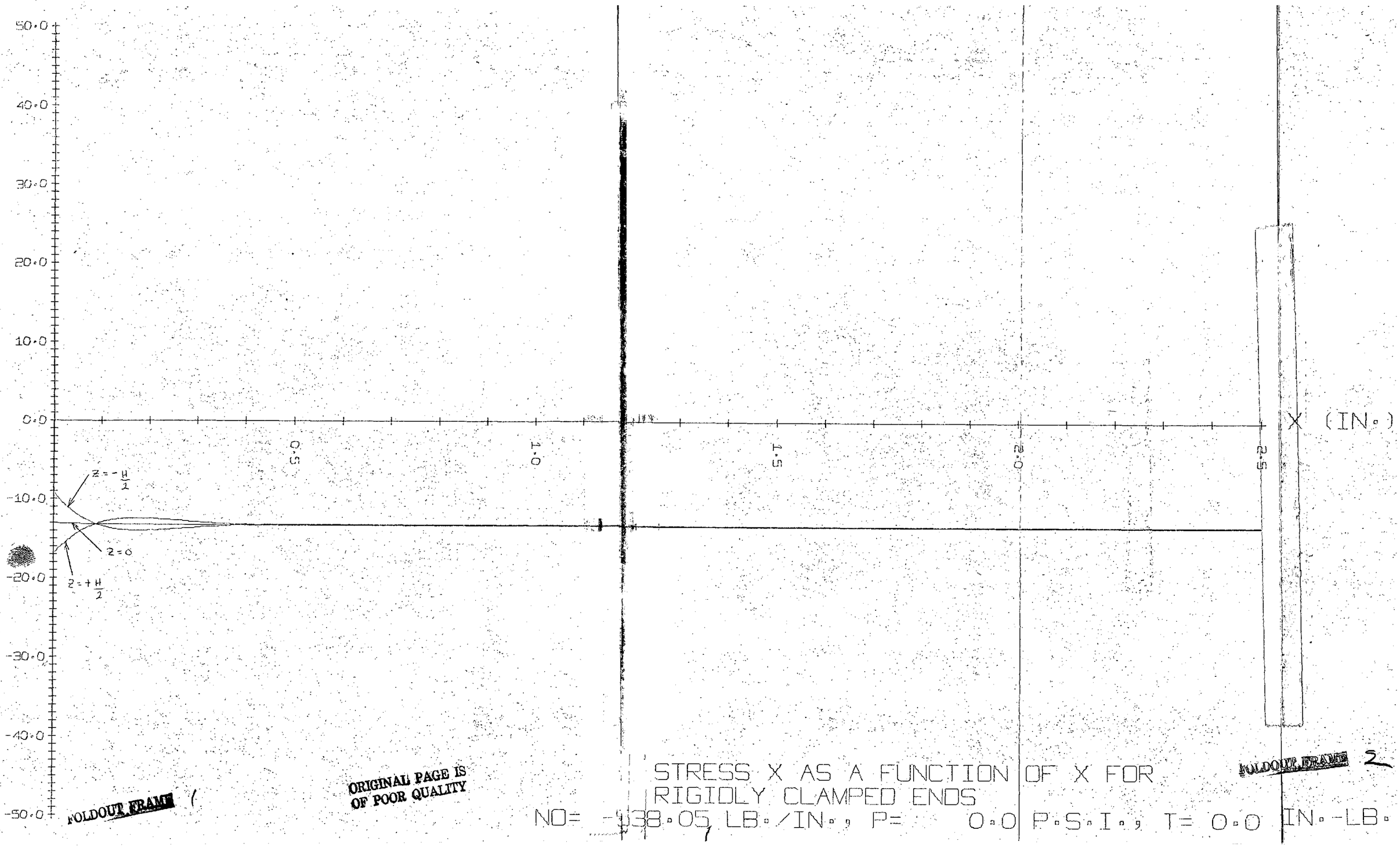

FOLDOUT FRAME 1

ORIGINAL PAGE IS OF POOR QUALITY

STRESS X AS A FUNCTION OF X FOR RIGIDLY CLAMPED ENDS

NO= -938.05 LB./IN., P= 0.0 P.S.I., T= 0.0 IN.-LB.

FOLDOUT FRAME 2

In this example, the tube was also wrapped circumferentially but it was under a more complex loading state. The tube was loaded in axial compression and internal pressure and the values of the load read into the computer program occurred at failure. The induced bending stresses were quite significant near the end of the tube that these rapidly converged to a uniform stress state.

X	Z	NO	P	T	STRESS X	STRESS Y	STRESS XY	W	WX	WXX
0.00	-0.015	-199.7	3225.0	0.0	0.9258E 05	0.3114E 05	0.0000E 00	0.3725E-08	0.4423E-07	0.5280E 01
0.05	-0.015	-199.7	3225.0	0.0	0.1456E 05	0.2671E 05	0.0000E 00	0.4582E-02	0.1487E 00	0.1127E 01
0.10	-0.015	-199.7	3225.0	0.0	-0.1956E 05	0.5280E 05	0.0000E 00	0.1247E-01	0.1518E 00	-0.6908E 00
0.15	-0.015	-199.7	3225.0	0.0	-0.2718E 05	0.8097E 05	0.0000E 00	0.1893E-01	0.1031E 00	-0.1098E 01
0.20	-0.015	-199.7	3225.0	0.0	-0.2305E 05	0.1006E 06	0.0000E 00	0.2276E-01	0.5227E-01	-0.8802E 00
0.25	-0.015	-199.7	3225.0	0.0	-0.1619E 05	0.1108E 06	0.0000E 00	0.2443E-01	0.1738E-01	-0.5152E 00
0.30	-0.015	-199.7	3225.0	0.0	-0.1061E 05	0.1144E 06	0.0000E 00	0.2479E-01	-0.4840E-03	-0.2189E 00
0.35	-0.015	-199.7	3225.0	0.0	-0.7326E 04	0.1145E 06	0.0000E 00	0.2458E-01	-0.6559E-02	-0.4371E-01
0.40	-0.015	-199.7	3225.0	0.0	-0.5910E 04	0.1133E 06	0.0000E 00	0.2423E-01	-0.6526E-02	0.3173E-01
0.45	-0.015	-199.7	3225.0	0.0	-0.5613E 04	0.1121E 06	0.0000E 00	0.2396E-01	-0.4373E-02	0.4764E-01
0.50	-0.015	-199.7	3225.0	0.0	-0.5803E 04	0.1113E 06	0.0000E 00	0.2380E-01	-0.2187E-02	0.3755E-01
0.55	-0.015	-199.7	3225.0	0.0	-0.6102E 04	0.1109E 06	0.0000E 00	0.2373E-01	-0.7073E-03	0.2171E-01
0.60	-0.015	-199.7	3225.0	0.0	-0.6339E 04	0.1107E 06	0.0000E 00	0.2371E-01	0.4107E-04	0.9066E-02
0.65	-0.015	-199.7	3225.0	0.0	-0.6478E 04	0.1107E 06	0.0000E 00	0.2372E-01	0.2886E-03	0.1678E-02
0.70	-0.015	-199.7	3225.0	0.0	-0.6537E 04	0.1108E 06	0.0000E 00	0.2374E-01	0.2802E-03	-0.1448E-02
0.75	-0.015	-199.7	3225.0	0.0	-0.6548E 04	0.1108E 06	0.0000E 00	0.2375E-01	0.1854E-03	-0.2064E-02
0.80	-0.015	-199.7	3225.0	0.0	-0.6540E 04	0.1109E 06	0.0000E 00	0.2376E-01	0.9147E-04	-0.1601E-02
0.85	-0.015	-199.7	3225.0	0.0	-0.6527E 04	0.1109E 06	0.0000E 00	0.2376E-01	0.2870E-04	-0.9148E-03
0.90	-0.015	-199.7	3225.0	0.0	-0.6517E 04	0.1109E 06	0.0000E 00	0.2376E-01	-0.2613E-05	-0.3750E-03
0.95	-0.015	-199.7	3225.0	0.0	-0.6511E 04	0.1109E 06	0.0000E 00	0.2376E-01	-0.1267E-04	-0.6372E-04
1.00	-0.015	-199.7	3225.0	0.0	-0.6508E 04	0.1109E 06	0.0000E 00	0.2376E-01	-0.1202E-04	0.6577E-04
1.05	-0.015	-199.7	3225.0	0.0	-0.6508E 04	0.1109E 06	0.0000E 00	0.2376E-01	-0.7855E-05	0.8936E-04
1.10	-0.015	-199.7	3225.0	0.0	-0.6508E 04	0.1109E 06	0.0000E 00	0.2376E-01	-0.3822E-05	0.6827E-04
1.15	-0.015	-199.7	3225.0	0.0	-0.6509E 04	0.1109E 06	0.0000E 00	0.2376E-01	-0.1161E-05	0.3851E-04
1.20	-0.015	-199.7	3225.0	0.0	-0.6509E 04	0.1109E 06	0.0000E 00	0.2376E-01	0.1477E-06	0.1549E-04
1.25	-0.015	-199.7	3225.0	0.0	-0.6509E 04	0.1109E 06	0.0000E 00	0.2376E-01	0.5559E-06	0.2383E-05
1.30	-0.015	-199.7	3225.0	0.0	-0.6510E 04	0.1109E 06	0.0000E 00	0.2376E-01	0.5159E-06	-0.2972E-05
1.35	-0.015	-199.7	3225.0	0.0	-0.6510E 04	0.1109E 06	0.0000E 00	0.2376E-01	0.3326E-06	-0.3865E-05
1.40	-0.015	-199.7	3225.0	0.0	-0.6510E 04	0.1109E 06	0.0000E 00	0.2376E-01	0.1596E-06	-0.2908E-05
1.45	-0.015	-199.7	3225.0	0.0	-0.6510E 04	0.1109E 06	0.0000E 00	0.2376E-01	0.4686E-07	-0.1620E-05
1.50	-0.015	-199.7	3225.0	0.0	-0.6510E 04	0.1109E 06	0.0000E 00	0.2376E-01	-0.7833E-08	-0.6394E-06
1.55	-0.015	-199.7	3225.0	0.0	-0.6510E 04	0.1109E 06	0.0000E 00	0.2376E-01	-0.2434E-07	-0.8750E-07
1.60	-0.015	-199.7	3225.0	0.0	-0.6510E 04	0.1109E 06	0.0000E 00	0.2376E-01	-0.2211E-07	0.1337E-06
1.65	-0.015	-199.7	3225.0	0.0	-0.6510E 04	0.1109E 06	0.0000E 00	0.2376E-01	-0.1408E-07	0.1670E-06
1.70	-0.015	-199.7	3225.0	0.0	-0.6510E 04	0.1109E 06	0.0000E 00	0.2376E-01	-0.6658E-08	0.1238E-06
1.75	-0.015	-199.7	3225.0	0.0	-0.6510E 04	0.1109E 06	0.0000E 00	0.2376E-01	-0.1885E-08	0.6813E-07
1.80	-0.015	-199.7	3225.0	0.0	-0.6510E 04	0.1109E 06	0.0000E 00	0.2376E-01	0.3985E-09	0.2635E-07
1.85	-0.015	-199.7	3225.0	0.0	-0.6510E 04	0.1109E 06	0.0000E 00	0.2376E-01	0.1064E-08	0.3132E-08
1.90	-0.015	-199.7	3225.0	0.0	-0.6510E 04	0.1109E 06	0.0000E 00	0.2376E-01	0.9473E-09	-0.5995E-08
1.95	-0.015	-199.7	3225.0	0.0	-0.6510E 04	0.1109E 06	0.0000E 00	0.2376E-01	0.5956E-09	-0.7211E-08
2.00	-0.015	-199.7	3225.0	0.0	-0.6510E 04	0.1109E 06	0.0000E 00	0.2376E-01	0.2775E-09	-0.5269E-08
2.05	-0.015	-199.7	3225.0	0.0	-0.6510E 04	0.1109E 06	0.0000E 00	0.2376E-01	0.7555E-10	-0.2863E-08
2.10	-0.015	-199.7	3225.0	0.0	-0.6510E 04	0.1109E 06	0.0000E 00	0.2376E-01	-0.1968E-10	-0.1084E-08
2.15	-0.015	-199.7	3225.0	0.0	-0.6510E 04	0.1109E 06	0.0000E 00	0.2376E-01	-0.4642E-10	-0.1076E-09
2.20	-0.015	-199.7	3225.0	0.0	-0.6510E 04	0.1109E 06	0.0000E 00	0.2376E-01	-0.4048E-10	0.2683E-09
2.25	-0.015	-199.7	3225.0	0.0	-0.6510E 04	0.1109E 06	0.0000E 00	0.2376E-01	-0.2509E-10	0.3110E-09
2.30	-0.015	-199.7	3225.0	0.0	-0.6510E 04	0.1109E 06	0.0000E 00	0.2376E-01	-0.1151E-10	0.2223E-09
2.35	-0.015	-199.7	3225.0	0.0	-0.6510E 04	0.1109E 06	0.0000E 00	0.2376E-01	-0.3135E-11	0.1152E-09
2.40	-0.015	-199.7	3225.0	0.0	-0.6510E 04	0.1109E 06	0.0000E 00	0.2376E-01	0.4734E-12	0.3503E-10
2.45	-0.015	-199.7	3225.0	0.0	-0.6510E 04	0.1109E 06	0.0000E 00	0.2376E-01	0.9619E-12	-0.9873E-11
2.50	-0.015	-199.7	3225.0	0.0	-0.6510E 04	0.1109E 06	0.0000E 00	0.2376E-01	-0.8910E-18	-0.2386E-10

X	Z	NO	P	T	STRESS X	STRESS Y	STRESS XY	W	WX	WXX
0.00	0.0000	-199.7	3225.0	0.0	-0.6171E 04	-0.2076E 04	0.0000E 00	0.3725E-08	0.4423E-07	0.5280E 01
0.05	0.0000	-199.7	3225.0	0.0	-0.6553E 04	0.1928E 05	0.0000E 00	0.4582E-02	0.1487E 00	0.1127E 01
0.10	0.0000	-199.7	3225.0	0.0	-0.6720E 04	0.5624E 05	0.0000E 00	0.1247E-01	0.1518E 00	-0.6908E 00
0.15	0.0000	-199.7	3225.0	0.0	-0.6758E 04	0.8651E 05	0.0000E 00	0.1893E-01	0.1031E 00	-0.1098E 01
0.20	0.0000	-199.7	3225.0	0.0	-0.6738E 04	0.1045E 06	0.0000E 00	0.2276E-01	0.5227E-01	-0.8802E 00
0.25	0.0000	-199.7	3225.0	0.0	-0.6704E 04	0.1123E 06	0.0000E 00	0.2443E-01	0.1738E-01	-0.5152E 00
0.30	0.0000	-199.7	3225.0	0.0	-0.6677E 04	0.1140E 06	0.0000E 00	0.2479E-01	-0.4840E-03	-0.2189E 00
0.35	0.0000	-199.7	3225.0	0.0	-0.6661E 04	0.1130E 06	0.0000E 00	0.2458E-01	-0.6559E-02	-0.4371E-01
0.40	0.0000	-199.7	3225.0	0.0	-0.6654E 04	0.1114E 06	0.0000E 00	0.2423E-01	-0.6526E-02	0.3173E-01
0.45	0.0000	-199.7	3225.0	0.0	-0.6652E 04	0.1101E 06	0.0000E 00	0.2396E-01	-0.4373E-02	0.4764E-01
0.50	0.0000	-199.7	3225.0	0.0	-0.6653E 04	0.1093E 06	0.0000E 00	0.2380E-01	-0.2187E-02	0.3755E-01
0.55	0.0000	-199.7	3225.0	0.0	-0.6654E 04	0.1090E 06	0.0000E 00	0.2373E-01	-0.7073E-03	0.2171E-01
0.60	0.0000	-199.7	3225.0	0.0	-0.6656E 04	0.1090E 06	0.0000E 00	0.2371E-01	0.4107E-04	0.9066E-02
0.65	0.0000	-199.7	3225.0	0.0	-0.6656E 04	0.1090E 06	0.0000E 00	0.2372E-01	0.2886E-03	0.1678E-02
0.70	0.0000	-199.7	3225.0	0.0	-0.6657E 04	0.1091E 06	0.0000E 00	0.2374E-01	0.2802E-03	-0.1448E-02
0.75	0.0000	-199.7	3225.0	0.0	-0.6657E 04	0.1091E 06	0.0000E 00	0.2375E-01	0.1854E-03	-0.2064E-02
0.80	0.0000	-199.7	3225.0	0.0	-0.6657E 04	0.1092E 06	0.0000E 00	0.2376E-01	0.9147E-04	-0.1601E-02
0.85	0.0000	-199.7	3225.0	0.0	-0.6657E 04	0.1092E 06	0.0000E 00	0.2376E-01	0.2870E-04	-0.9148E-03
0.90	0.0000	-199.7	3225.0	0.0	-0.6657E 04	0.1092E 06	0.0000E 00	0.2376E-01	-0.2613E-05	-0.3750E-03
0.95	0.0000	-199.7	3225.0	0.0	-0.6657E 04	0.1092E 06	0.0000E 00	0.2376E-01	-0.1267E-04	-0.6372E-04
1.00	0.0000	-199.7	3225.0	0.0	-0.6656E 04	0.1092E 06	0.0000E 00	0.2376E-01	-0.1202E-04	0.6577E-04
1.05	0.0000	-199.7	3225.0	0.0	-0.6656E 04	0.1092E 06	0.0000E 00	0.2376E-01	-0.7855E-05	0.8936E-04
1.10	0.0000	-199.7	3225.0	0.0	-0.6656E 04	0.1092E 06	0.0000E 00	0.2376E-01	-0.3822E-05	0.6827E-04
1.15	0.0000	-199.7	3225.0	0.0	-0.6656E 04	0.1092E 06	0.0000E 00	0.2376E-01	-0.1161E-05	0.3851E-04
1.20	0.0000	-199.7	3225.0	0.0	-0.6656E 04	0.1092E 06	0.0000E 00	0.2376E-01	0.1477E-06	0.1549E-04
1.25	0.0000	-199.7	3225.0	0.0	-0.6656E 04	0.1092E 06	0.0000E 00	0.2376E-01	0.5559E-06	0.2383E-05
1.30	0.0000	-199.7	3225.0	0.0	-0.6656E 04	0.1092E 06	0.0000E 00	0.2376E-01	0.5159E-06	-0.2972E-05
1.35	0.0000	-199.7	3225.0	0.0	-0.6657E 04	0.1092E 06	0.0000E 00	0.2376E-01	0.3326E-06	-0.3865E-05
1.40	0.0000	-199.7	3225.0	0.0	-0.6657E 04	0.1092E 06	0.0000E 00	0.2376E-01	0.1596E-06	-0.2908E-05
1.45	0.0000	-199.7	3225.0	0.0	-0.6657E 04	0.1092E 06	0.0000E 00	0.2376E-01	0.4686E-07	-0.1620E-05
1.50	0.0000	-199.7	3225.0	0.0	-0.6657E 04	0.1092E 06	0.0000E 00	0.2376E-01	-0.7833E-08	-0.6394E-06
1.55	0.0000	-199.7	3225.0	0.0	-0.6657E 04	0.1092E 06	0.0000E 00	0.2376E-01	-0.2434E-07	-0.8750E-07
1.60	0.0000	-199.7	3225.0	0.0	-0.6657E 04	0.1092E 06	0.0000E 00	0.2376E-01	-0.2211E-07	0.1337E-06
1.65	0.0000	-199.7	3225.0	0.0	-0.6657E 04	0.1092E 06	0.0000E 00	0.2376E-01	-0.1408E-07	0.1670E-06
1.70	0.0000	-199.7	3225.0	0.0	-0.6657E 04	0.1092E 06	0.0000E 00	0.2376E-01	-0.6658E-08	0.1238E-06
1.75	0.0000	-199.7	3225.0	0.0	-0.6657E 04	0.1092E 06	0.0000E 00	0.2376E-01	-0.1885E-08	0.6813E-07
1.80	0.0000	-199.7	3225.0	0.0	-0.6657E 04	0.1092E 06	0.0000E 00	0.2376E-01	0.3985E-09	0.2635E-07
1.85	0.0000	-199.7	3225.0	0.0	-0.6657E 04	0.1092E 06	0.0000E 00	0.2376E-01	0.1064E-08	0.3132E-08
1.90	0.0000	-199.7	3225.0	0.0	-0.6657E 04	0.1092E 06	0.0000E 00	0.2376E-01	0.9473E-09	-0.5995E-08
1.95	0.0000	-199.7	3225.0	0.0	-0.6657E 04	0.1092E 06	0.0000E 00	0.2376E-01	0.5956E-09	-0.7211E-08
2.00	0.0000	-199.7	3225.0	0.0	-0.6657E 04	0.1092E 06	0.0000E 00	0.2376E-01	0.2775E-09	-0.5269E-08
2.05	0.0000	-199.7	3225.0	0.0	-0.6657E 04	0.1092E 06	0.0000E 00	0.2376E-01	0.7555E-10	-0.2863E-08
2.10	0.0000	-199.7	3225.0	0.0	-0.6657E 04	0.1092E 06	0.0000E 00	0.2376E-01	-0.1968E-10	-0.1084E-08
2.15	0.0000	-199.7	3225.0	0.0	-0.6657E 04	0.1092E 06	0.0000E 00	0.2376E-01	-0.4642E-10	-0.1076E-09
2.20	0.0000	-199.7	3225.0	0.0	-0.6657E 04	0.1092E 06	0.0000E 00	0.2376E-01	-0.4048E-10	0.2683E-09
2.25	0.0000	-199.7	3225.0	0.0	-0.6657E 04	0.1092E 06	0.0000E 00	0.2376E-01	-0.2509E-10	0.3110E-09
2.30	0.0000	-199.7	3225.0	0.0	-0.6657E 04	0.1092E 06	0.0000E 00	0.2376E-01	-0.1151E-10	0.2223E-09
2.35	0.0000	-199.7	3225.0	0.0	-0.6657E 04	0.1092E 06	0.0000E 00	0.2376E-01	-0.3135E-11	0.1152E-09
2.40	0.0000	-199.7	3225.0	0.0	-0.6657E 04	0.1092E 06	0.0000E 00	0.2376E-01	0.4734E-12	0.3503E-10
2.45	0.0000	-199.7	3225.0	0.0	-0.6657E 04	0.1092E 06	0.0000E 00	0.2376E-01	0.9619E-12	-0.9873E-11
2.50	0.0000	-199.7	3225.0	0.0	-0.6657E 04	0.1092E 06	0.0000E 00	0.2376E-01	-0.8910E-18	-0.2386E-10

X	Z	NO	P	T	STRESS X	STRESS Y	STRESS XY	W	WX	WXX
0.00	0.0150	-199.7	3225.0	0.0	-0.1049E 06	-0.3529E 05	0.0000E 00	0.3725E-08	0.4423E-07	0.5280E 01
0.05	0.0150	-199.7	3225.0	0.0	-0.2766E 05	0.1187E 05	0.0000E 00	0.4582E-02	0.1487E 00	0.1127E 01
0.10	0.0150	-199.7	3225.0	0.0	0.6125E 04	0.5971E 05	0.0000E 00	0.1247E-01	0.1518E 00	-0.6908E 00
0.15	0.0150	-199.7	3225.0	0.0	0.1367E 05	0.9209E 05	0.0000E 00	0.1893E-01	0.1031E 00	-0.1098E 01
0.20	0.0150	-199.7	3225.0	0.0	0.9587E 04	0.1084E 06	0.0000E 00	0.2276E-01	0.5227E-01	-0.8802E 00
0.25	0.0150	-199.7	3225.0	0.0	0.2785E 04	0.1138E 06	0.0000E 00	0.2443E-01	0.1738E-01	-0.5152E 00
0.30	0.0150	-199.7	3225.0	0.0	-0.2731E 04	0.1136E 06	0.0000E 00	0.2479E-01	-0.4840E-03	-0.2189E 00
0.35	0.0150	-199.7	3225.0	0.0	-0.5991E 04	0.1115E 06	0.0000E 00	0.2458E-01	-0.6559E-02	-0.4371E-01
0.40	0.0150	-199.7	3225.0	0.0	-0.7393E 04	0.1095E 06	0.0000E 00	0.2423E-01	-0.6526E-02	0.3173E-01
0.45	0.0150	-199.7	3225.0	0.0	-0.7687E 04	0.1081E 06	0.0000E 00	0.2396E-01	-0.4373E-02	0.4764E-01
0.50	0.0150	-199.7	3225.0	0.0	-0.7498E 04	0.1074E 06	0.0000E 00	0.2380E-01	-0.2187E-02	0.3755E-01
0.55	0.0150	-199.7	3225.0	0.0	-0.7203E 04	0.1072E 06	0.0000E 00	0.2373E-01	-0.7073E-03	0.2171E-01
0.60	0.0150	-199.7	3225.0	0.0	-0.6968E 04	0.1072E 06	0.0000E 00	0.2371E-01	0.4107E-04	0.9066E-02
0.65	0.0150	-199.7	3225.0	0.0	-0.6830E 04	0.1073E 06	0.0000E 00	0.2372E-01	0.2886E-03	0.1678E-02
0.70	0.0150	-199.7	3225.0	0.0	-0.6772E 04	0.1074E 06	0.0000E 00	0.2374E-01	0.2802E-03	-0.1448E-02
0.75	0.0150	-199.7	3225.0	0.0	-0.6761E 04	0.1075E 06	0.0000E 00	0.2375E-01	0.1854E-03	-0.2064E-02
0.80	0.0150	-199.7	3225.0	0.0	-0.6769E 04	0.1075E 06	0.0000E 00	0.2376E-01	0.9147E-04	-0.1601E-02
0.85	0.0150	-199.7	3225.0	0.0	-0.6782E 04	0.1075E 06	0.0000E 00	0.2376E-01	0.2870E-04	-0.9148E-03
0.90	0.0150	-199.7	3225.0	0.0	-0.6792E 04	0.1075E 06	0.0000E 00	0.2376E-01	-0.2613E-05	-0.3750E-03
0.95	0.0150	-199.7	3225.0	0.0	-0.6798E 04	0.1075E 06	0.0000E 00	0.2376E-01	-0.1267E-04	-0.6372E-04
1.00	0.0150	-199.7	3225.0	0.0	-0.6800E 04	0.1075E 06	0.0000E 00	0.2376E-01	-0.1202E-04	0.6577E-04
1.05	0.0150	-199.7	3225.0	0.0	-0.6801E 04	0.1075E 06	0.0000E 00	0.2376E-01	-0.7855E-05	0.8936E-04
1.10	0.0150	-199.7	3225.0	0.0	-0.6800E 04	0.1075E 06	0.0000E 00	0.2376E-01	-0.3822E-05	0.6827E-04
1.15	0.0150	-199.7	3225.0	0.0	-0.6800E 04	0.1075E 06	0.0000E 00	0.2376E-01	-0.1161E-05	0.3851E-04
1.20	0.0150	-199.7	3225.0	0.0	-0.6799E 04	0.1075E 06	0.0000E 00	0.2376E-01	0.1477E-06	0.1549E-04
1.25	0.0150	-199.7	3225.0	0.0	-0.6799E 04	0.1075E 06	0.0000E 00	0.2376E-01	0.5559E-06	0.2383E-05
1.30	0.0150	-199.7	3225.0	0.0	-0.6799E 04	0.1075E 06	0.0000E 00	0.2376E-01	0.5159E-06	-0.2972E-05
1.35	0.0150	-199.7	3225.0	0.0	-0.6799E 04	0.1075E 06	0.0000E 00	0.2376E-01	0.3326E-06	-0.3865E-05
1.40	0.0150	-199.7	3225.0	0.0	-0.6799E 04	0.1075E 06	0.0000E 00	0.2376E-01	0.1596E-06	-0.2908E-05
1.45	0.0150	-199.7	3225.0	0.0	-0.6799E 04	0.1075E 06	0.0000E 00	0.2376E-01	0.4686E-07	-0.1620E-05
1.50	0.0150	-199.7	3225.0	0.0	-0.6799E 04	0.1075E 06	0.0000E 00	0.2376E-01	-0.7833E-08	-0.6394E-06
1.55	0.0150	-199.7	3225.0	0.0	-0.6799E 04	0.1075E 06	0.0000E 00	0.2376E-01	-0.2434E-07	-0.8750E-07
1.60	0.0150	-199.7	3225.0	0.0	-0.6799E 04	0.1075E 06	0.0000E 00	0.2376E-01	-0.2211E-07	0.1337E-06
1.65	0.0150	-199.7	3225.0	0.0	-0.6799E 04	0.1075E 06	0.0000E 00	0.2376E-01	-0.1408E-07	0.1670E-06
1.70	0.0150	-199.7	3225.0	0.0	-0.6799E 04	0.1075E 06	0.0000E 00	0.2376E-01	-0.6658E-08	0.1238E-06
1.75	0.0150	-199.7	3225.0	0.0	-0.6799E 04	0.1075E 06	0.0000E 00	0.2376E-01	-0.1885E-08	0.6813E-07
1.80	0.0150	-199.7	3225.0	0.0	-0.6799E 04	0.1075E 06	0.0000E 00	0.2376E-01	0.3985E-09	0.2635E-07
1.85	0.0150	-199.7	3225.0	0.0	-0.6799E 04	0.1075E 06	0.0000E 00	0.2376E-01	0.1064E-08	0.3132E-08
1.90	0.0150	-199.7	3225.0	0.0	-0.6799E 04	0.1075E 06	0.0000E 00	0.2376E-01	0.9473E-09	-0.5995E-08
1.95	0.0150	-199.7	3225.0	0.0	-0.6799E 04	0.1075E 06	0.0000E 00	0.2376E-01	0.5956E-09	-0.7211E-08
2.00	0.0150	-199.7	3225.0	0.0	-0.6799E 04	0.1075E 06	0.0000E 00	0.2376E-01	0.2775E-09	-0.5269E-08
2.05	0.0150	-199.7	3225.0	0.0	-0.6799E 04	0.1075E 06	0.0000E 00	0.2376E-01	0.7555E-10	-0.2863E-08
2.10	0.0150	-199.7	3225.0	0.0	-0.6799E 04	0.1075E 06	0.0000E 00	0.2376E-01	-0.1968E-10	-0.1084E-08
2.15	0.0150	-199.7	3225.0	0.0	-0.6799E 04	0.1075E 06	0.0000E 00	0.2376E-01	-0.4642E-10	-0.1076E-09
2.20	0.0150	-199.7	3225.0	0.0	-0.6799E 04	0.1075E 06	0.0000E 00	0.2376E-01	-0.4048E-10	0.2683E-09
2.25	0.0150	-199.7	3225.0	0.0	-0.6799E 04	0.1075E 06	0.0000E 00	0.2376E-01	-0.2509E-10	0.3110E-09
2.30	0.0150	-199.7	3225.0	0.0	-0.6799E 04	0.1075E 06	0.0000E 00	0.2376E-01	-0.1151E-10	0.2223E-09
2.35	0.0150	-199.7	3225.0	0.0	-0.6799E 04	0.1075E 06	0.0000E 00	0.2376E-01	-0.3135E-11	0.1152E-09
2.40	0.0150	-199.7	3225.0	0.0	-0.6799E 04	0.1075E 06	0.0000E 00	0.2376E-01	0.4734E-12	0.3503E-10
2.45	0.0150	-199.7	3225.0	0.0	-0.6799E 04	0.1075E 06	0.0000E 00	0.2376E-01	0.9619E-12	-0.9873E-11
2.50	0.0150	-199.7	3225.0	0.0	-0.6799E 04	0.1075E 06	0.0000E 00	0.2376E-01	-0.8910E-18	-0.2386E-10

B2= 0.4249E 00 4D2= 0.1974E 06

COF

0.1000E 01	0.1053E 02	-0.5836E 23	-0.1099E 25
0.0000E 00	0.1054E 02	0.4598E 23	-0.1312E 24
0.1000E 01	-0.1053E 02	-0.1057E-22	0.2347E-22
0.0000E 00	0.1054E 02	0.8329E-23	-0.1992E-21

COF^{-1}

0.0000E 00	0.0000E 00	0.1000E 01	0.9985E 00
0.0000E 00	0.0000E 00	0.0000E 00	0.9480E-01
-0.2253E-23	0.1888E-22	0.2253E-23	-0.1438E-22
-0.7897E-24	-0.1002E-23	0.7897E-24	0.2579E-23

0.5355E-25	-0.4488E-24	-0.2376E-01	-0.2372E-01
↑	↑	↑	↑
A	B	C	D

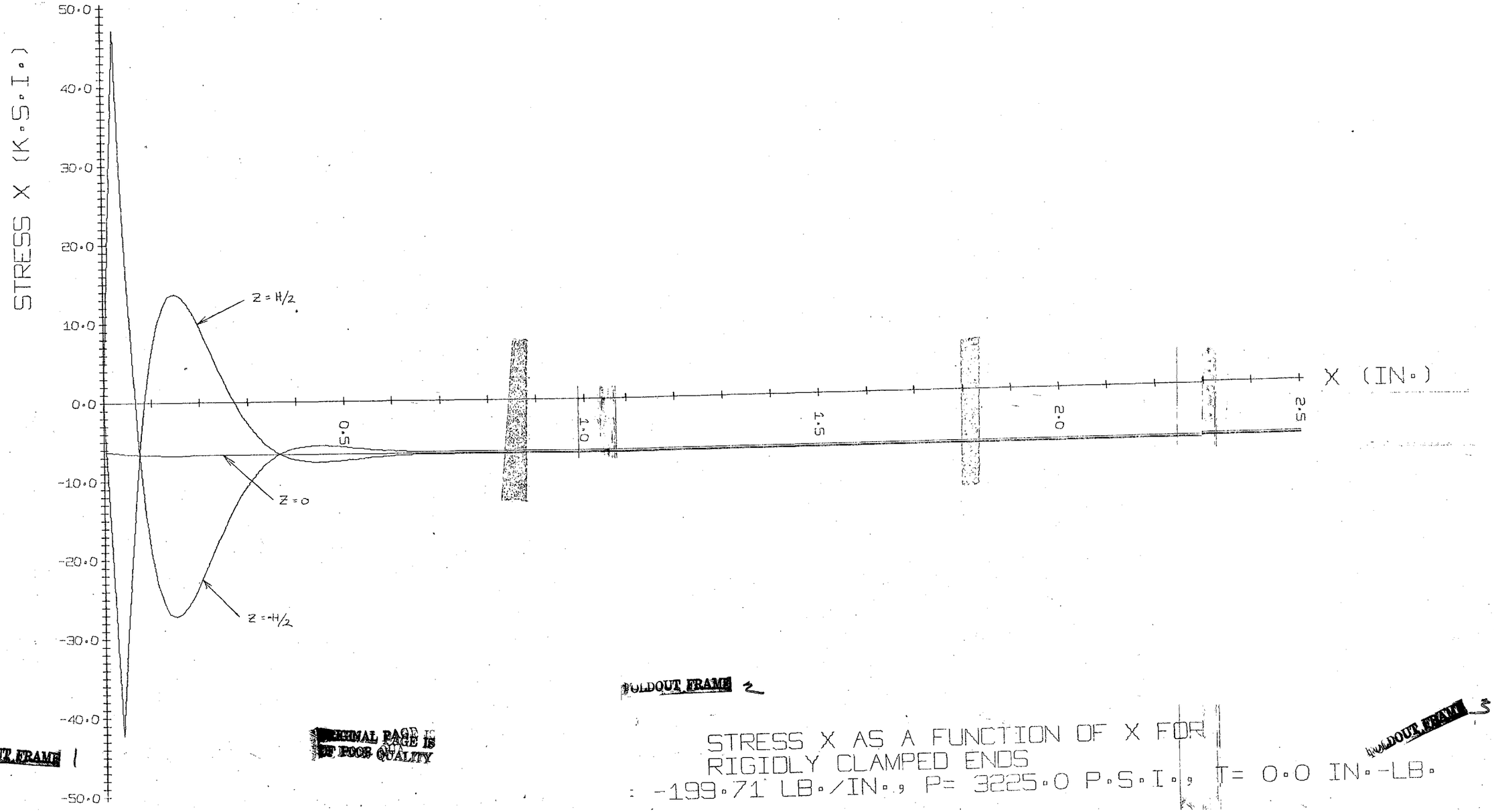

FOLDOUT FRAME 1

ORIGINAL PAGE IS OF POOR QUALITY

FOLDOUT FRAME 2

FOLDOUT FRAME 3

STRESS X AS A FUNCTION OF X FOR
RIGIDLY CLAMPED ENDS
: -199.71 LB./IN., P= 3225.0 P.S.I., T= 0.0 IN.-LB.

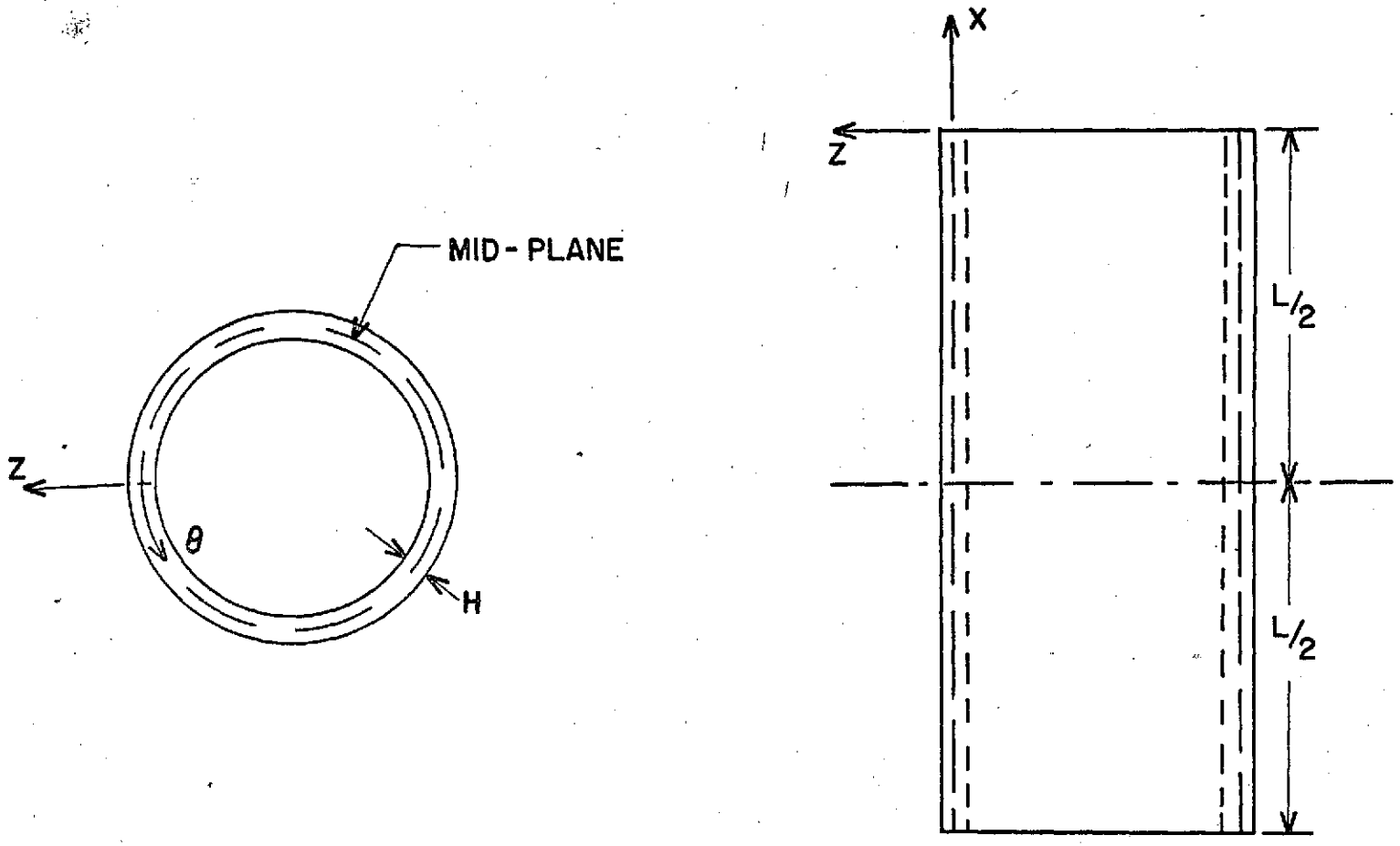

FIG. A-1 CYLINDER GEOMETRY

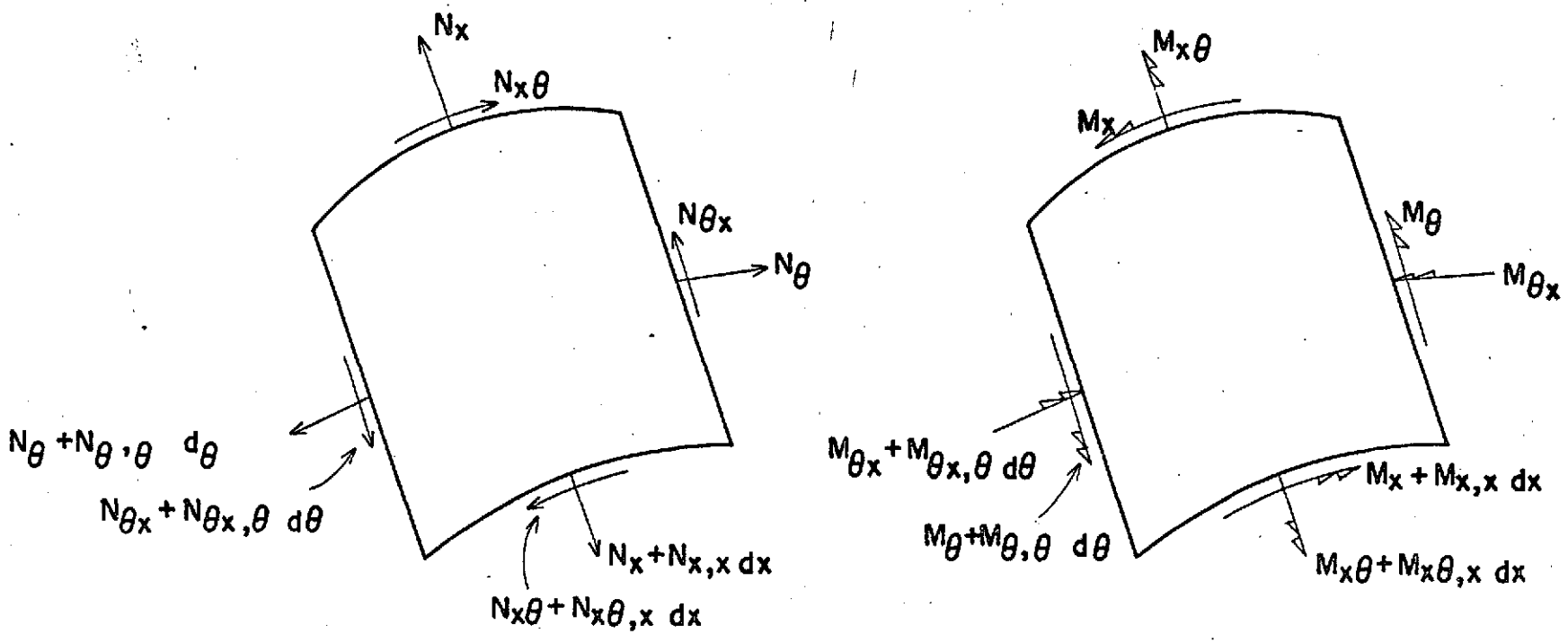

FIG. A-2 SHELL ELEMENT

APPENDIX B

THE EFFECTS OF TEMPERATURE ON THE MATERIAL PROPERTIES OF FIBREGLASS/EPOXY COMPOSITES

B.1 INTRODUCTION

With the increased use in recent years of advanced composites by the aerospace industry for the design of primary load carrying structures, ever increasing consideration has been given to the effects that varying environmental conditions may have upon the integrity of these materials. Some of the most common of the advanced composites are those made using glass fibres embedded in a polymer matrix; an example of which is Scotchply 1002. Although some references exist on the effects of temperature on these materials it is desirable to have specific data on the specific material in question. This study has been performed in order to evaluate the effect of various temperatures on the elastic constants and burst strength of circular cylindrical tubes made using Scotchply 1002. The results of this investigation are reported in the following sections.

B.2 Test Procedure

All sixteen of the tubes used in this investigation were tested under internal pressure and subsequently loaded to failure. The various phases of the testing procedure are shown in Figures B.1 to B.3. Each of the eleven strain gauged tubes was subjected to two separate loading constraints; the

first being free expansion under internal pressure (ie., both ϵ_x and ϵ_y being non-zero) and the second being clamped expansion under internal pressure such that $\epsilon_x = 0$ with, however, ϵ_y remaining non-zero. By using the data obtained from the axial and circumferential strain gauges when the tubes were loaded as stated above, it was possible to solve the constitutive equations for the elastic constants of the material (ie., E_{11}, E_{22}, ν_{12} and ν_{21}). Section 3 describes in detail the method of solution used. Figures B.4 through B.10 show the pressure vs. strain curves from which the data was obtained to perform the calculations.

In-situ test temperatures were varied over the range of -80°F to 250°F so that the effect of test temperature on the elastic constants of the material could be studied. Once this data was obtained the specimens were then loaded to failure under internal pressure in order to evaluate the effect of temperature on the transverse burst strength of the material.

For these tests, temperatures in excess of ambient room temperature were obtained using a Blue "M" Oven, whereas temperatures below ambient were achieved using a Tenny Junior environmental chamber. In order to ensure that consistent in-situ test temperatures were obtained, each of the specimens was equipped with thermocouples which were monitored at all times during each test. The temperature of each tube was allowed to stabilize at the desired value before testing began. This nominally required 0.75 hours for each test. By

using the Blue "M" Oven and the Tenny Junior Chamber it was possible to achieve a temperature stability of $\pm$ 1°F during each test run.

B.3 Basic Equations

For any anisotropic material it is possible to write the constitutive or Hooke's Law relations in the following form:

$$\begin{bmatrix} \sigma_x \\ \sigma_y \\ \sigma_{xy} \end{bmatrix}^k = \begin{bmatrix} \bar{Q}_{11} & \bar{Q}_{12} & \bar{Q}_{16} \\ \bar{Q}_{12} & \bar{Q}_{22} & \bar{Q}_{26} \\ \bar{Q}_{16} & \bar{Q}_{26} & \bar{Q}_{66} \end{bmatrix}^k \begin{bmatrix} \epsilon_x \\ \epsilon_y \\ \epsilon_{xy} \end{bmatrix}^k \qquad \text{(B1)}$$

where the superscript, k, denotes the k^{th} lamina of the material. Since all of the tubes used in this investigation were 3 ply, 90° laminates the superscript may, in this case, be omitted.

The components of the stiffness matrix, $[\bar{Q}]$ are given by the relations:

$$\begin{aligned}
\bar{Q}_{11} &= Q_{11}\cos^4\theta + 2(Q_{12} + 2Q_{66})\sin^2\theta\cos^2\theta + Q_{22}\sin^4\theta \\
\bar{Q}_{22} &= Q_{11}\sin^4\theta + 2(Q_{12} + 2Q_{66})\sin^2\theta\cos^2\theta + Q_{22}\cos^4\theta \\
\bar{Q}_{12} &= (Q_{11} + Q_{22} - 4Q_{66})\sin^2\theta\cos^2\theta + Q_{66}(\sin^4\theta + \cos^4\theta) \\
\bar{Q}_{66} &= (Q_{11} + Q_{22} - 2Q_{12} - 2Q_{66})\sin^2\theta\cos^2\theta + Q_{66}(\sin^4\theta + \cos^4\theta) \\
\bar{Q}_{16} &= (Q_{11} - Q_{12} - 2Q_{66})\sin\theta\cos^3\theta + (Q_{12} - Q_{22} + 2Q_{66})\sin^3\theta\cos\theta \\
\bar{Q}_{26} &= (Q_{11} - Q_{12} - 2Q_{66})\sin^3\theta\cos\theta + (Q_{12} - Q_{22} + 2Q_{66})\sin\theta\cos^3\theta
\end{aligned} \qquad \text{(B2)}$$

where the Q_{ij} (i,j = 1,2,6) are the components of the stiffness matrix for the lamina coordinate system, and may be ex-

pressed as:

$$Q_{11} = E_{11}/(1 - \nu_{12}\nu_{21})$$

$$Q_{22} = E_{22}/(1 - \nu_{12}\nu_{21})$$

$$Q_{12} = \nu_{21}\, E_{11}/(1 - \nu_{12}\nu_{21}) = \nu_{12}\, E_{22}/(1 - \nu_{12}\nu_{21}) \qquad (B3)$$

$$Q_{66} = G_{12}$$

$$Q_{16} = Q_{26} = 0$$

Thus, with a wrap angle of 90° as for the tubes being considered here, equations (B2) reduce to:

$$\bar{Q}_{11} = Q_{22} = E_{22}/(1 - \nu_{12}\nu_{21})$$

$$\bar{Q}_{22} = Q_{11} = E_{11}/(1 - \nu_{12}\nu_{21})$$

$$\bar{Q}_{12} = Q_{12} = \nu_{21}\, E_{11}/(1 - \nu_{12}\nu_{21}) \qquad (B4)$$

$$\bar{Q}_{66} = Q_{66} = G_{12}$$

$$\bar{Q}_{16} = \bar{Q}_{26} = 0$$

The constitutive equation (B1) can therefore be expressed in matrix form as:

$$\begin{bmatrix} \sigma_x \\ \sigma_y \\ \sigma_{xy} \end{bmatrix} = \begin{bmatrix} Q_{22} & Q_{12} & 0 \\ Q_{12} & Q_{11} & 0 \\ 0 & 0 & Q_{66} \end{bmatrix} \begin{bmatrix} \epsilon_x \\ \epsilon_y \\ \epsilon_{xy} \end{bmatrix} \qquad (B5)$$

Equation (B5) can now be expanded taking into consideration the two separate loading cases:

$$\sigma_{x1} = \frac{E_{22}}{\beta}\epsilon_{x1} + \frac{\nu_{12}\, E_{22}}{\beta}\epsilon_{y1} \qquad (B6.a)$$

$$\sigma_{y1} = \frac{\nu_{12}\, E_{22}}{\beta}\epsilon_{x1} + \frac{E_{11}}{\beta}\epsilon_{y1} \qquad (B6.b)$$

$$\sigma_{xy1} = G_{12}\,\epsilon_{xy1} \tag{B6.c}$$

and,
$$\sigma_{x2} = \frac{\nu_{12}\,E_{22}}{\beta}\,\epsilon_{y2} \tag{B6.d}$$

$$\sigma_{y2} = \frac{E_{11}}{\beta}\,\epsilon_{y2} \tag{B6.e}$$

$$\sigma_{xy2} = G_{12}\,\epsilon_{xy2} \tag{B6.f}$$

where the subscripts 1 and 2 denote the free expansion and clamped loading conditions, respectively, and $\beta = 1 - \nu_{12}\,\nu_{21}$.

By setting $\sigma_{y1} = \sigma_{y2}$, equation (B6) can be reduced to the set:

$$\sigma_{x1} = \frac{E_{22}}{\beta}\,\epsilon_{x1} + \frac{\nu_{12}\,E_{22}}{\beta}\,\epsilon_{y1} \tag{B7.a}$$

$$\sigma_{y1} = \frac{\nu_{12}\,E_{22}}{\beta}\,\epsilon_{x1} + \frac{E_{11}}{\beta}\,\epsilon_{y1} \tag{B7.b}$$

$$\sigma_{y2} = \sigma_{y1} = \frac{E_{11}}{\beta}\,\epsilon_{y2} \tag{B7.c}$$

which may be readily solved for E_{11}, E_{22}, ν_{12} and ν_{21} as follows,

$$\frac{E_{11}}{\beta} = \frac{\sigma_{y2}}{\epsilon_{y2}} \tag{B8}$$

$$\frac{E_{22}}{\beta} = \frac{1}{\epsilon_{x1}}\left(\sigma_{x1} - \frac{\sigma_{y1}\,\epsilon_{y1}\,(\epsilon_{y2} - \epsilon_{y1})}{\epsilon_{x1}\,\epsilon_{y2}}\right) \tag{B9}$$

$$\nu_{12} = \frac{\sigma_{y1}\,(\epsilon_{y2} - \epsilon_{y1})\,\epsilon_{x1}}{\sigma_{x1}\,\epsilon_{x1}\,\epsilon_{y2} - \sigma_{y1}\epsilon_{y1}(\epsilon_{y2} - \epsilon_{y1})} \tag{B10}$$

$$\nu_{21} = \frac{(\epsilon_{y2} - \epsilon_{y1})}{\epsilon_{x1}} \qquad (B11)$$

It should be noted that the condition that $\sigma_{y1} = \sigma_{y2}$ is easily accomplished experimentally by ensuring that under both of the loading conditions the tubes are loaded to the same internal pressure.

The above calculations were performed for each tube and the results are listed in TableIV. The geometric properties of each of the tubes tested can be found in Table B.1.

B.4 Discussion of Experimental Results

As can be seen from the graphs in Figures B.11 to B.15, the testing temperature has little effect on the value of E_{11}. The calculated values are well within $\pm$ 10% of the average value of about 5.9×10^6 psi. It was expected that the range of temperatures investigated would not affect the properties of the brittle fibres as much as it would affect those of the ductile epoxy matrix. Therfore, since E_{11} is primarily a function of the fibre modulus it should not change very much.

The test temperature had a greater effect on the value of E_{22} since it is primarily a function of the modulus of the matrix. At high temperatures the matrix is very plastic and strains easily so that E_{22} takes on a very low value. At lower temperatures the matrix becomes brittle and strains less than it would at higher temperatures. This increased slope of the stress-strain curve results in a higher value for E_{22}.

The same reasoning applies to the effect of temperature on the transverse burst strength of the material. Since it strains easier at higher temperatures, fracture will occur at a lower value of internal pressure and the opposite is true for the lower temperatures.

B.5 Conclusions

The effects of testing temperature on the transverse burst strength and the material properties of a fibreglass/epoxy composite have been reported in this Appendix. It has been shown that variations in the temperature over the range being investigated have pronounced effects on the properties of the matrix material but do not affect the fibres significantly. Since it is the matrix material which is most affected by the temperature changes, the effects on other mechanical properties such as shear strength and modulus which are directly related to the matrix should be investigated fully in order to obtain a more complete understanding of the changes taking place in the composite at different temperatures.

Table B.1
Geometry of Laminated Tubes

TABLE B.1 TUBE GEOMETRIES

TUBE NO.	$\bar{E}$ AVERAGE THICKNESS (IN.)	R AVERAGE RADIUS (IN.)
11c 90°	0.0295	1.006
12c 90°	0.0295	1.006
13c 90°	0.0295	1.006
14a 90°	0.0282	1.005
14b 90°	0.0298	1.006
14c 90°	0.0288	1.005
15a 90°	0.0282	1.005
16a 90°	0.0301	1.006
19a 90°	0.0297	1.006
19b 90°	0.0296	1.006
22b 90°	0.0304	1.006
22c 90°	0.0292	1.006

23a 90°	0.0307	1.0¢b
23b 90°	0.0308	1.0¢b
23c 90°	0.0302	1.0¢b
24b 90°	0.0304	1.0¢b

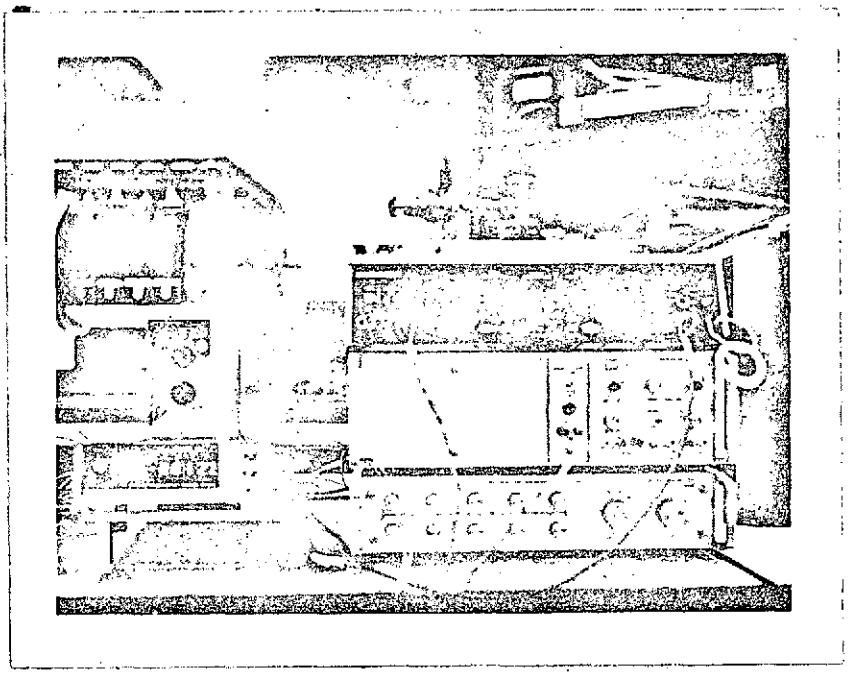

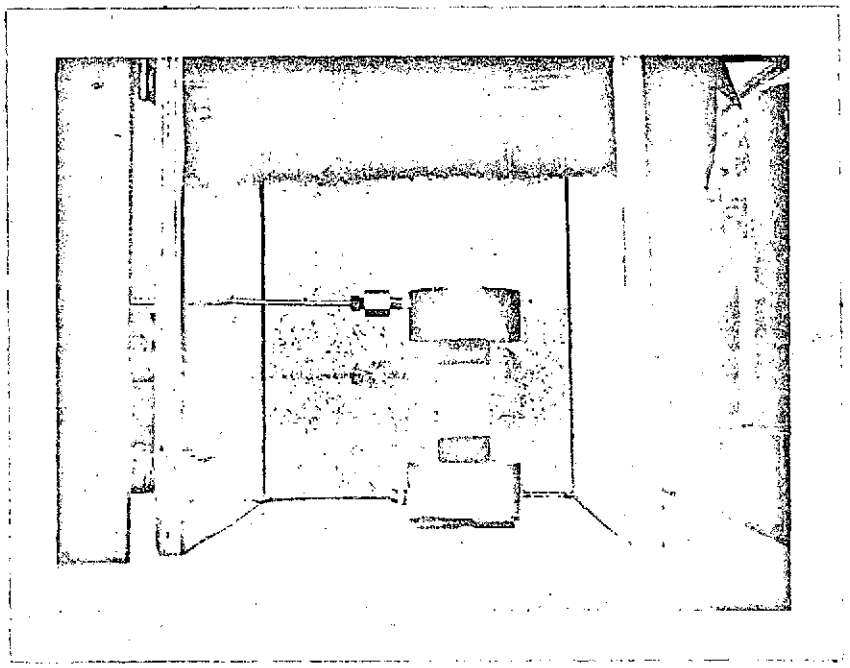

FIGURE B.1

INSTRUMENTATION AND A TUBE READY FOR TESTING

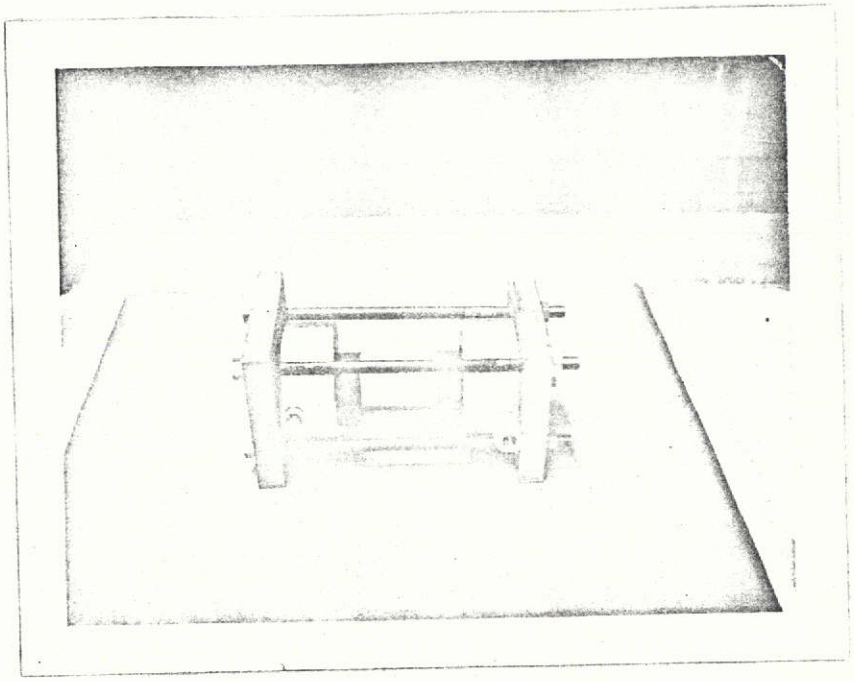

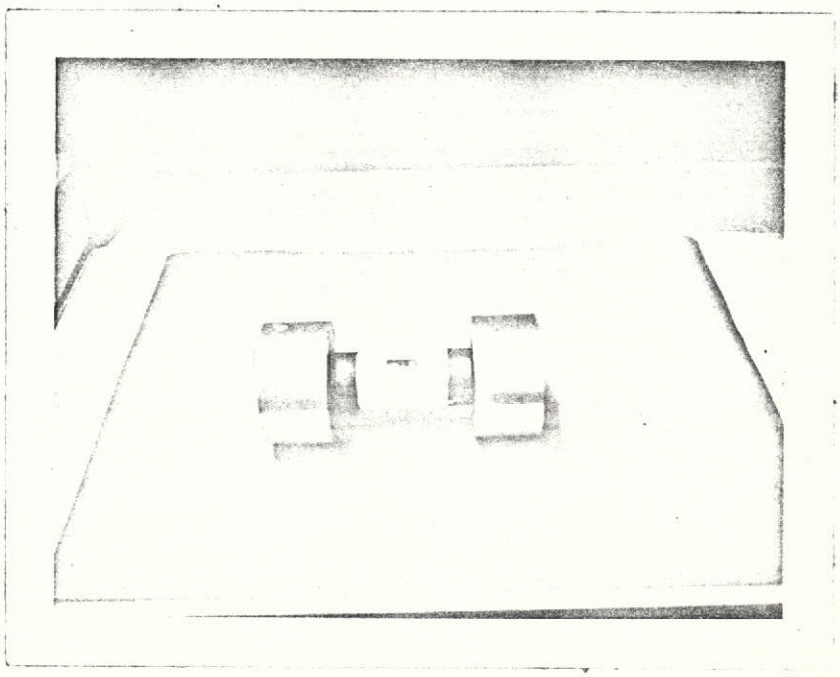

FIGURE B.2

CLAMPING APPARATUS AND A FRACTURED TUBE

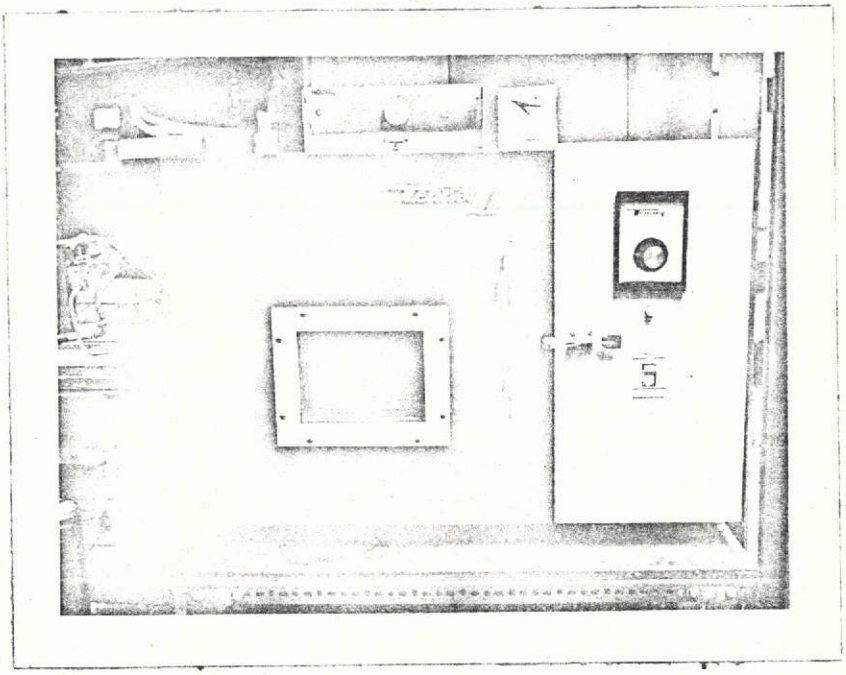

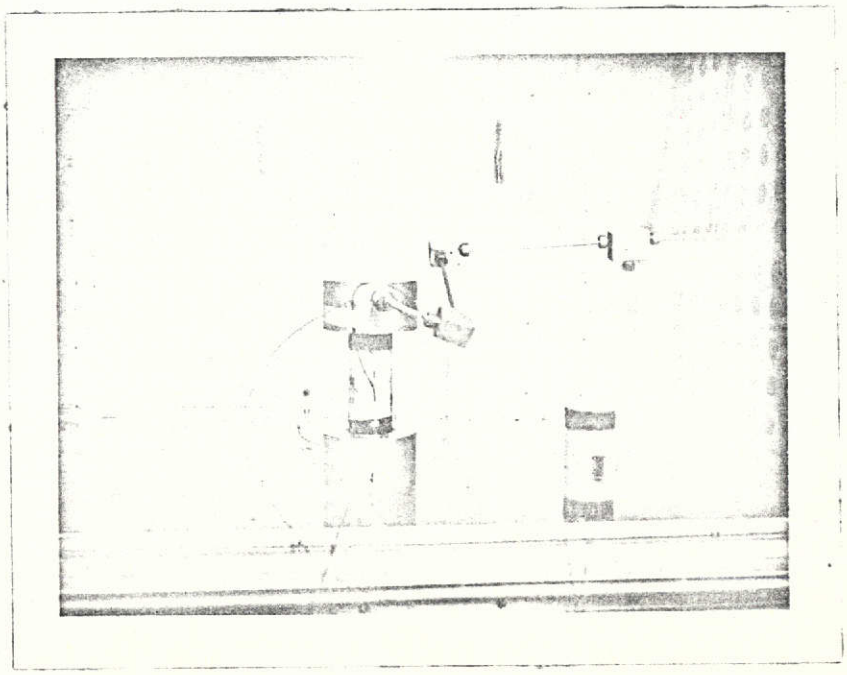

FIG. B3 CHAMBERS FOR THE COLD AND HOT TEMPERATURE TESTS

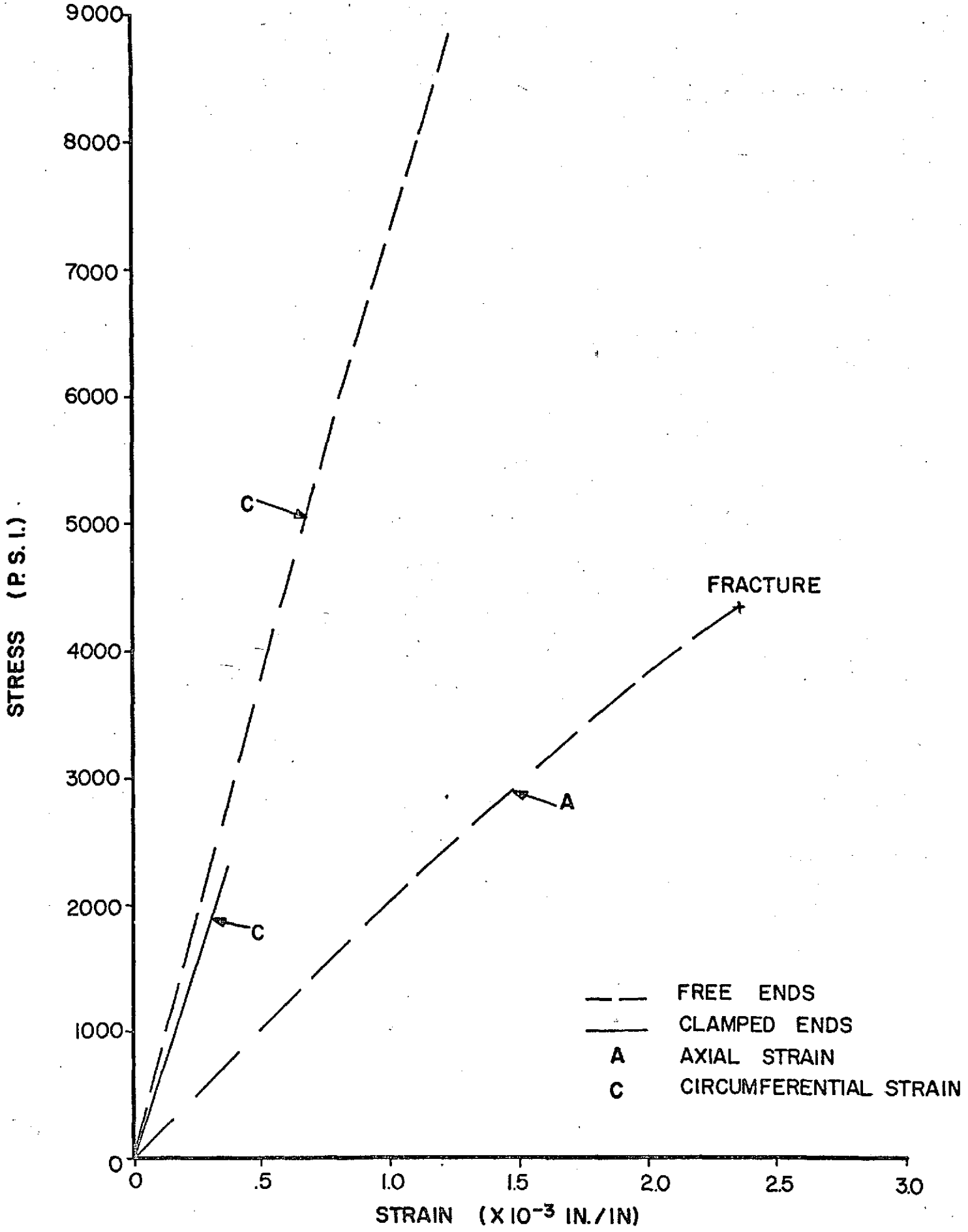

FIG. 8.4 STRESS-STRAIN CURVES FOR TUBE 24 b 90° (TEMP.- 80° F)

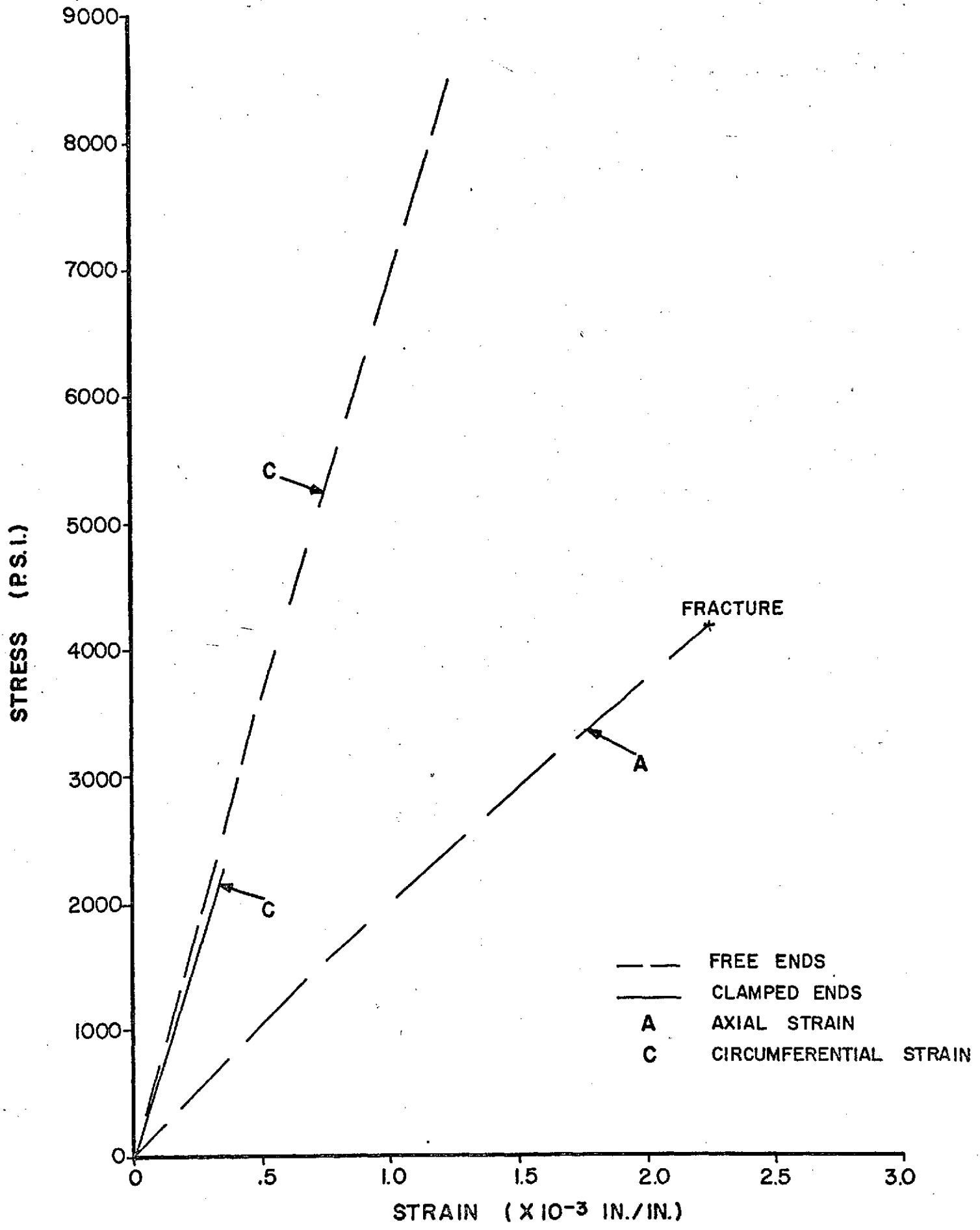

FIG. B5 STRESS-STRAIN CURVES FOR TUBE 23b 90° (TEMP.-45° F)

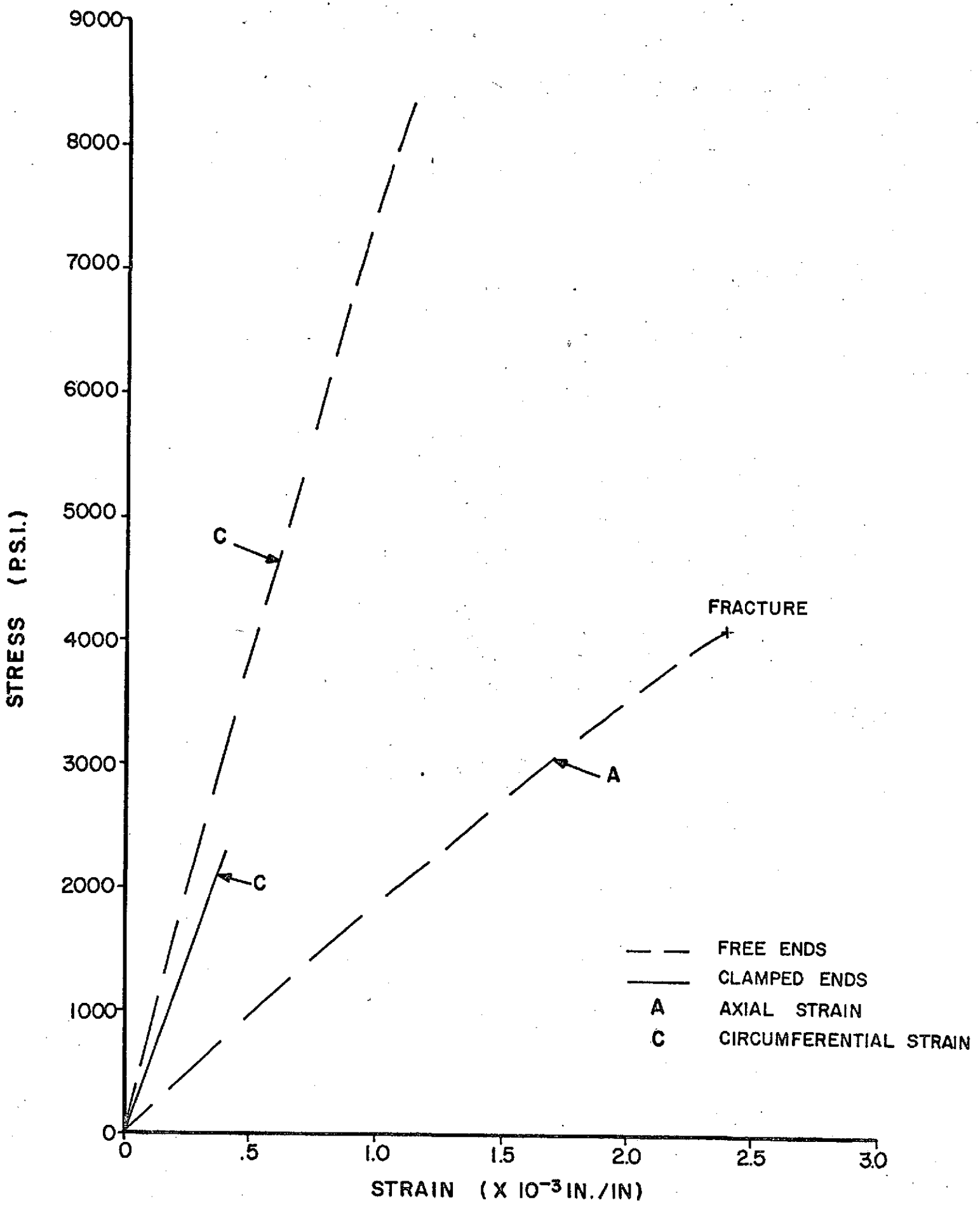

FIG. B6 STRESS-STRAIN CURVES FOR TUBE 23a 90° (TEMP.-20° F)

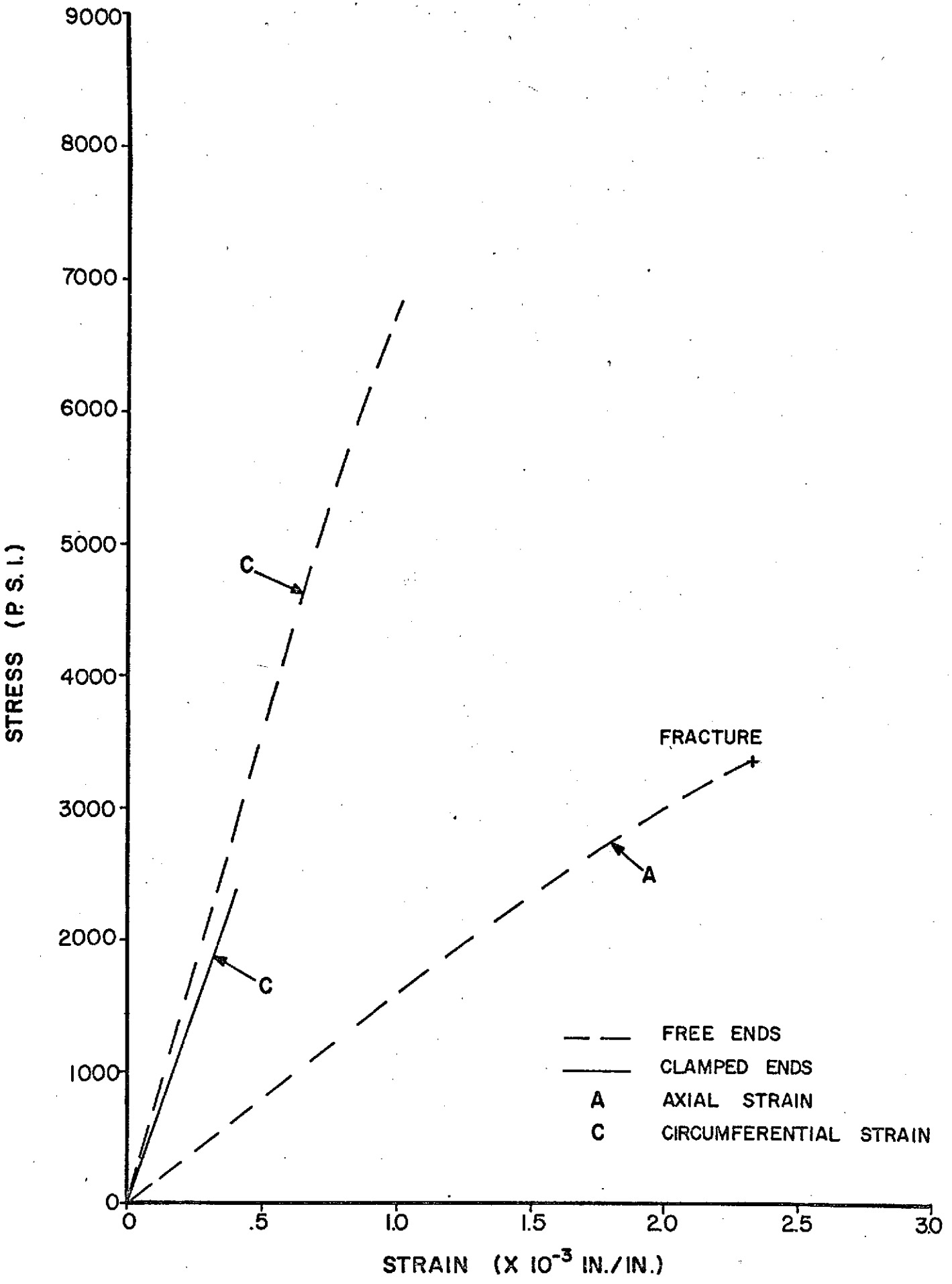

FIG. 57 STRESS-STRAIN CURVES FOR TUBE # 13c 90° (TEMP. 70° F)

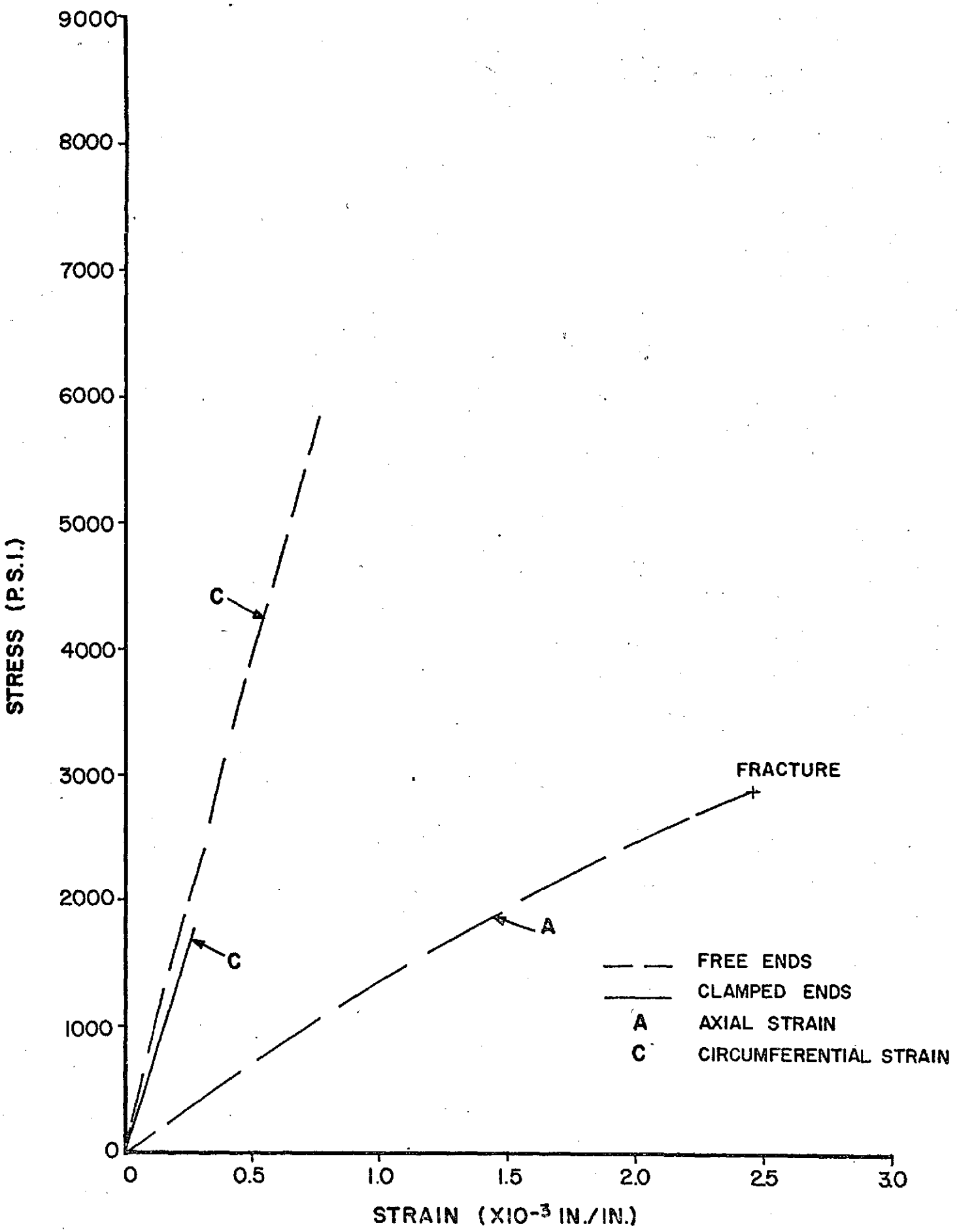

FIG. B8 STRESS-STRAIN CURVES FOR TUBE 16a 90° (TEMP. 58° F)

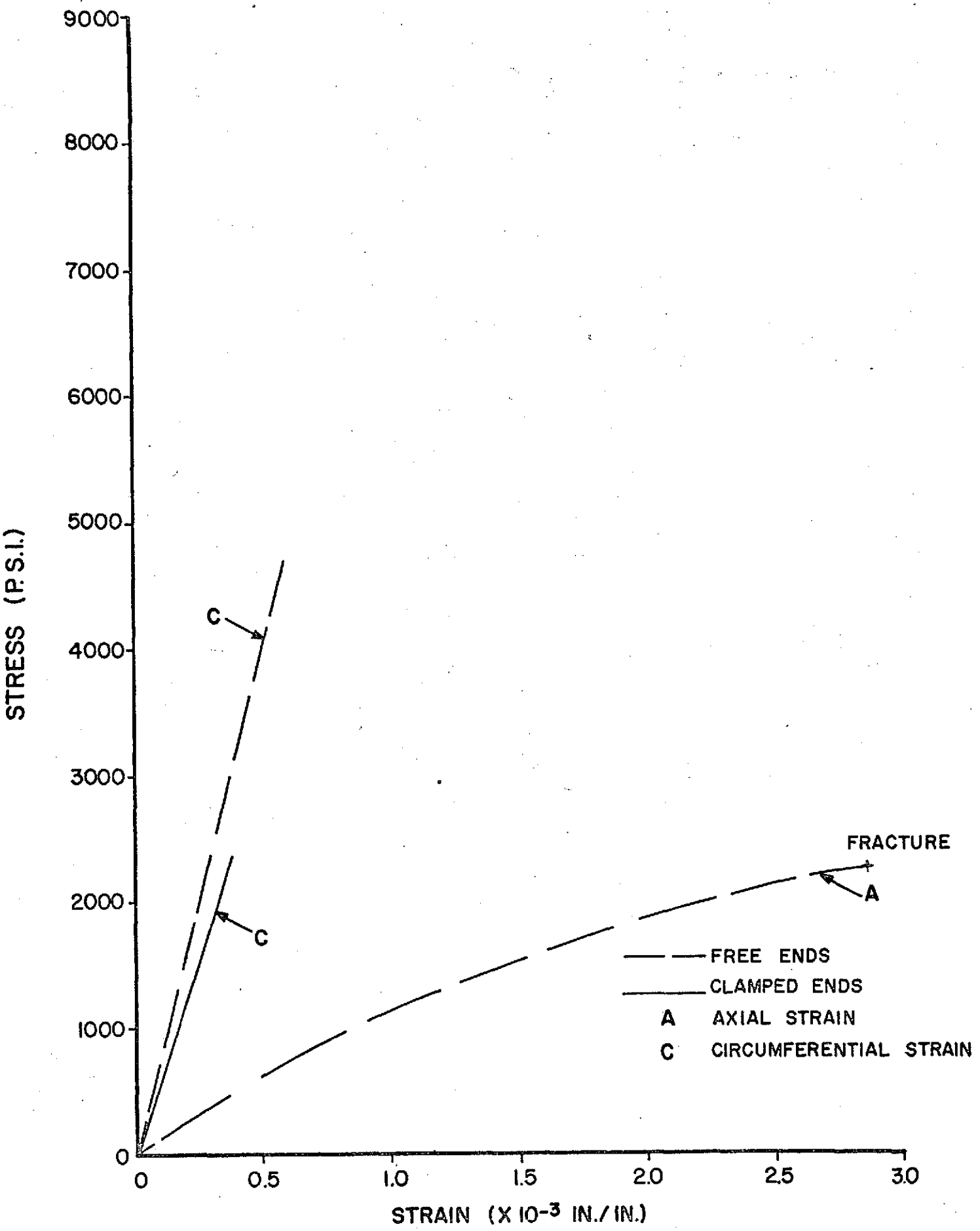

FIG. B9 STRESS-STRAIN CURVES FOR TUBE 19a 90° (TEMP 200° F)

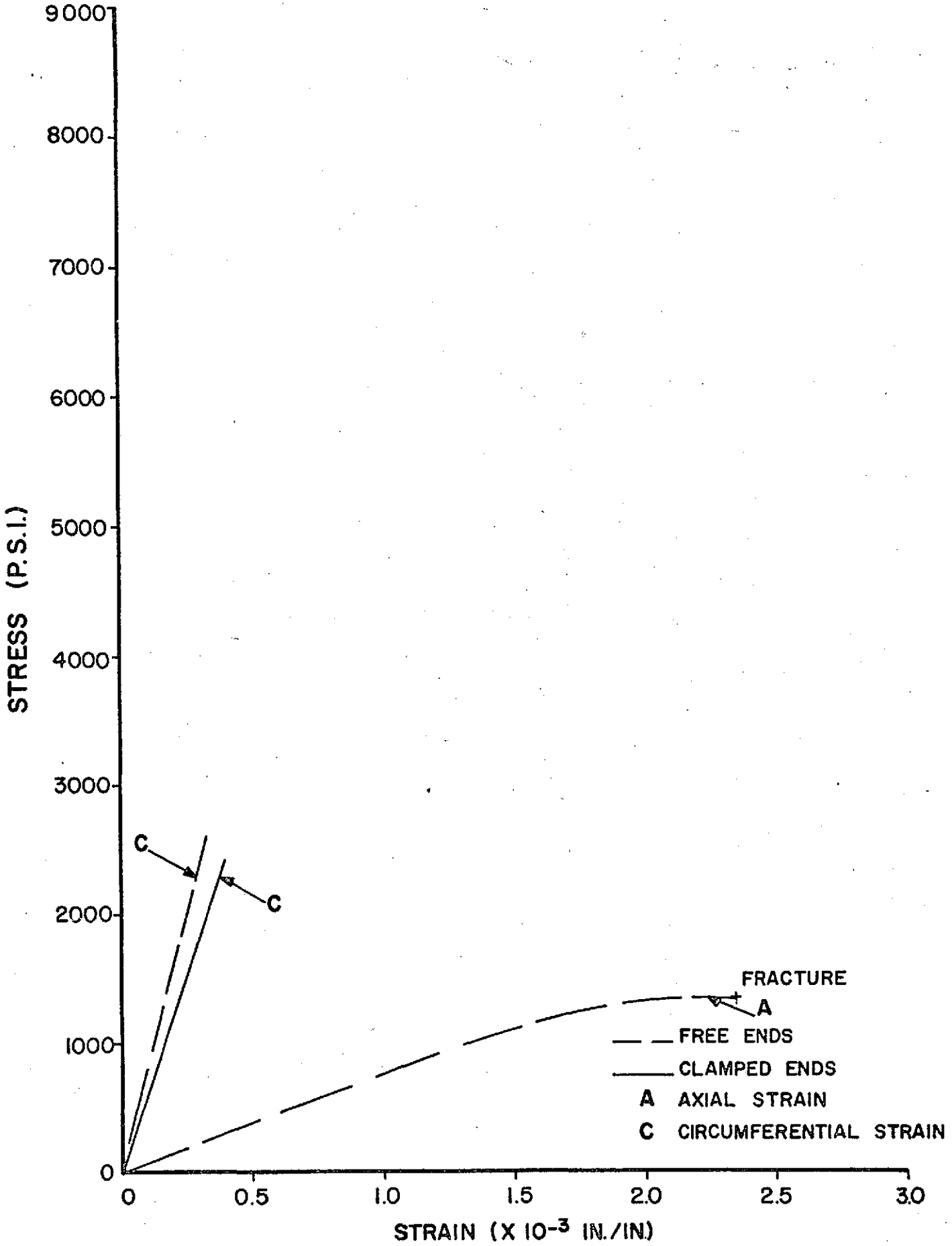

FIG. B.10 STRESS-STRAIN CURVES FOR TUBE 14c 90° (TEMP. 250° F)

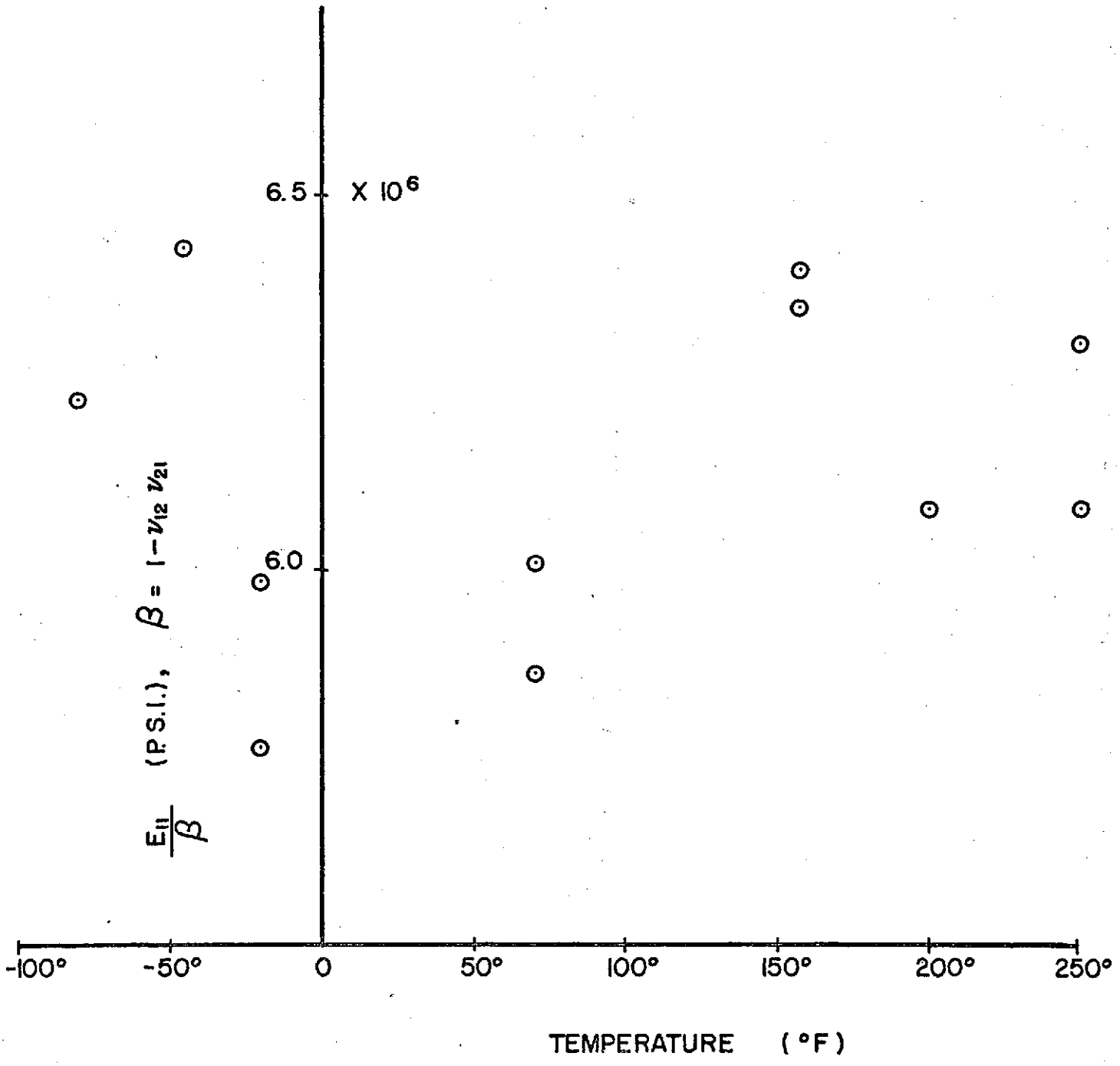

FIG. B.11 THE EFFECT OF TEMPERATURE ON E_{11}/β OF SCOTCHPLY (1000) TUBES

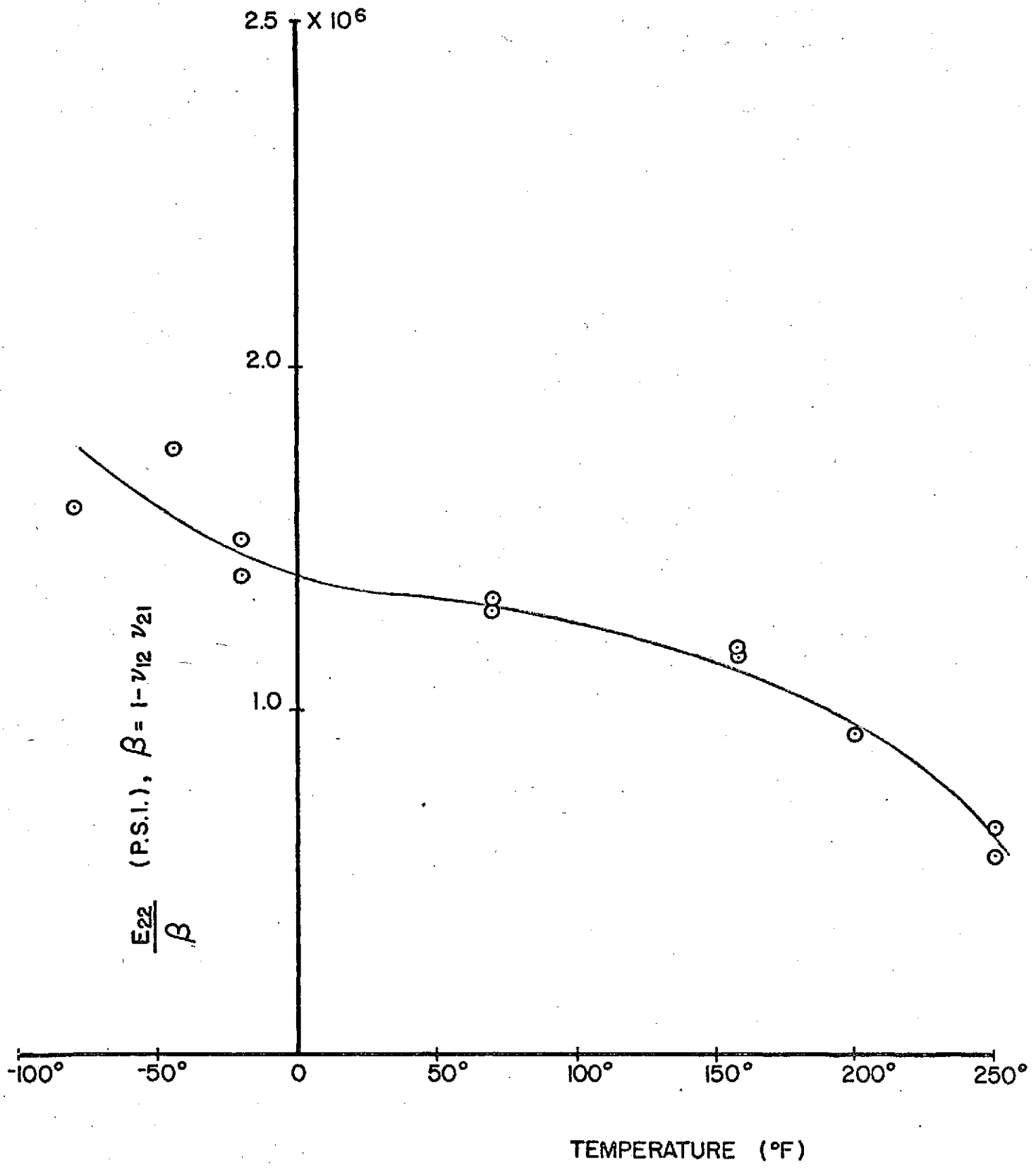

FIG. B-12 THE EFFECT OF TEMPERATURE ON E_{22}/β OF SCOTCHPLY (1000) TUBES

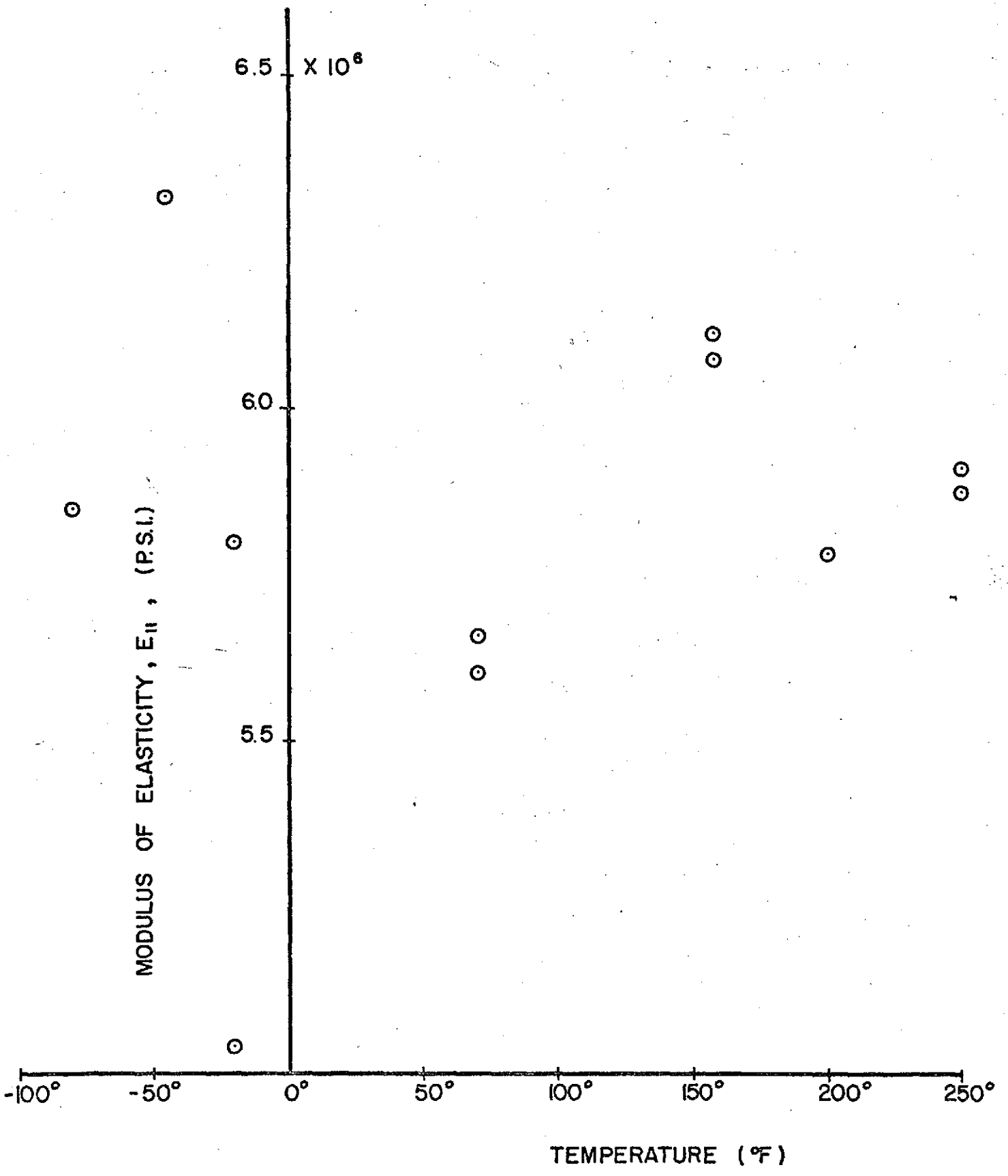

FIG. B-13 THE EFFECT OF TEMPERATURE ON E_{11} FOR SCOTCHPLY (1002) TUBES

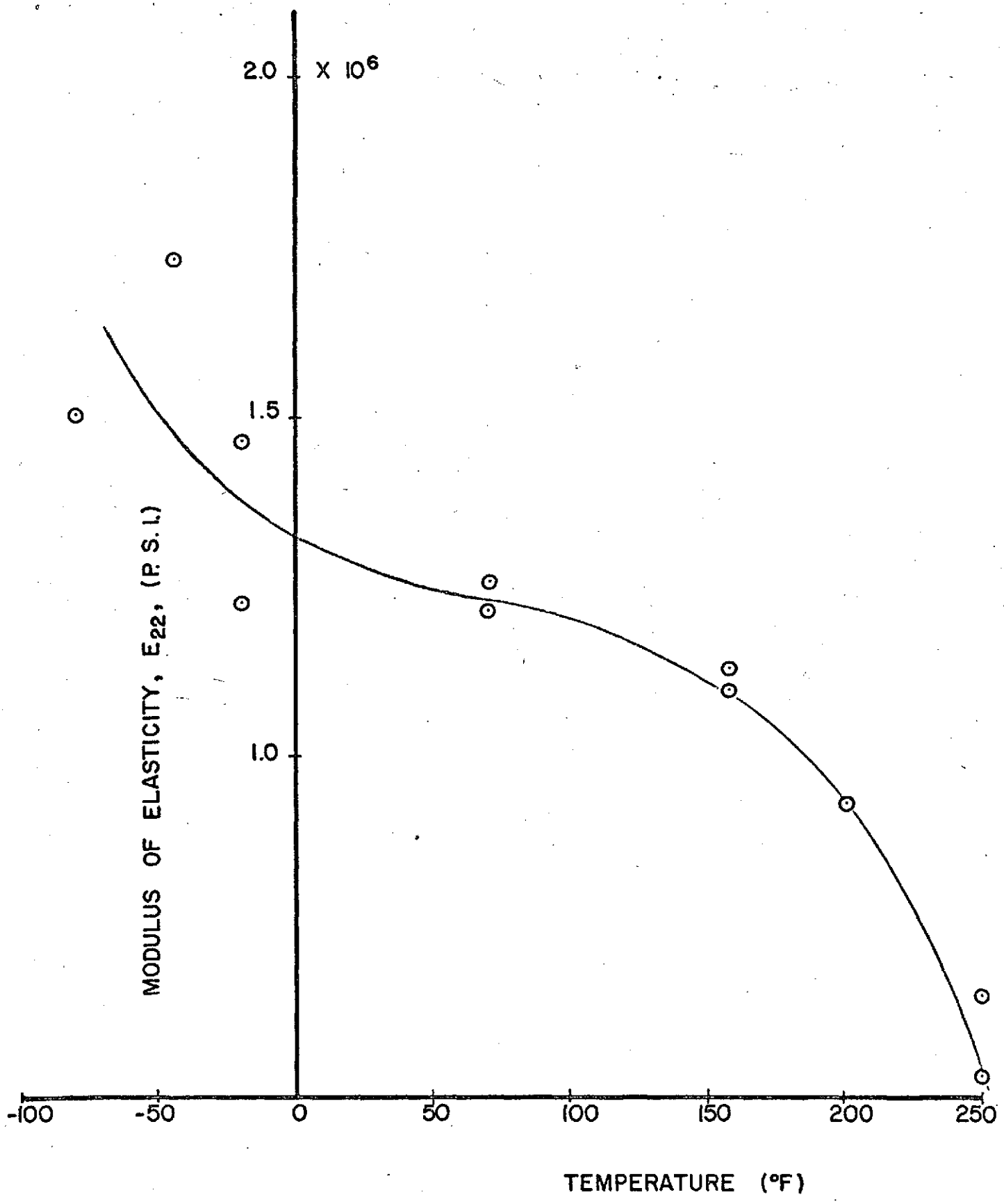

FIG. B-14 THE EFFECT OF TEMPERATURE ON E_{22} FOR SCOTCHPLY (1000) TUBES

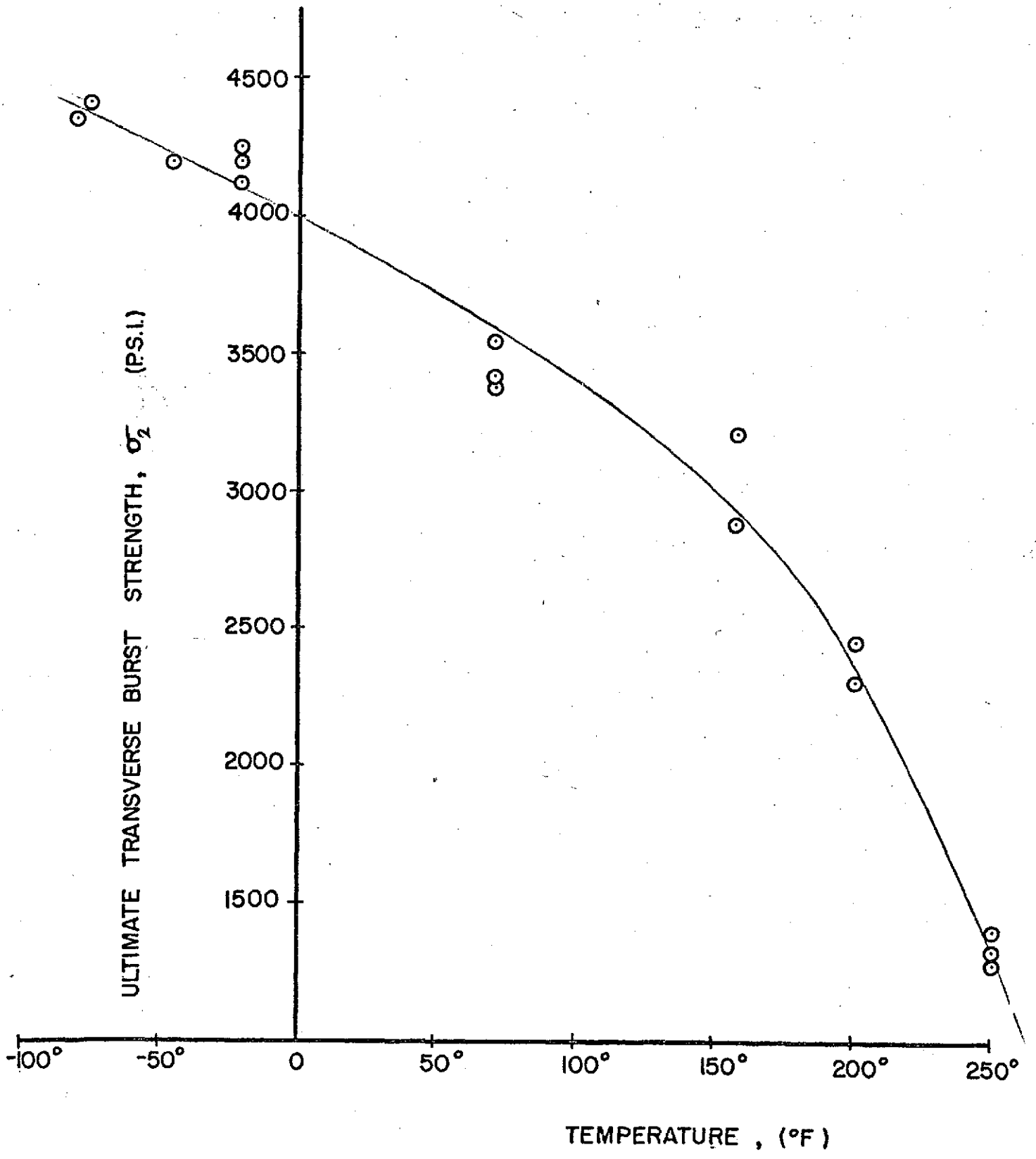

FIG. B-15 THE EFFECT OF TEMPERATURE ON THE ULTIMATE TRANSVERSE BURST STRENGTH OF SCOTCHPLY (1002) TUBES

APPENDIX C

THE EFFECTS OF LENGTH OF POST CURE ON THE MATERIAL PROPERTIES OF FIBREGLASS/EPOXY COMPOSITES.

C.1 INTRODUCTION

Many fibreglass/epoxy components can be manufactured from preimpregnated (prepreg) sheets of oriented fibre impregnated with uncured epoxy resin. Data sheets provided by the manufacturer of the prepreg tapes usually give a specified length of time as well as the temperature and pressure at which the component must be cured to achieve optimum properties. However, these specifications rarely give the effects of a deviation from the normal cure time on the properties of the composite.

Here, the results of a preliminary investigation on the variation in certain mechanical properties which result from variations in the length of post cure time will be reported.

C.2 Test Procedure

All of the tubes were tested under internal pressure. Two tubes from each batch of three were equipped with an axial and a circumferential strain gauge. The elastic constants (E_{11}, E_{22}, ν_{12}, and ν_{21}) of the material can be solved for when the responses from these strain gauges to two different loadings are substituted into the constitutive equations (see Appendix B for details). The two types of loadings are free expansion under internal pressure ($\epsilon_x \neq 0$ and $\epsilon_y \neq 0$)

and clamped expansion under internal pressure where the tube is clamped in such a way that $\epsilon_x = 0$ but $\epsilon_y \neq 0$.

The required pressure vs. strain curves were obtained for each strain gauged specimen (Fig.C.1 to C.4) and then the tubes were burst in order to find the effect of length of post cure on the ultimate transverse burst strength of the material (Fig.C.5).

A general view of the testing apparatus is given in Figures B.1 and B.2.

All of the tubes used in these tests were wrapped with a fibre angle of 90°, ie., the fibres were aligned in the circumferential direction.

The equations used in the calculations are the same as those derived in the previous Appendix.

C.3 Conclusions

The various elastic constants and ultimate transverse strength were calculated from the strain gauge responses for the two different loadings. These results are shown in Table V and are plotted in Figures C.6 to C.9.

As can be seen from the graphs, the length of post curing time has little effect on the values of E_{11}. The calculated average values vary little from about 5.6×10^6 psi. This was expected because E_{11} is essentially the value obtained by multiplying the fibre modulus by the fibre volume fraction.

The effect of the matrix modulus on E11 is negligible. Also, the lengths of post curing times considered in this investigation shouldn't have had any degrading or harmful effects on the fibres. For the 24 hour post cure case, there was quite a variation in the values calculated for E_{11}. This was determined to be a Poisson's ratio effect. The Poisson's ratio, ν_{12}, is directly proportional to the difference in the strain ϵ_{y2} and ϵ_{y1} (a very small number) and is therefore very difficult to determine accurately. The difference in the two values is approximately 0.2 which gives a $\pm$ 33% inaccuracy in the value of ν_{12}. E_{11} was directly proportional to ν_{12} ($E_{11} = \nu_{12} E_{22}/\nu_{21}$) and this is the reason for the great variation in E_{11} at 24 hours postcure. The quantity $\beta = (1 - \nu_{12}\nu_{21})$ was a much more accurate number to determine and so the quantities E_{11}/β and E_{22}/β were calculated so that the variation in the moduli would be reduced.

The difference in post curing time has a more pronounced effect on the value of E_{22}. As the length of post curing time increases, E_{22} steadily decreases. This is also to be expected because the length of post cure affects the matrix more than the fibres and E_{22} is more dependent on the modulus of the matrix.

Using the same reasoning as above, the ultimate transverse strength, σ_{2u}, increases a good deal as the length of post cure increases.

From these two facts it is deduced that an increase in

the length of post cure causes the matrix to become more ductile.

The amount of post cure will probably affect other mechanical properties of the composite more than was noted in this investigation. Some of these other properties would be the interlaminar shear strength and shear modulus, the transverse compressive strength and the fatigue strength. The effects on these properties will probably be quite pronounced since they are quite dependent on the state of the matrix. Other investigations should provide the effects of differences in post cure temperature as well as time in order to determine the optimum curing time for any given curing temperature to obtain the optimum value for any particular mechanical property of the composite. Curing conditions will probably vary with the property that is required and so, different components can be fabricated to optimize the specific mechanical property that is required.

TABLE C.1

GEOMETRY OF TUBES USED IN POST CURE STUDY

TUBE DESIGNATION	R (IN)	$\bar{t}$ (IN)
11c 90°	1.016	.0295
12c 90°	1.016	.0295
13c 90°	1.016	.0295
18a 90°	1.016	.0292
18b 90°	1.016	.0297
18c 90°	1.016	.0300
20a 90°	1.016	.0299
20b 90°	1.016	.0298
20c 90°	1.016	.0292
21a 90°	1.016	.0294
21b 90°	1.016	.0303
21c 90°	1.016	.0303

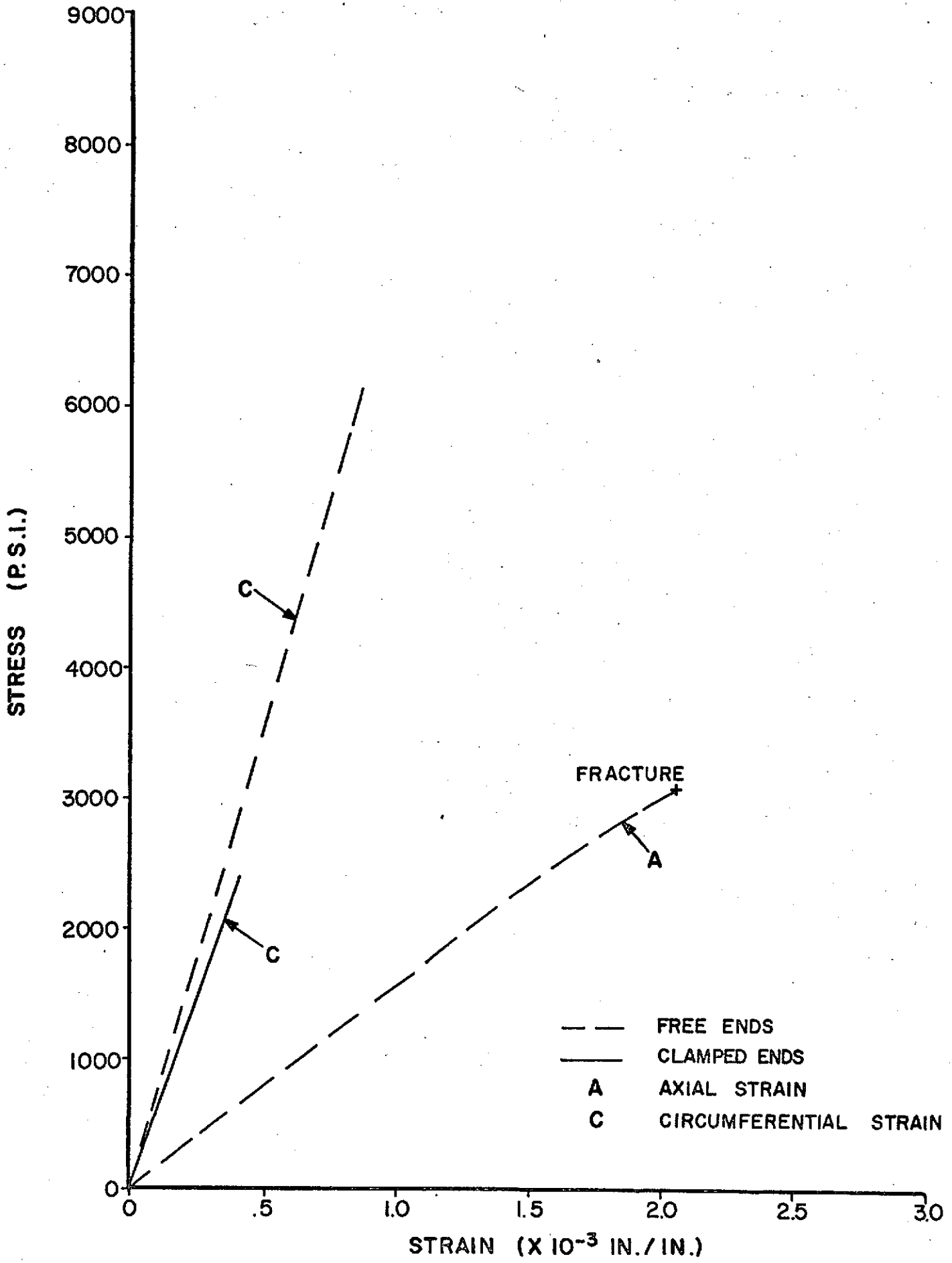

FIG. C-1 STRESS-STRAIN CURVES FOR TUBE # 18a 90° (0 HOURS POSTCURE)

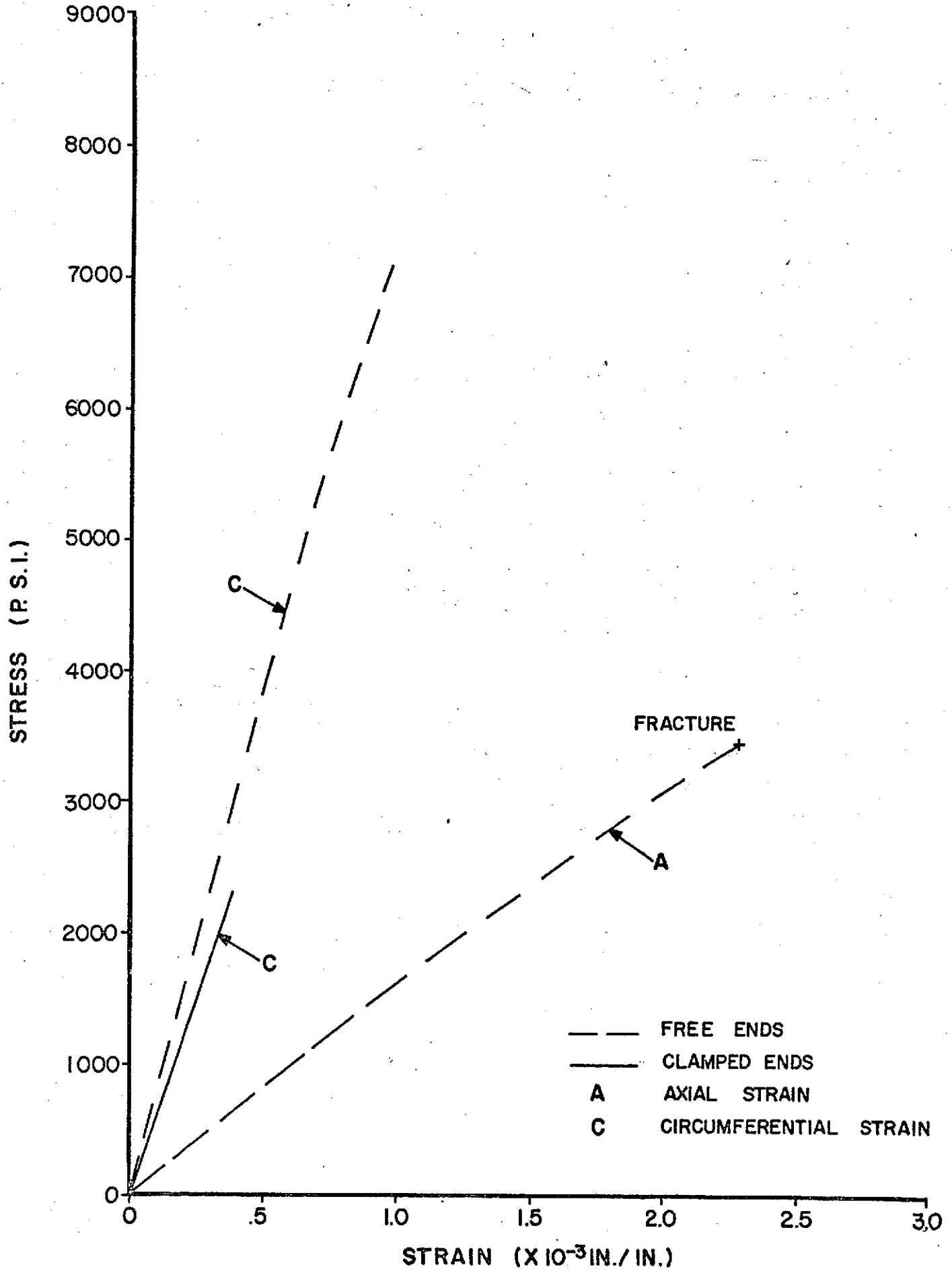

FIG. C.2 STRESS-STRAIN CURVES FOR TUBE #21b 90° (7 HOURS POSTCURE)

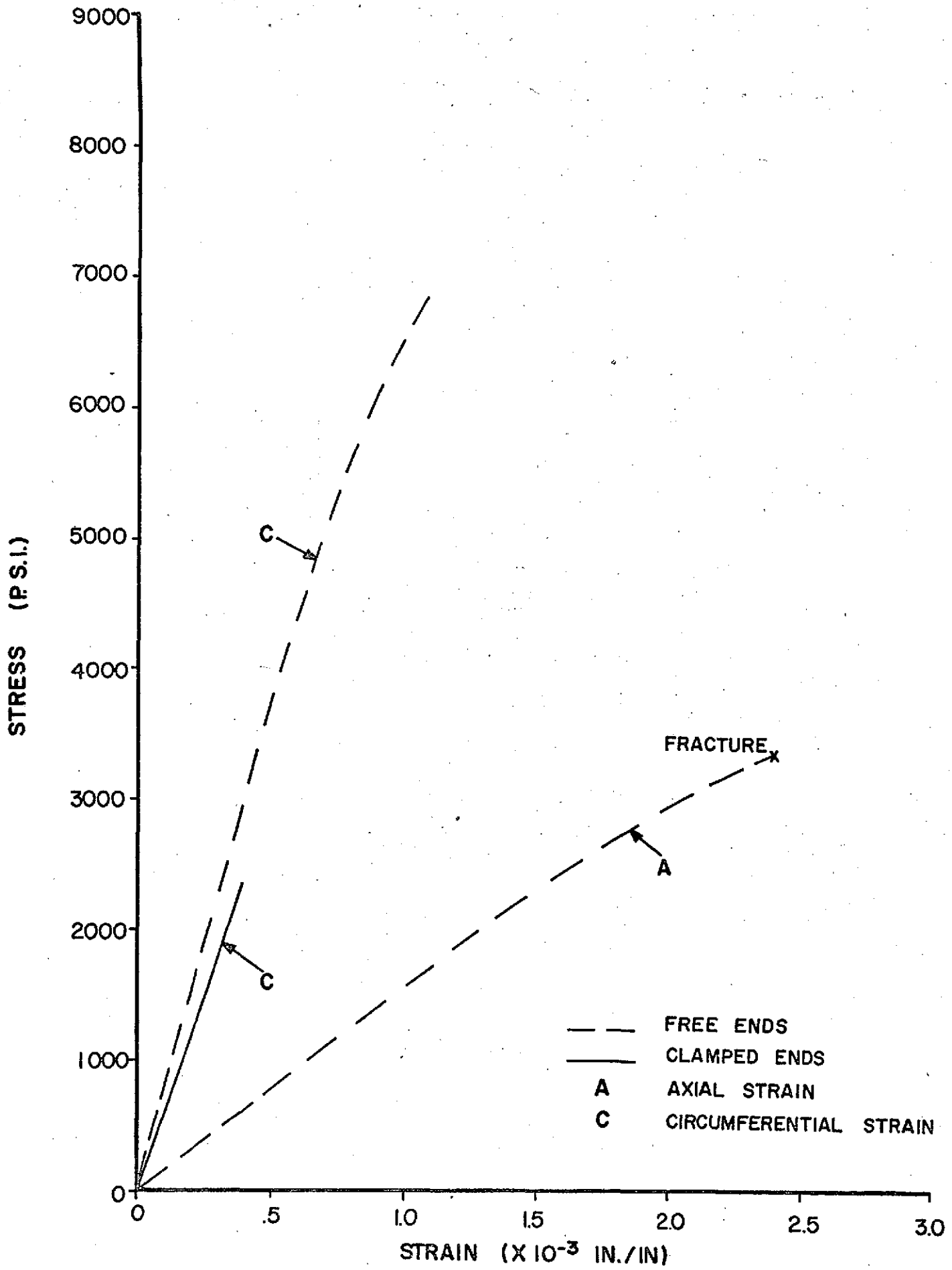

FIG. C.3 STRESS-STRAIN CURVES FOR TUBE # 11c 90° (16.75 HOURS POSTCURE)

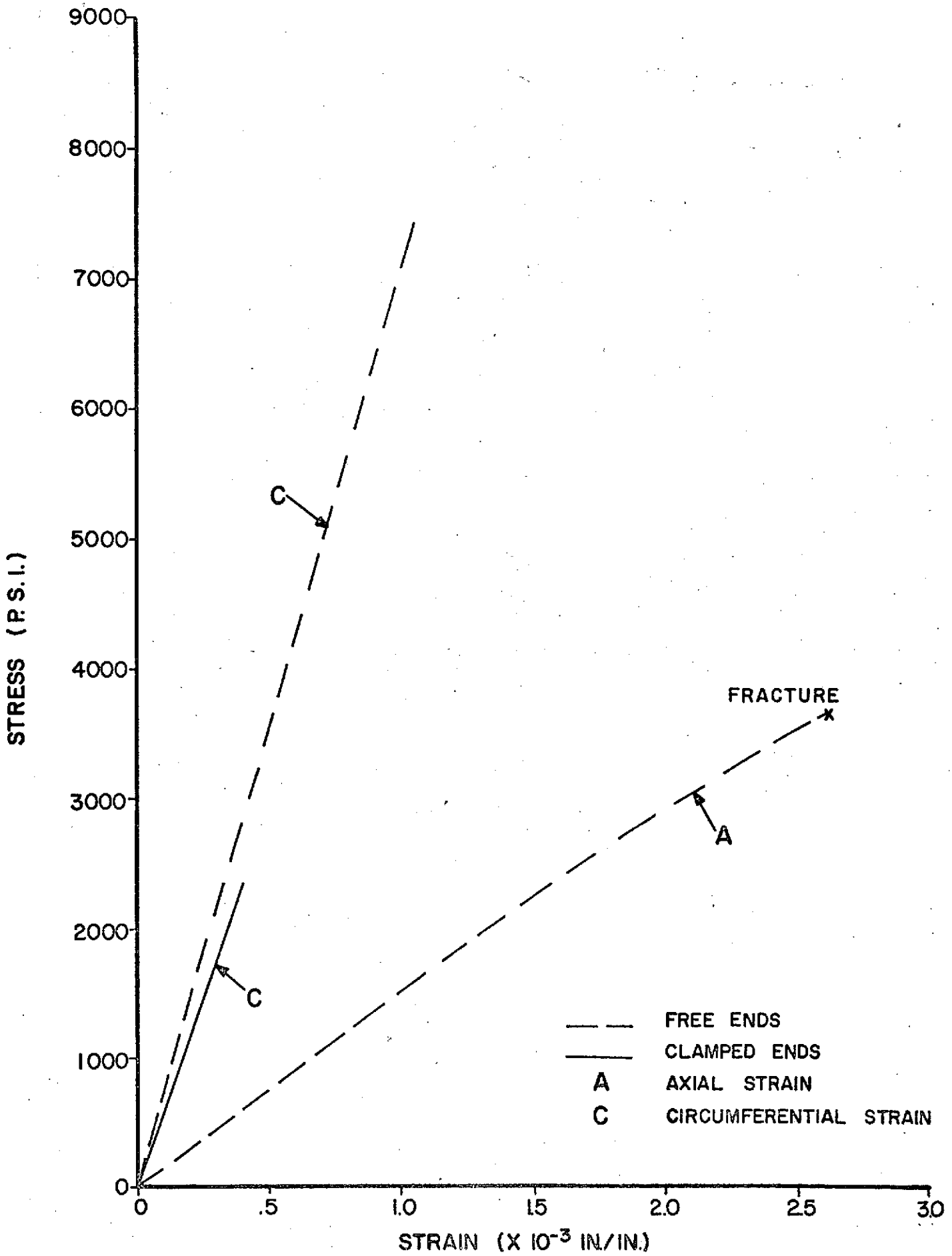

FIG. C.4 STRESS-STRAIN CURVES FOR TUBE 20a 90° (24 HOURS POSTCURE)

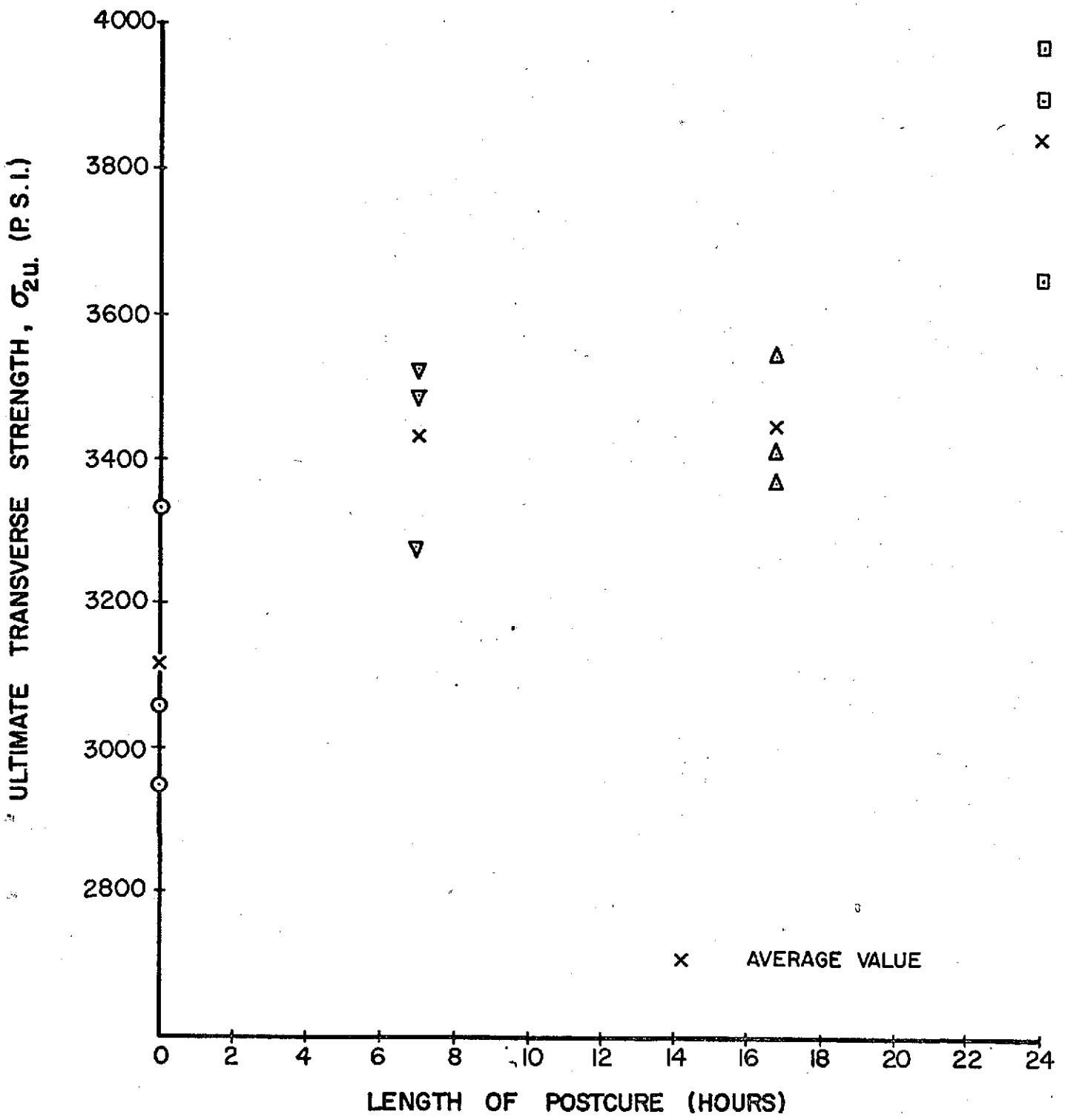

FIG. 6.5 EFFECT OF CURE TIME ON THE TRANSVERSE BURST STRENGTH, $\sigma_{2u.}$

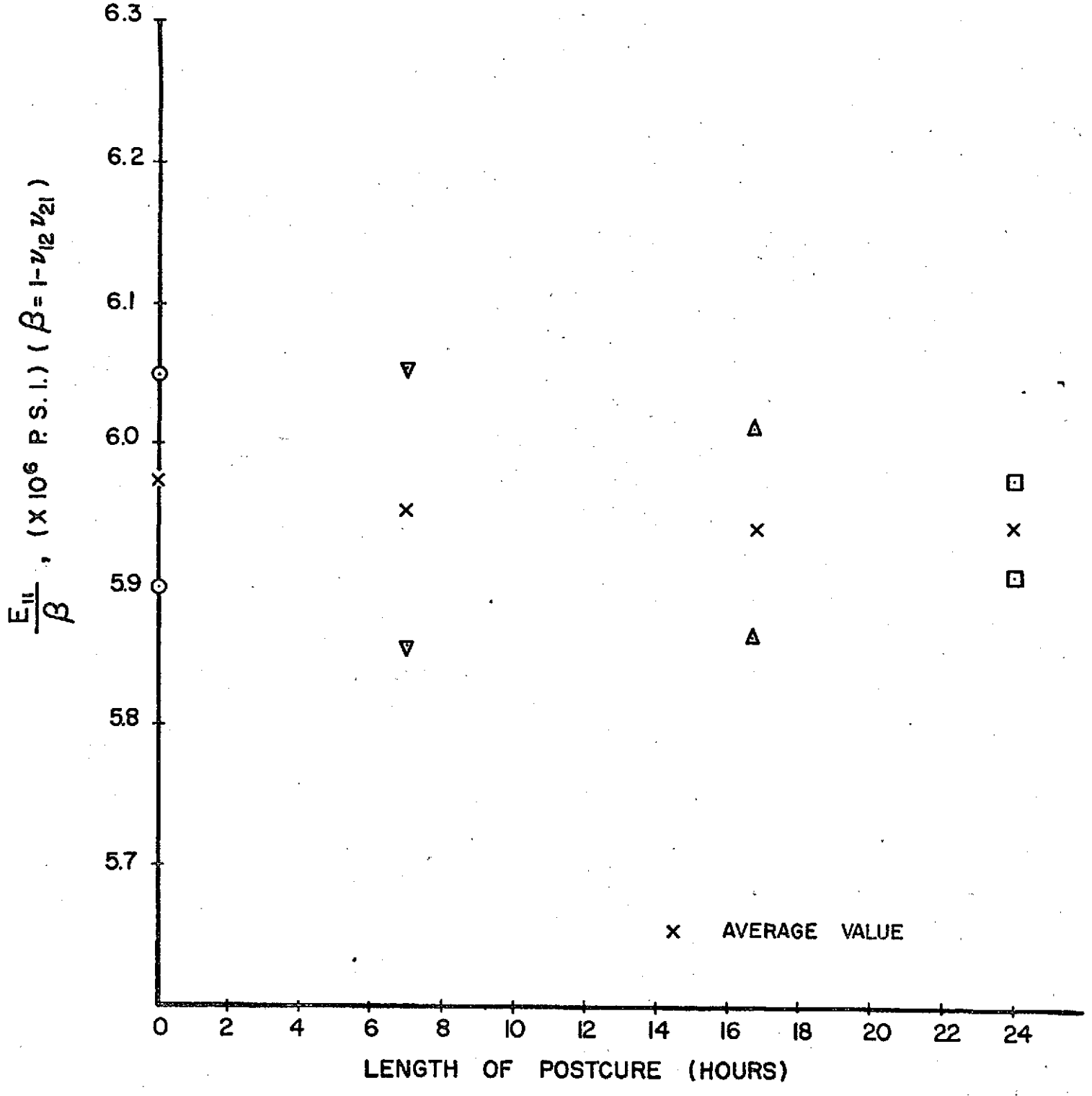

FIG. C.6 EFFECT OF CURE TIME ON THE QUANTITY, $\frac{E_{11}}{\beta}$

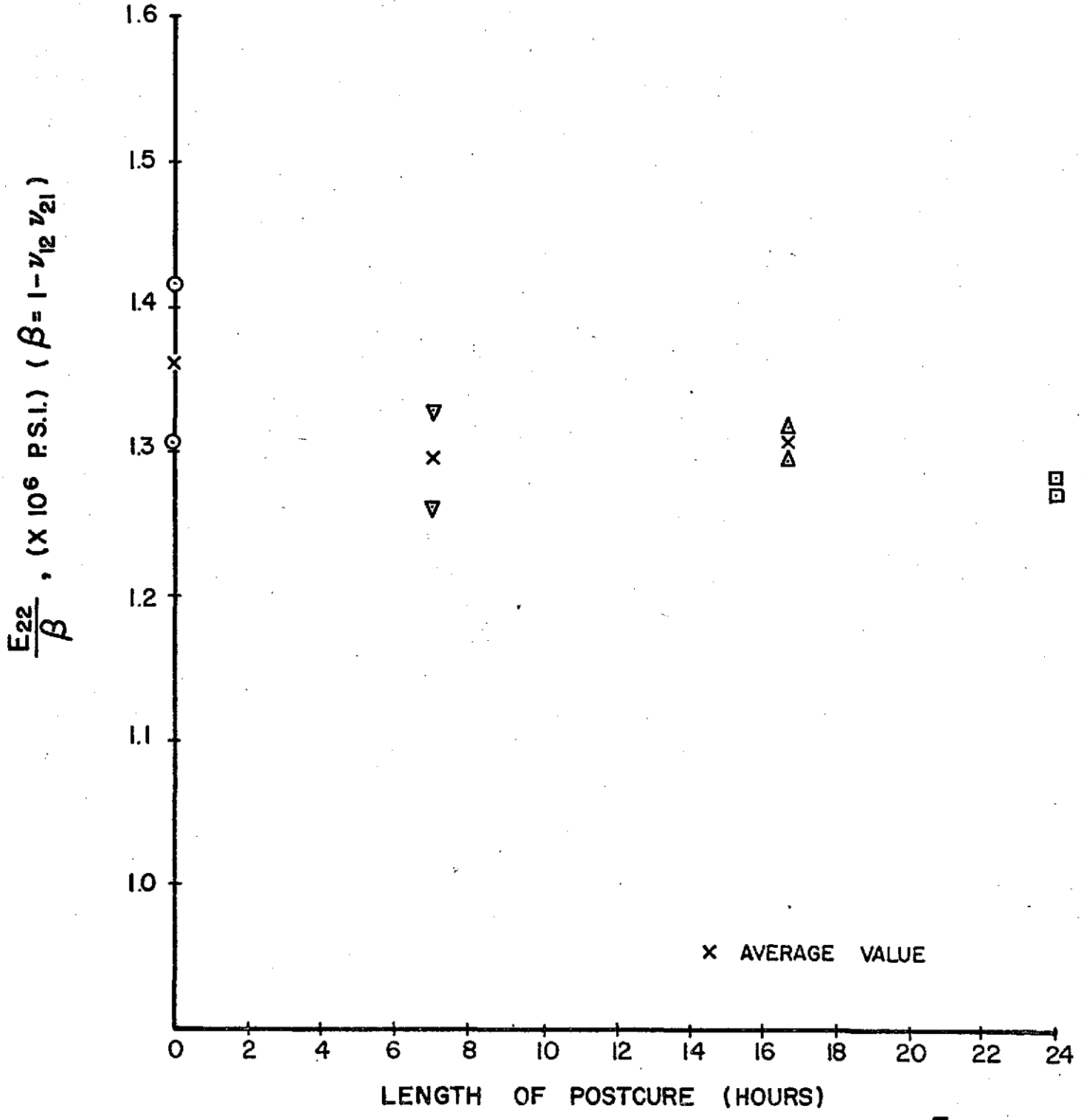

FIG. C.7 EFFECT OF CURE TIME ON THE QUANTITY, $\frac{E_{22}}{\beta}$

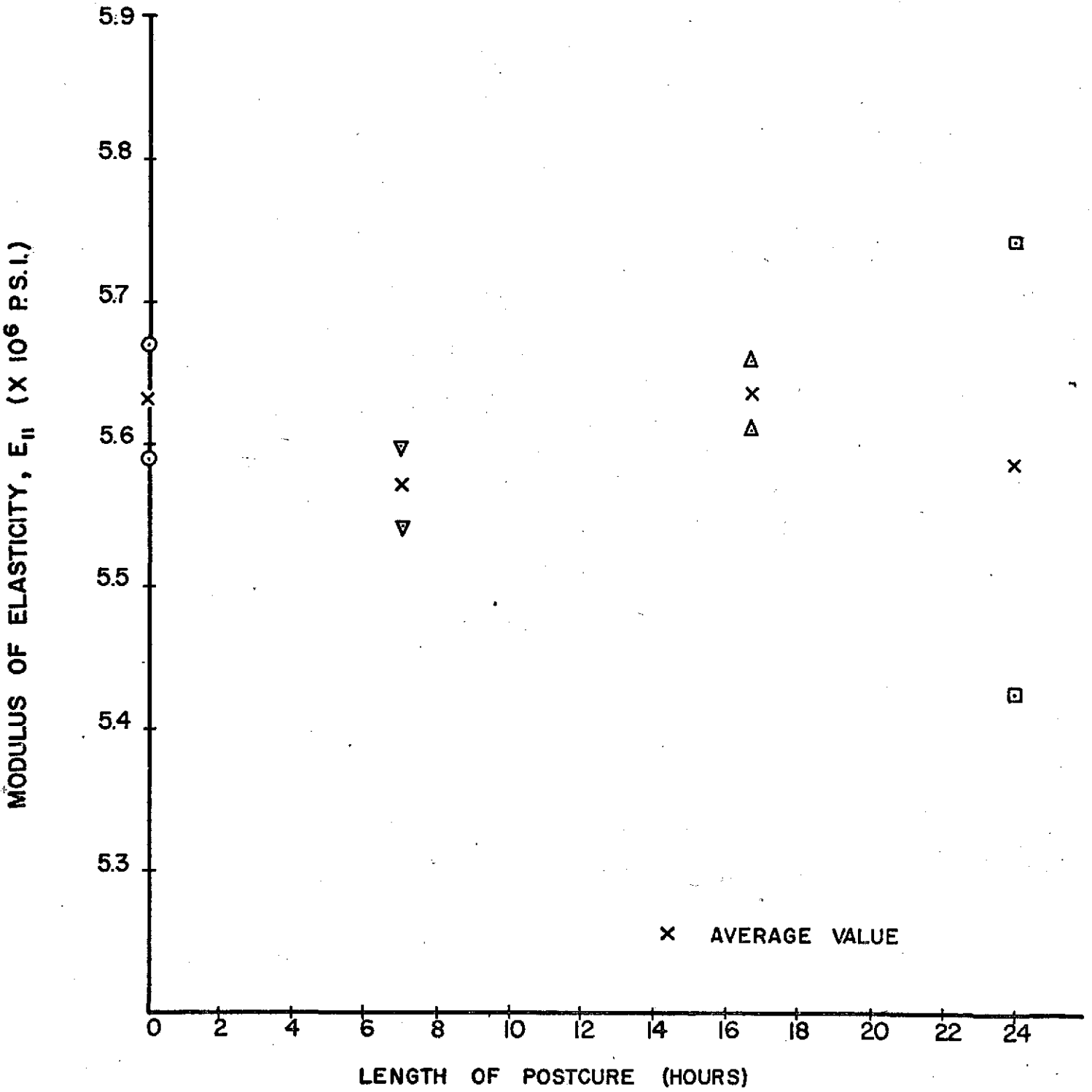

FIG. C-8 EFFECT OF CURE TIME ON MODULUS OF ELASTICITY, E_{11}

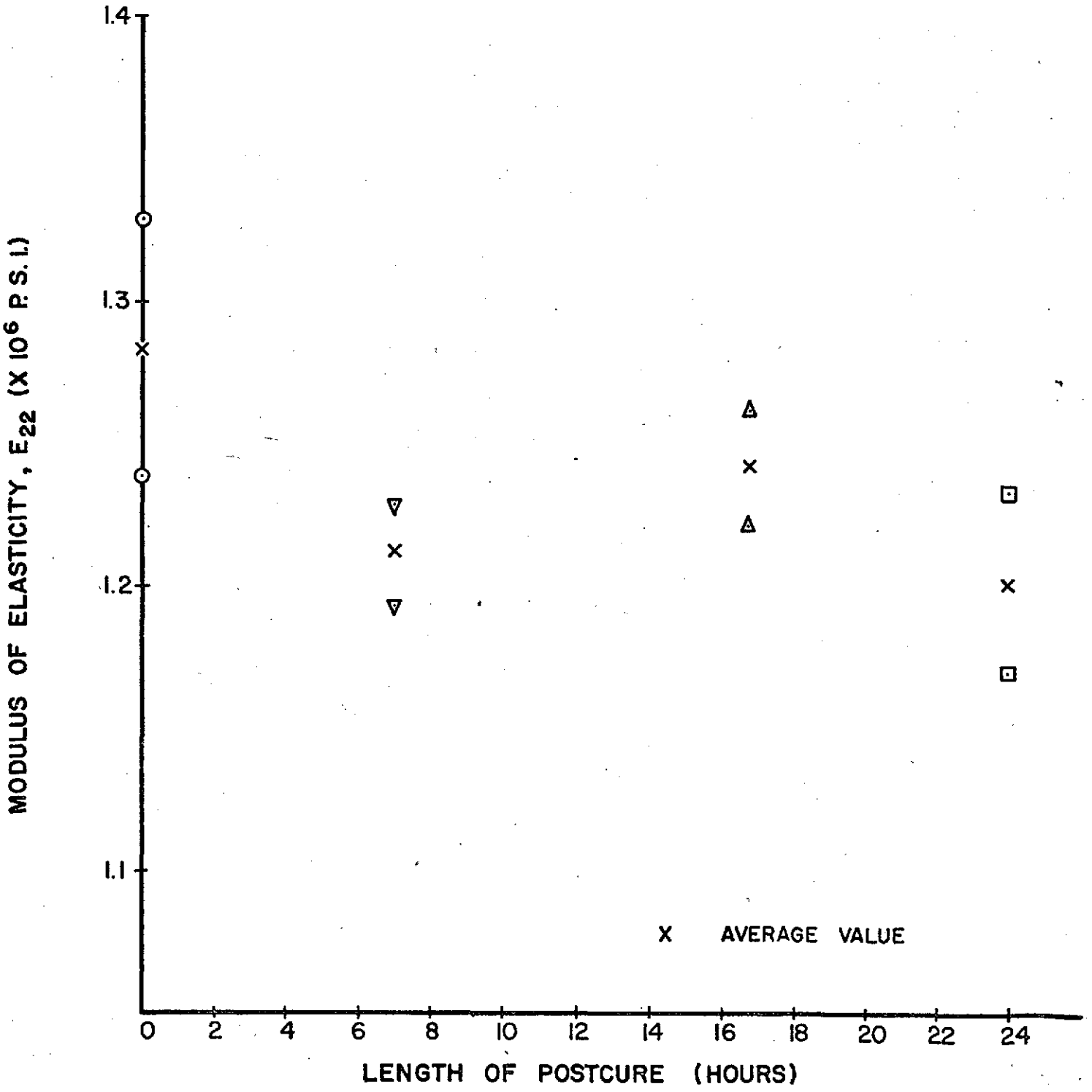

FIG. C-9 EFFECT OF CURE TIME ON THE MODULUS OF ELASTICITY, E_{22}

APPENDIX D

COMPUTER PROGRAMMES FOR EVALUATING CUBIC TERMS AND FAILURE PRESSURES FOR LAMINATED TUBES UNDER INTERNAL PRESSURE- WITH AND WITHOUT TORQUE

EVALUATION OF CUBIC COEFFICIENTS

```
      IMPLICIT REAL*8(A-H,O-Z)
      COMMON /AAA/E11,E22,V12,V21,G12
      DIMENSION PRR(4),ENXY(4),DTI(4),TR(3,3),SIG(4,3),A(4,4),B(4),
     1 IR(4),IC(4)
      READ(5,2) E11,E22,V12,V21,G12
    2 FORMAT(5D16.4)
      READ(5,5) F1,F2,F11,F22,F12,F66
    5 FORMAT(6D13.7)
      READ(5,10) (PRR(I),I=1,4)
   10 FORMAT(4D20.5)
      READ(5,10) (ENXY(I),I=1,4)
      READ(5,10) (DTI(I),I=1,4)
      READ(5,1) LR
    1 FORMAT(I10)
      TH=.040D0
      RAD=1.02D0
      NL=4
      DO 40 I=1,4
      DT=DTI(I)
      CALL CMAT(TR,DT,TH,NL,LR)
      SIG(I,1)=TR(1,1)*PRR(I)/2.D0+TR(1,2)*PRR(I)+TR(1,3)*ENXY(I)
      SIG(I,2)=TR(2,1)*PRR(I)/2.D0+TR(2,2)*PRR(I)+TR(2,3)*ENXY(I)
      SIG(I,3)=TR(3,1)*PRR(I)/2.D0+TR(3,2)*PRR(I)+TR(3,3)*ENXY(I)
   40 CONTINUE
      DO 50 I=1,4
      A(I,1)=3.D0*SIG(I,1)*SIG(I,1)*SIG(I,2)
      A(I,2)=3.D0*SIG(I,1)*SIG(I,2)*SIG(I,2)
      A(I,3)=3.D0*SIG(I,2)*SIG(I,3)*SIG(I,3)
      A(I,4)=3.D0*SIG(I,1)*SIG(I,3)*SIG(I,3)
      B(I)=1.D0-(F1*SIG(I,1)+F2*SIG(I,2)+2.D0*F12*SIG(I,1)*SIG(I,2)
     1 +F11*SIG(I,1)*SIG(I,1)+F22*SIG(I,2)*SIG(I,2)+F66*SIG(I,3)*SIG(I,3
     1 ))
   50 CONTINUE
      CALL LNEQND(A,4,4,4,B,IR,IC,IER)
      WRITE(6,60)
   60 FORMAT('1',T10,'F112',T30,'F221',T50,'F266',T70,'F166',//)
      WRITE(6,70) (B(I),I=1,4)
   70 FORMAT(4D20.7)
      STOP
      END
      .4765D+07       .1211D+07       .3363D+00       .0855D+00       .4230D+06
-.3075589D-02+.2344010D+00+.9397711D-04+.2269570D-01-.6387300D-03+.2142418D-02
        .67422D+00      .67422D+00      .60180D+00      .60180D+00
        .00000D+00      .07650D+00      .07650D+00      .00000D+00
        .60000D+02      .60000D+02      .45000D+02      .45000D+02
     1
```

```
$PRINTOFF
      IMPLICIT REAL*8(A-H,O-Z)
      COMMON/AAA/E11,E22,V12,V21,G12
      DIMENSION TR(3,3)
      READ(5,2) E11,E22,V12,V21,G12
    2 FORMAT(5D16.4)
      READ(5,5) F1,F2,F11,F22,F12,F66
    5 FORMAT(6D13.7)
      LR=2
      ENXY=.0765D0
      DT=80.D0
      F112=.1667067D-03
      F221=-.1057499D-02
      F266=-.1372627D-02
      F166=.3998496D-03
      TH=.040D0
      DP=.005D0
      RAD=1.02D0
      ALIM=.8D0
      NL=4
      WRITE(6,10) DT,ENXY
   10 FORMAT('1',T10,'THETA=',F10.2,T30,'NXY=',F12.4,//)
      CALL CMAT(TR,DT,TH,NL,LR)
      PRR=0.D0
   40 CONTINUE
      SIG1=TR(1,1)*PRR/2.D0+TR(1,2)*PRR+TR(1,3)*ENXY
      SIG2=TR(2,1)*PRR/2.D0+TR(2,2)*PRR+TR(2,3)*ENXY
      SIG6=TR(3,1)*PRR/2.D0+TR(3,2)*PRR+TR(3,3)*ENXY
      VALF=F1*SIG1+F2*SIG2+F11*SIG1*SIG1+F22*SIG2*SIG2+F66*SIG6*SIG6+
     1 2.D0*F12*SIG1*SIG2+3.D0*F112*SIG1*SIG1*SIG2+3.D0*F221*SIG2*SIG2*
     1 SIG1+3.D0*F266*SIG6*SIG6*SIG2-1.D0+3.D0*F166*SIG1*SIG6*SIG6
      PR=PRR
      WRITE(6,850) PR,VALF,SIG1,SIG2,SIG6
  850 FORMAT(' ','PR=',F10.5,2X,'VALF=',D15.5,2X,'SIG1=',D15.5,2X,'SIG2
     1=',D15.5,2X,'SIG6=',D15.5)
      PRR=PRR+DP
      IF(PR .GE. ALIM) GO TO 100
      GO TO 40
  100 CONTINUE
      STOP
      END
C
      SUBROUTINE CMAT(TR,DT,TH,NL,LR)
      IMPLICIT REAL*8(A-H,O-Z)
      COMMON /AAA/E11,E22,V12,V21,G12
      DIMENSION T(4),DTA(4),TA(4),TR(3,3),TRI(3,3),Q(3,3),H(5),
     1 QQ(3,3,4),A(3,3),AA(3,3),LL(3),MM(3),QR(3,3),W(3)
      DO 88 K=1,NL
```

```
 88 T(K)=TH/NL
    DTA(1)=-DT
    DTA(2)= DT
    DTA(3)= DT
    DTA(4)=-DT
    DO 21 K=1,NL
C       CONVERSION OF DEGREES INTO RADIANS
 21   TA(K)=DTA(K)*.01745329250
      C1=DCOS(TA(LR))
      S1=DSIN(TA(LR))
     C2=C1*C1
     S2=S1*S1
     TR(1,1)=C2
     TR(1,2)=S2
      TR(1,3)=2.D0*C1*S1
     TR(2,1)=S2
     TR(2,2)=C2
      TR(2,3)=-2.D0*C1*S1
     TR(3,1)=-C1*S1
     TR(3,2)=C1*S1
     TR(3,3)=C2-S2
C       THE INVERSE TRANSFORMATION MATRIX
     TRI(1,1)=C2
     TRI(1,2)=S2
      TRI(1,3)=-2.D0*C1*S1
     TRI(2,1)=S2
     TRI(2,2)=C2
      TRI(2,3)=2.D0*C1*S1
     TRI(3,1)=C1*S1
     TRI(3,2)=-C1*S1
     TRI(3,3)=C2-S2
C       CALCULATE Q,QQ,A,AA MATRICES
      VV=1.D0-V12*V21
     Q(1,1)= E11/VV
     Q(2,2) = E22/VV
     Q(1,2) = (V21*E11)/VV
     Q(2,1) = Q(1,2)
     Q(3,3) = G12
      Q(1,3)=0.D0
      Q(3,1)=0.D0
      Q(2,3)=0.D0
      Q(3,2)=0.D0
      Q12=Q(1,1)-Q(1,2)-2.D0*Q(3,3)
      Q23=Q(1,2)-Q(2,2)+2.D0*Q(3,3)
      Q13=2.D0*(Q(1,2)+2.D0*Q(3,3))
      Q14=Q(1,1)+Q(2,2)-4.D0*Q(3,3)
      Q22=Q(1,1)+Q(2,2)-2.D0*Q(1,2)-2.D0*Q(3,3)
C         CONVERSION OF THICKNESS INTO H WITH MEDIAN SURFACE AS REFERENCE
      H(1)=-TH/2.D0
    DO 777 K=1,NL
777 H(K+1) = H(K)+T(K)
    DO 9 K= 1,NL
     C1=DCOS(TA(K))
     S1=DSIN(TA(K))
    C2 = C1**2
    S2 = S1**2
    C4 = C2**2
    S4 = S2**2
    QQ(1,1,K) = Q(1,1)*C4+Q13*S2*C2+Q(2,2)*S4
    QQ(2,2,K) = Q(1,1)*S4+Q13*S2*C2+Q(2,2)*C4
```

```
      QQ(1,2,K) = Q14*S2*C2+Q(1,2)*(S4+C4)
      QQ(2,1,K) = QQ(1,2,K)
      QQ(3,3,K) = Q22*S2*C2+Q(3,3)*(S4+C4)
      QQ(1,3,K) = (Q12*C2+Q23*S2)*S1*C1
      QQ(3,1,K) = QQ(1,3,K)
      QQ(2,3,K) = (Q12*S2+Q23*C2)*S1*C1
    9 QQ(3,2,K) = QQ(2,3,K)
      DO 10 J=1,3
      DO 10 I=1,3
       A(I,J)=0.DO
      DO 10 K=1,NL
      A(I,J)=QQ(I,J,K)*(H(K+1)-H(K)) + A(I,J)
   10 AA(I,J) = A(I,J)
C        SUBROUTINE MINV ENTER AA AND REPLACE IT WITH THE INVERSE MATRIX
C        MM,LL ARE WORK VECTORS FOR SUBROUTINE MINV (MATRIX INVERSION)
       CALL MINVRD(AA,3,3,DET,IER,LL,MM)
      DO 12 I=1,3
      DO 12 J=1,3
   12 QR(I,J)=QQ(I,J,LR)
       CALL MAMP1D(TR,3,3,QR,3,3,3,3,3,W,3)
       CALL MAMP1D(TR,3,3,AA,3,3,3,3,3,W,3)
       RETURN
       END
$DATA
$DATA
       .4765D+07        .1211D+07        .3363D+00        .0855D+00        .4230D+06
-.30755890-02+.2344010D+00+.9397711D-04+.2269570D-01-.6387300D-03+.2142418D-02

STATISTICS -    136 CARDS READ,-    150 LINES PRINTED
```